Anti-Cancer Thesis

A Thesis

Submitted to Bahauddin Zakariya University, Multan in the partial fulfilment of the requirement of a Degree of

Master of Philosophy In
the Subject of
PHARMACOLOGY
By

Laiqa Qayyum Rao
Roll no: 11-PHL-S-23
Session: 2023-2025

SUPERVISOR
DR. Waseem Ashraf

DEPARTMENT OF PHARMACOLOGY
FACULTY OF PHARMACY BAHAUDDIN ZAKARIYA UNIVERSITY MULTAN,
PAKISTAN


بسم الله الرحمن الرحيم

ACKNOWLEDGEMENT

Bismillahir-Rahmanir-Rahim.

"In the name of ALLAH, the Most Gracious, the Most Merciful."

I seek His blessings, guidance, and mercy in the search for my knowledge. May this effort be a means of acquiring beneficial knowledge, and understanding, and contributing positively to the academic dissertation.

All praise is for Almighty ALLAH, the benevolent creator of all the universe. The Lord created a man with the abilities of learning, speech, and understanding. All respects to our Holy Prophet Muhammad ﷺ who illuminated our souls with the importance of knowledge.

I would like to express my sincere gratitude to the individuals and my institution for their valuable support and guidance throughout the completion of this thesis. I am indebted to people whose support and guidance have played a great role in the understanding of this endeavor. First and foremost, I express my sincere gratitude to my esteemed Supervisor, Assistant Professor [**Dr. Waseem Ashraf**], for his commitment, encouragement, feedback, and continuous support. His mentorship and expertise have not only improved my academic knowledge but have also shaped the route of this research. Working under his supervision was a knowledgeable experience for me. I'm thankful for the time he invested to guide me in my research reviewing my work and providing me with great and knowledgeable feedback on my research.

I am grateful for my siblings' support and understanding, their encouragement, and their belief in my abilities. I am thankful to my colleague fellows Alya Shezadi, Nida Rasheed, and Hafiza Khushbakht, who have been a constant source of motivation. Their cooperation and encouragement have proved supportive throughout this journey. A special thanks to all my lab fellows, who have made my MPhil journey enjoyable and memorable.

This thesis would not have been possible without the support and collaboration of these individuals and organizations. Thank you all for being an integral part of this academic journey.

DEDICATION

To my beloved parents and spouse

This thesis is lovingly dedicated to my parents, whose unwavering support, endless sacrifices, and profound belief in my abilities have been my guiding light throughout this journey. Your encouragement and values have been the foundation of all my accomplishments. To my beloved spouse, your support, patience, and understanding have been my strength during challenging times. Your unwavering faith in me and constant motivation have made this achievement possible.

Thank you for being my pillars of support and inspiration. This work is a testament to your unconditional support and the enduring impact you have on my life.

With love and gratitude,

Laiqa Qayyum Rao

Table of Contents

Abstract

Introduction: In the present paper, we evaluate the safety and pharmacokinetic properties of 2-amino-3-hydroxy-anthraquinone, a single compound shown to possess anti-cancer activities. Thus, the study employing a BALB/c female mouse model seeks to harness the shortcomings of existing cancer therapies including toxicity, drug resistance, and nonspecific effects. Tolerability and metabolic study were undertaken using different dosing schedules, namely; single day IV, 3 days IV, and 7 days IP. Neurological and behavioral effects were investigated using the Open Field Test (OFT) to evaluate anxiety, locomotor and exploratory activity, and the inverted screen test to evaluate motor coordination strength and general neurological condition.

Methodology: The compound was first isolated and characterized using HPLC; standard samples that were used confirmed clear peaks. After optimization; in vivo studies were conducted using 8-week-old female BALB/c mice. These dosing paradigms ranged from single-day intravenous to three-day intravenous and seven-day intraperitoneal, with very precise concentrations to prevent toxicity while optimizing efficacy. The pharmacokinetic evaluation assessed the drug's action on absorption, distribution, metabolism, and elimination. The hematological findings were carried out to determine the changes on the part of the red and white blood cells, changes in the hemoglobin concentrations, and the blood platelets. Behavioral assessments that included OFT to assess anxiety and locomotion and inverted screen tests for motor coordination and muscle strength were done. These methodologies afforded an extensive assessment of the compound's safety and pharmacokinetics.

Results: This was done through the use of High-Pressure Liquid Chromatography or HPLC analysis whereby the presence of 2-amino-3-hydroxy-anthraquinone was confirmed due to the consistency of peaks obtained. At six hours post-dosing, pharmacokinetic analysis showed stable drug uptake with maximum activity without polarity shift when administered with longer interval dosing. Biochemical and hematological investigations revealed only a slight rise in red, and white blood cell count that was still within the permissible limits, and thus no severe complications were observed. There were no observed deleterious effects on anxiety as measured

through the Open Field Test, locomotion, exploratory activity, muscle coordination, or strength through the inverted screen test.

Findings: The result concluded that the 2-amino-3-hydroxy-anthraquinone compound showed low toxicity, good pharmacokinetic properties, and no effect on hematology and neurology. These results demonstrate the absence of substantial systemic toxicity and distribution effects of the compound, suggesting its ability to alleviate existing shortcomings of cancer treatments.

Keywords: Pharmacokinetics of anthraquinone derivatives, Peak area analysis in \HPLC, Cross-species validation of drug effects, Behavioural statistics in animal models

LIST OF ABBREVIATION

Abbreviation	Full Form
HPV	Human Papillomavirus
ATP	Adenosine Triphosphate
BALB/c	Bagg Albino Laboratory-Bred Mouse/c inbred strain
DMSO	Dimethyl Sulfoxide
HPLC	High-Performance Liquid Chromatography
IP	Intraperitoneal
IV	Intravenous
NIH	National Institutes of Health
EBV	Epstein-Barr Virus
OFT	Open Field Test
AQ	Anthraquinone
MCPyV	Merkel Cell Polyomavirus
WHO	World Health Organization
CSV	Cancer Stem Cells
MTD	Maximum Tolerated Dose

LIST OF FIGURES

LIST OF TABLES

Chapter 1: Introduction

Anti-Cancer Drug (2-Amino, 3-Hydroxy-Anthraquinone)

1. Introduction of Disease Cancer:

Cancer is a complex genetic disease brought on by intricate genome alterations. A cell can develop a malignant phenotype through a combination of gain-of-function mutations that activate oncogenes, loss-of-function mutations that deactivate **tumor** suppressor genes, and mutations that deactivate stability genes involved in proliferative cell division. However, the world's leading cause of death is cancer. According to the 2020 WHO report, cancer claimed 10.1 million lives. Cancer accounts for 13% of all human deaths and is regarded as the second most common cause of death. Gene alterations and the possibility of metastasis to other organs are the causes of cancer. Cancer is also brought on by disruptions in cellular regulatory systems and epigenetic changes. (Rao, et al., 2022).

Reprogramming metabolic pathways gives these cancerous cells the energy and materials they need to maintain their traits. The most well-known altered metabolic pathways in cancer cells are glycolysis and glucose metabolism, though other pathways have also been observed to be altered. Complex mechanisms and the cooperation of multiple signaling molecules, including non-coding RNAs, are required for the reprogramming of these pathways. Because of the intricacy of these pathways, cancer cells can display plasticity that is not seen in healthy cells. According to Otto Warburg's theory, the Warburg Effect, which is mediated by alterations in oxidative metabolism, oncogene activation, and the loss of tumor suppressor genes, cancer cells depend on aerobic glycolysis to produce ATP. (Schiliro & Firestein, 2021).

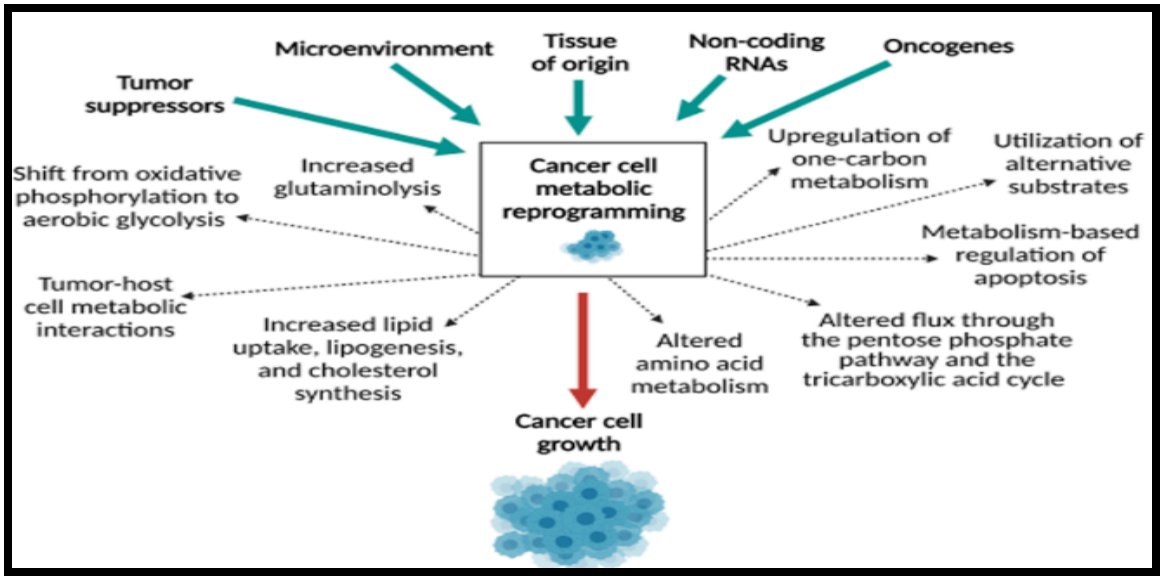

Figure 1: Cancer Cell Metabolic Reprogramming in different ways like in microenvironment, tissue of origin, non-coding RNAs, and oncogenes *(Schiliro & Firestein, 2021)*

1.1 Epidemiology Prevalence:

Effective prevention, screening, and diagnosis policies are supported by timely and appropriate healthcare interventions that are made possible by a thorough and accurate understanding of cancer epidemiology, which offers crucial information on the probable causes and population trends of these conditions. This brief report updates the 115 cancer regions' frequency, mortality, and survival expectancy, which offers a succinct summary of current cancer epidemiologic data gathered from the World Health Organization's (WHO) and IARC's official databases. This is because accurate data on cancer epidemiology is always needed to create reliable healthcare policies across the globe. (Mattiuzzi & Lippi, Current Cancer Epidemiology, 2019).

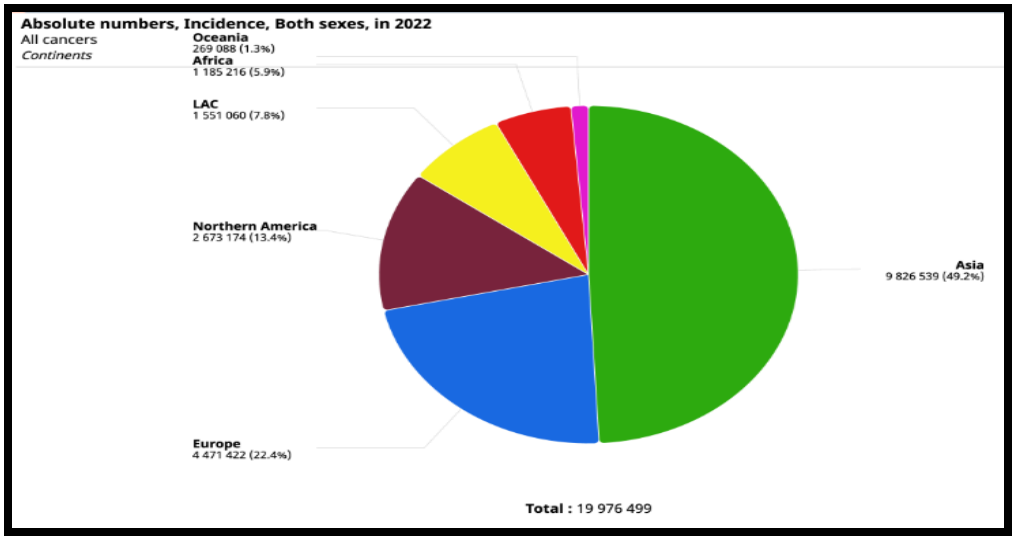

Figure 2: Cancer Prevalence Worldwide IARC Report

The International Agency for Research on Cancer (IARC) report thoroughly assesses the worldwide cancer burden based on a survey of 115 countries. 20 million new cases of cancer were reported in 2022, and 9.7 million deaths were attributed to the disease. It was predicted that prevalence rates would increase by 25% every ten years, peaking at 28.4 million cases by 2040. One in nine men and one in twelve women are expected to die from cancer. It indicates that a higher incidence of cancer disease was noted in women than in men. (Globocan, 2024). This expanding rate was predicted to be influenced by a growing economy, growing globalization-related risk factors, as well as dietary and lifestyle factors that predispose. With 11.7% (2.3 million) of new cases in 2020, female breast cancer was the most common cancer to be diagnosed. In 2020, breast cancer was the leading cause of cancer-related deaths among women worldwide, with an estimated 6.9% mortality rate. (Lawal, Kuo, Sumitra, & Wu, 2021).

However, new developments in medicine have led to lower death rates. Overall cancer mortality has dropped by 33% since 1991, according to the American Cancer Society's most recent Cancer Statistics 2023 report. The observed decline in death rates has been largely attributed to new anti-cancer treatments as well as improvements in early detection and cancer

prevention. Thanks to these cutting-edge therapies, patients with leukemia, melanoma, kidney cancer, and lung cancer have particularly improved survival rates (Mattiuzzi & Lippi, Current Cancer Epidemiology, 2019).

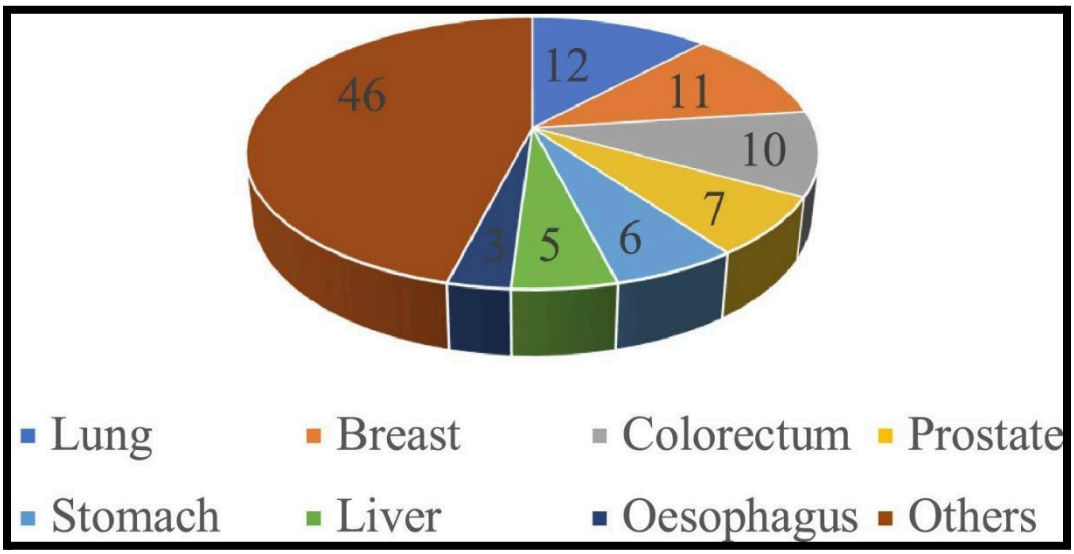

Figure 3: Different Cancer %ages worldwide *(Karati & Kumar, 2022)*

Breast cancer has the highest percentage of any cancer type worldwide, at 46%, according to the WHO 2023 report and figure. Following breast cancer, the majority of patients (12%) had lung cancer. Prostate cancer accounts for 7%, oesophageal cancer for 3%, and liver cancer for 5%. While prostate cancer is more common in men than in women, breast cancer is more common in women. (Schwartz, 2024). Changes in risk factor exposure, many of which are connected to socioeconomic development, as well as population growth and aging, are the causes of the rapidly rising global cancer burden.

1.2 Risk Factors:

Most cancer risk (and protective) factors are initially identified through epidemiology studies. Researchers compare individuals who develop cancer with those who do not in these large-scale studies. These studies may show that being exposed to certain substances or engaging

in specific behaviors increases or decreases the likelihood that a person will develop cancer. Tobacco use is the primary cause of cancer globally. Chemicals in tobacco smoke have the potential to cause lung cancer in addition to several other cancers. Inhaling someone else's smoke, also known as passive smoking, increases the risk of developing cancer. The risk of developing cancer is increased by certain chronic infections; this is particularly problematic in low- and middle-income countries (Azees, Natarajan, Amaechi, Thajuddin, & Phuong, 2022).

About 13% of cancer diagnoses worldwide in 2018 were caused by carcinogenic infections, including Helicobacter pylori, human papillomavirus (HPV), hepatitis B, hepatitis C, and Epstein-Barr viruses. Drinking alcohol increases your risk of getting cancers of the mouth, throat, oesophagus, larynx (voice box), breast, and liver. The more alcohol you drink, the higher the risk. The risk of cancer is considerably higher for those who smoke and consume alcohol. It is well known that a class of female sex hormones called estrogens can cause cancer in humans. Despite having essential physiological functions in both males and females, these hormones have been connected to an increased risk of developing certain types of cancer (NIH Cancer, 2024).

For instance, taking combined menopausal hormone therapy, which includes estrogen and progestin, a synthetic form of the female hormone progesterone, may raise a woman's risk of breast cancer (NSW, 2024). Only women who have had a hysterectomy are treated with menopausal hormone therapy, which uses estrogen alone and raises the risk of endometrial cancer. Additionally, according to the domain studied, different subgroups of cancer patients have different kinds of needs, and the predictors of reporting some unmet needs for assistance differ (NIH Cancer, 2024). The comprehensive needs of cancer patients were linked to sociodemographic traits. Generally speaking, these female patients with low family monthly incomes should receive comprehensive care at their own expense from highly educated

caregivers. Female cancer patients are more likely than male patients to have unmet needs, particularly those related to psychological issues, and gender is a significant factor in the likelihood of having more comprehensive needs. This discrepancy has been explained by similar findings, such as the correlation between female gender and higher rates of anxiety and/or depressive disorders.

is a greater need for psychological problems, health care personnel, physical symptoms, social and religious/spiritual support, and practical support because female cancer patients are more psychologically affected than male patients and consider more aspects of the disease. As a result, female cancer patients need closer observation and might be the group that receives more intensive treatment. Similarly, many patients who pay for their care also experience financial strain due to a lack of insurance, which may result in a high need for psychosocial support, particularly financial support. Cancer-related financial stress and strain have been linked to poor psychological outcomes in patients with breast and prostate cancer however it is not surprising that these factors would intersect with psychologically unmet needs. Therefore, it should be recommended that interventions be developed to help with cancer patient screening and resource identification to close the gap between the growing needs of cancer patients and the limited resources available (Zhao, Wang, Zhang, Liu, & Chen, 2019).

1.3 Pathogens Mechanism:

The pathophysiological understanding of how molecular and cellular processes contribute to the transformation of benign tumors into malignant ones is known as cancer pathogenesis. In solid tumors and blood cells, this frequently entails genetic, epigenetic, proteomic, and metabolic changes. In general, pathogens can be classified as either direct or indirect carcinogens.

There are several commonalities among the direct carcinogenic pathogens, including HPV,

HTLV-1, EBV, MCPyV, and KSVH. Each cancer cell typically contains at least a significant amount of the viral genome, which leads to the expression of viral oncogenes that interfere with cell-cycle checkpoints, prevent apoptosis, and promote cell immortality.

Tumours are made up of stromal fibroblasts, blood vessels, and immune cells in addition to cell-intrinsic factors, all of which are involved in the development of tumours Chemicals and drugs (Animesh & Revandkar, 2024). Cancer cells can accomplish this in several ways, including by producing an excess of growth factors for autocrine signalling or by producing signalling molecules that cause the surrounding stromal tissue to produce growth factors that in turn promote the growth of cancer cells (Noorani, 2020).

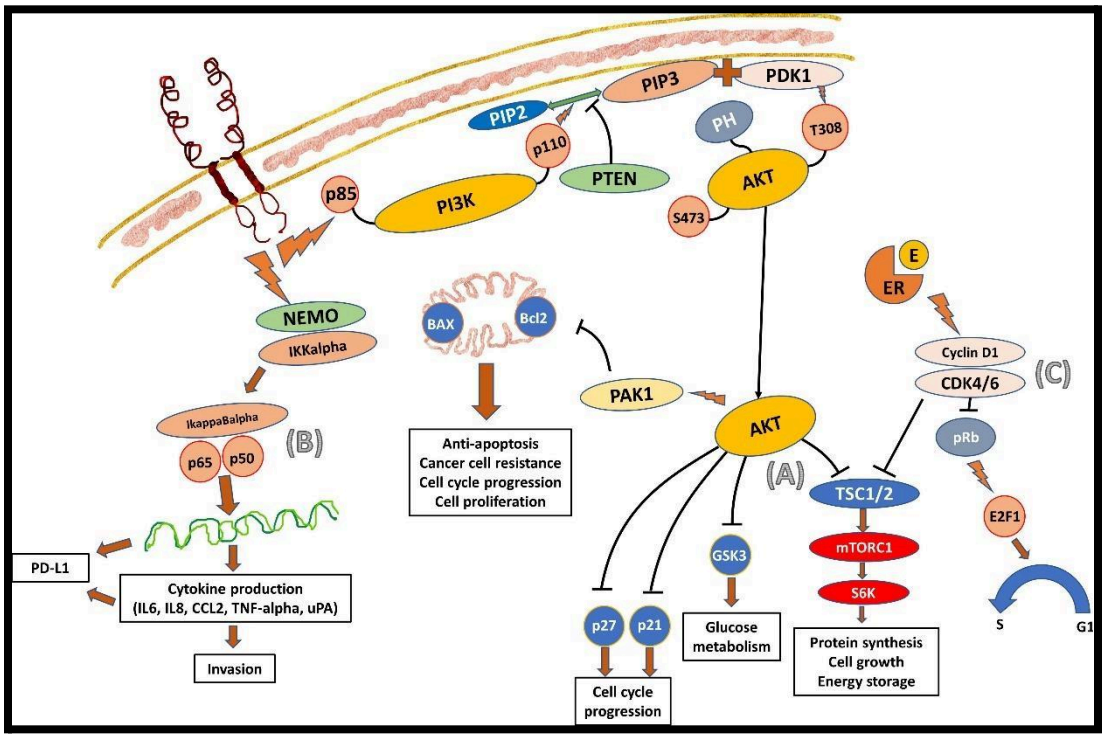

Figure 4: Different chemicals are activated in cancer. The primary transcription factors that control the expression of genes implicated in lipogenesis *(Chow, Lie, & Wu, 2022).*

The PI3K-AKT and Ras-MAPK pathways, which activate transcriptional programs that support cell cycle entry and progression, are examples of how these diverse approaches to cellular signaling activation commonly converge on similar pathways. For example, about 40%

of melanomas have activating mutations in B-raf that increase signaling through the Raf to MAPK pathway, and about 40% of gliomas have activating mutations in EGFR (epidermal growth factor receptor) that activate the PI3K-AKT pathway. Normal cells contain a variety of negative feedback loops that regulate cell division and prevent excessive division by lowering the activation of signaling circuits. For example, the PTEN phosphatase negatively regulates PI3K signaling by degrading PIP3. Cancers often have a loss of function mutations or deletions of the PTEN gene, which raises proliferative PI3K signaling (Junwei, et al., 2020).

Mutations in tumour suppressor genes (TSGs), which normally suppress proliferative pathways, and oncogenes, which activate them like Ras, are typically acquired by the cells early in the formation of cancer. These mutations work in concert to maximize proliferative stimuli in the cells. Senescence and apoptosis are two processes that may be triggered by excessive oncogenic signalling in normal cells as a protective mechanism, according to numerous studies. It is believed that by inhibiting senescence or apoptosis processes, cancer cells have gotten past these defence mechanisms (Puneet & Lim, 2022).

In contrast to normal cells, which have a finite number of divisions before entering a crisis state and dying by senescence, cancers have developed a unique property known as immortalization that allows them to divide endlessly. Overcoming the telomeres' natural shortening with subsequent cell divisions is a crucial step in immortalization. Cells enter a crisis state when their telomeres multiple tandem hexanucleotide repeats that shield chromosomal ends are destroyed. By expressing telomerase, a DNA polymerase that can regenerate telomere DNA, cancers gain the capacity to halt telomerase erosion. This enzyme is expressed in 90% of immortalized cells but is typically absent in normal tissue, indicating that it is a crucial early prerequisite for cellular immortalization and, consequently, carcinogenesis (Nilmani et al., 2022).

By turning on an angiogenic switch, cancers can disrupt the oxygen and nutrition that tumours need to survive. To support growth, new blood vessels and micro vessels are produced, which frequently result in abnormal vessels. Because preneoplastic lesions exhibit aberrant blood vessels, angiogenesis is acquired early in the development of cancer.

Because preneoplastic cells express unique antigens that immune cells can recognize, immune surveillance programs are essential for preventing the early development of cancer (Neha et al., 2012). By concentrating on the interactions between cancer cells and T-cells and inducing T-cell immune destruction of tumor cells, PD-L1 inhibitors have been successful in improving patient survival in certain cases of advanced melanoma, renal cell carcinoma, and non-small cell lung cancer. It will be crucial to increase our knowledge of CSCs to create more precisely targeted treatments, as clinical evidence suggests that high numbers of these cells are linked to a shorter time to recurrence, a worse prognosis, and resistance to chemotherapy and radiation (Lei et al., 2023).

1.4 Impact of Disease on Lifespan:

Every individual uniquely reacts to treatment. The effectiveness of cancer treatment is unknown in advance. Furthermore, it is impossible to predict a person's life expectancy, whether they have cancer or not. The rate of survival depends on cancer patients during and after treatment. Life expectancy can be detected for cancer patients and is often reported as a five-year survival rate. The entire mortality profile seen in the population group under consideration determines this (Livestrong, 2024). For this reason, it can be used as a standardized indicator to compare the overall mortality patterns of various populations. Conditional survival, or the expected survival after a patient has lived for a specific amount of time, has been reported

recently (8–10). Although each of these survival metrics is significant, using percentages or probabilities has limitations.

A 75% 10-year survival estimate, for instance, might not mean much to someone who doesn't know how long they should expect to live. Furthermore, all net survival metrics represent the relatively uninformative likelihood of survival (Baade, Youlden, Kimlin, Aitken, & Biggar, 2024). The financial cost of incorrectly diagnosing a patient with thyroid cancer can range from hundreds to thousands of dollars, depending on the intricacy of the treatment and follow-up, as well as the extent of the tests performed. Avoiding histologic examination of nodules ≤1.0 cm that do not have additional risk factors is one of the many recommendations that have recently been made to avoid these costs and the inconveniences of unnecessary treatment.

1.5 Current Treatment Regime of Disease

Chemotherapy:

These drugs are often delivered intravenously or intraperitoneally. Doxorubicin, cisplatin, and paclitaxel are commonly administered to induce tumor regression. Chemotherapy is frequently used to treat cancer. It employs medications to stop tumor growth and kill cancer cells. It might be used with other cancer treatments like surgery or radiation therapy. Chemotherapy is typically administered intravenously (Izzah & Ibharm, 2020). Despite being a successful treatment, side effects are possible. Chemotherapy is a treatment that can either cure cancer or lessen the chance that it will return by reducing the rate at which cancer cells divide. It is commonly used in combination with other cancer treatments, depending on the type of cancer, its spread, and other medical conditions.

Topically, intraperitoneally (IP), intra-arterially (IA), intravenously (IV), or orally, chemotherapy can be administered. To administer IV chemotherapy, a tiny needle is typically

placed into a vein on the patient's hand or lower arm. Chemotherapy is delivered through ports or catheters, and its dosage and rate are managed by pumps. The patient's cancer type, its spread, and other medical conditions determine the kind of chemotherapy that is used. Throughout treatment, it's critical to keep an eye out for any indications of infection near the catheter and port (Cleveland, 2024).

Radiation:

High doses of radiation therapy harm cancer cells' DNA, which either stops the cells from growing or kills them. When a cancer cell's DNA is irreparably damaged, it either dies or stops growing. The body breaks down and eliminates the damaged cells when they die. Radiation therapy does not immediately kill cancer cells. Treatment must be administered for days or weeks before the DNA is sufficiently damaged to destroy cancer cells.

Targeted Therapies:

One type of cancer treatment called targeted therapy focuses on particular proteins that aid in the growth and metastasis of tumors. By marking cancer cells, it aids the immune system in eliminating them and improves the immune system's capacity to combat cancer. Certain targeted treatments slow the unchecked growth of cancer by blocking signals that lead to cancer cells proliferating and dividing randomly. By interfering with signals that aid in the formation of blood vessels, angiogenesis inhibitors stop tumors from growing larger than they need to. Precision medicine is built on targeted therapy, which is commonly found in monoclonal antibodies and small-molecule medications.

These antibodies are made to adhere to particular cancer cell targets, either to directly stop or self-destruct cancer cells or to mark them for improved immune detection. Certain targeted therapies cause cancer cells to die by combining them with substances that kill cells.

Certain targeted treatments can starve cancer of the hormones it needs to proliferate and induce apoptosis, the death of cancer cells. When it comes to treating metastatic breast cancer with low HER2 protein levels, Enhertu is anticipated to become the new standard (NIH Cancer, 2022).

Immunotherapy:

Checkpoint inhibitors, like (anti-PD-1, anti-CTLA-4) and CAR-T cells are immune-modulating agents utilized to evaluate and enhance immune system responses. By identifying and eliminating aberrant cells, the immune system stops or slows the spread of cancer. Tumour-infiltrating lymphocytes, or TILs, are a sign of the immune system's response to a tumour. Cancer cells can avoid destruction by altering their genes, proteins on their surface, or the healthy cells that surround the tumour. Immunotherapy strengthens the immune system's defences against cancer. Immunotherapies include vaccines, immune system modulators, monoclonal antibodies, T-cell transfer therapy, and immune checkpoint inhibitors (NIH Cancer, 2024).

By blocking immune checkpoints, immune checkpoint inhibitors strengthen the immune cells' defense against cancer. T-cell transfer therapy involves removing immune cells from the tumour and transforming them into more active T cells. Monoclonal antibodies target specific cancer cells, while treatment vaccines boost the immune system's response to cancer cells. Only 20 to 40 percent of Immunotherapy works for patients, and these medications can sometimes trigger severe auto-immune reactions due to their ability to activate a wide range of immune cells. If clinicians can determine which patients won't respond, they can save money on treatment and shield patients from side effects (Nature, 2024).

Table 1: Cancer Drugs and their mechanism of action with side effects

Treatment/Drug	Mechanism of Action	Side Effects	
Doxorubicin	Interferes with the DNA replication of cancer cells by inhibiting topoisomerase II and generating free radicals.	Nausea, vomiting, hair loss, bone marrow suppression, cardiotoxicity, and risk of secondary cancers.	
Cisplatin	Forms crosslinks with DNA, preventing DNA replication and transcription, leading to cancer cell death.	Kidney damage, nausea, vomiting, hearing loss, peripheral neuropathy, and bone marrow suppression.	
Paclitaxel	Stabilizes microtubules and inhibits their disassembly, preventing mitosis in cancer cells.	Peripheral neuropathy, allergic reactions, bone marrow suppression, muscle pain, and nausea.	
Radiation Therapy	Damages DNA of cancer cells by high-energy radiation, preventing replication and leading to cell death.	Fatigue, skin irritation, localized tissue damage, and risk of secondary malignancies.	
Targeted Therapy (e.g., Enhertu)	Blocks specific proteins or pathways necessary for cancer growth, such as HER2 receptors in breast cancer, and promotes apoptosis.	Nausea, diarrhea, fatigue, low blood counts, and potential for heart and lung damage.	
Checkpoint Inhibitors	Block immune checkpoints (e.g., PD-1, CTLA-4) to enhance the immune system's ability to attack cancer cells.	Severe auto-immune reactions, fatigue, rash, diarrhoea, and inflammation of organs (e.g., liver, lungs).	
CAR-T Cells	Genetically modifies T-cells to recognize and attack specific antigens on cancer cells.	Cytokine release syndrome (CRS), neurotoxicity, fever, and low blood pressure.	

1.6 Shortcomings of Disease:

The effectiveness of current cancer treatment therapies is limited by some flaws in the disease. Immunosuppression, organ toxicity, nausea, and exhaustion are just a few of the serious

side effects of the most popular cancer treatments, such as radiation therapy and chemotherapy. These methods, which are referred to as non-specific methods, are unable to distinguish between cancerous and healthy cells. These restrictions lower the quality of life for patients. The majority of cancer cells frequently develop resistance to targeted and chemotherapies, which makes cancer treatment and growth disease ineffective. A lot of people wish to actively contribute to bettering their general health. They wish to expedite their recuperation from chemotherapy and strengthen their body's defences against cancer. It is not surprising that many cancer patients take high doses of one or more vitamins, as most people believe that taking vitamins is a safe way to improve their health. However, some vitamins may reduce the effectiveness of chemotherapy (Mylène, et al., 2021).

Because of their size and composition, nanoparticles can be dangerous and are quickly removed from the bloodstream by the spleen and liver. To improve circulation, polyethene glycol (PEG) is used as a particle camouflage agent. However, because PEG is used in cosmetics, 25% of people have developed PEG antibodies. The target's accumulation of nanoparticles stops them from deeply penetrating the tissue. A gene-modified cell therapy called CAR-T has demonstrated 83% remission rates in patients with acute lymphoblastic leukaemia that has relapsed or is refractory. Genetic alterations, the use of various immune cell types, and treatment of cytokine release syndrome are some solutions. Low transfection efficiency and high cell toxicity are problems for non-viral techniques like electroporation (Evans, 2024).

1.7 Anti-Cancer Drug (2-Amino, 3-Hydroxy-Anthraquinone) its Benefits and Structure:

An anti-cancer drug named 2-amino 3-hydroxy-anthraquinone is a chemical compound used for the treatment of cancer (Zaayter, et al., 2019). Natural anthraquinone compounds are

expensive to obtain from natural sources, which restricts their use for cancer patients, particularly in developing nations. Finding economical, effective substitutes requires research. The ability of a molecule to cross cell membranes is its most crucial biological characteristic. Research on interactions between drugs and surfactants is crucial because it sheds light on interactions between drugs and membranes. Micellar systems can increase the bioavailability of hydrophobic drugs by solubilizing them. They can also be used as models for drug carriers and bio membranes (Herck & Geest, 2020). These molecules' structure-activity relationship may help create novel treatments for a range of illnesses. The compound's molecular formula is C14H9NO3, and its PubChem ID is 67029. Spectroscopic and computational measurements were made to understand the electronic state and hydrogen bonding of 2-amino-3-hydroxyanthraquinone (AQ).

This study investigated the ability of anthraquinone (AQ) to cross a biological membrane using cationic and anionic surfactant micelles (Feeney & Villanueva, 2023). The construction between an anti-cancer drug AQ and surfactants is of interest to biology and drug development research. The drug AQ was chosen due to its cost-effectiveness when compared to other drugs and its planar anthraquinone unit. UV-Vis spectroscopy was used to examine how AQ is bound to a micellar system (Das, et al., 2016). AQ, on the other hand, has evolved into a systematic procedure that combines many calming modalities and treatment tactics. The significant cumulative benefit of AQ cancer medication indications that have been brought to market over the last 20 years must thus be acknowledged. (Michaeli, Michaeli, & Michaeli, 2023). The 3D structure of the AQ compound is as follows:

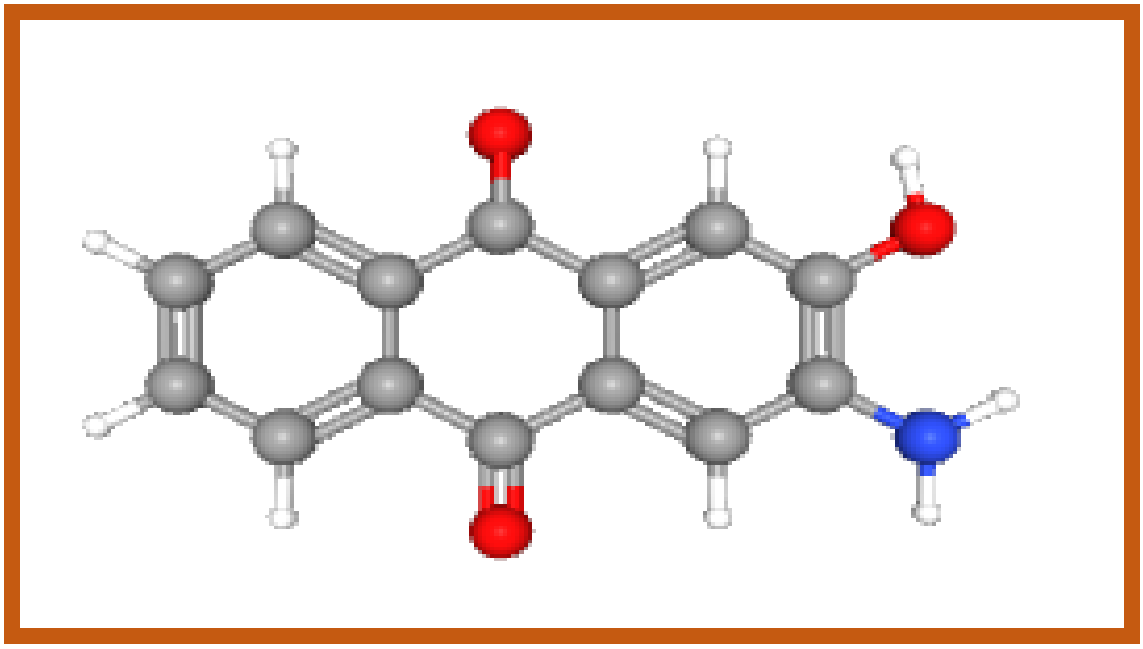

Figure 5: 3D Structure of 2-Amino, 3 Hydroxy Anthraquinone:

Types of Cancer:

Cancer is a generic name for over one hundred diseases form of disease characterized by the uncontrolled growth of cells. The most common types include:

Breast Cancer

The second most prevalent cancer type in women and one of the leading causes of cancer deaths all over the world, breast cancer begins when cells in the breast tissue alter. Although it is noticed that this disease is common in women, men can also get this disease. Breast cancer molecular classes include HER2-positive breast cancer and hormone receptor-positive breast cancer, which have a direct relation to the treatment approach and prognosis (Korde et al., 2020).

Lung Cancer

Lung cancer is usually divided into two groups: non-microcellular carcinoma of the lung (NTEC-NSCLC) which is the largest and microcellular carcinoma of the lung (SCLC). Smoking

continues to be a leading cause of the disease but patients who have never smoked can also get the disease through genetic mutations or exposure to other hazards (Roth et al., 2020).

Prostate Cancer

This cancer is found in the prostate gland of men and it most commonly affects the elderly. According to nature, most prostate cancer is androgen-dependent and slow-growing, whereas there exist some deadly subtypes that trigger metastasis. Using genetic biomarkers, such as BRCA1/2, there are potential impacts on the diagnosis and treatment plan (Cheng et al., 2021).

Colorectal Cancer

Colorectal cancer begins in the colon or rectum, and it is the third most frequent cancer in the world. Some of the diseases' risk factors include diet, inclusive of red meat, processed foods and foods that contain high amounts of fat and sugars, family and genetic profile especially having Lynch syndrome (Phipps et al., 2021).

Leukaemia

Leukaemia originates from the uncontrolled production of mature or immature white blood cells and is classified as acute or chronic. CLL and AML are two of the most prevalent forms (Jabbour et al., 2019).

Even these cancers that are morphologically similar and grouped under one type of cancer have different pathophysiologic characteristics and have different management strategies; thus, the therapeutic strategies should depend on genetic and environmental endowment.

High-Performance Liquid Chromatography (HPLC) in Cancer Therapy Research:

As will be discussed in the paper, conventional cancer treatments like chemotherapy, radiation treatment and surgery demonstrate different effectiveness when applied to new entrant

therapeutic intervention. Besides showing an interest in the anti-cancer agents such as 2-amino and 3-hydroxy anthraquinone this study covers issues such as the global incidence, structure and the mechanisms of cancer. These agents diplomatic both antimicrobial and antitumor personalities, assumption to approximate of various biological actions. Moreover, the focus on the evaluation of the effectiveness of such agents is given to using High-Performance Liquid Chromatography (HPLC) as one of the most effective methods (Sabourian et al., 2020).

The main purpose of this study is to evaluate the pharmacokinetics of 2-amino,3-hydroxy anthraquinone known as AQ (Antonetti et al., 2001). HPLC is used to quantify this compound in blood plasma and many other biological fluids. The technique is also crucial in testing important absorption rates, half-life, bioavailability and in vivo status of the drug (LCNEC, 2022).

Most conventional chemotherapy agents have severe side effects because they are highly reactive substances that can also kill cancer cells and have toxicity. On the other hand, the pharmacological features of AQ are to be less toxic and more stable to improve the safety of the treatment. Due to a very high separation capacity, LC, particularly HPLC, is widely used in the analysis of anti-cancer drugs. Of all the indicated forms of LC, reversed-phase HPLC or RP-HPLC for short is the most commonly used method for drug analysis since it’s easy to use, highly selective, precise and reproducible. This method is widely used in the development of pharmaceutical drugs and the determination of drugs and metabolites in the biological matrix (Kim et al., 2022).

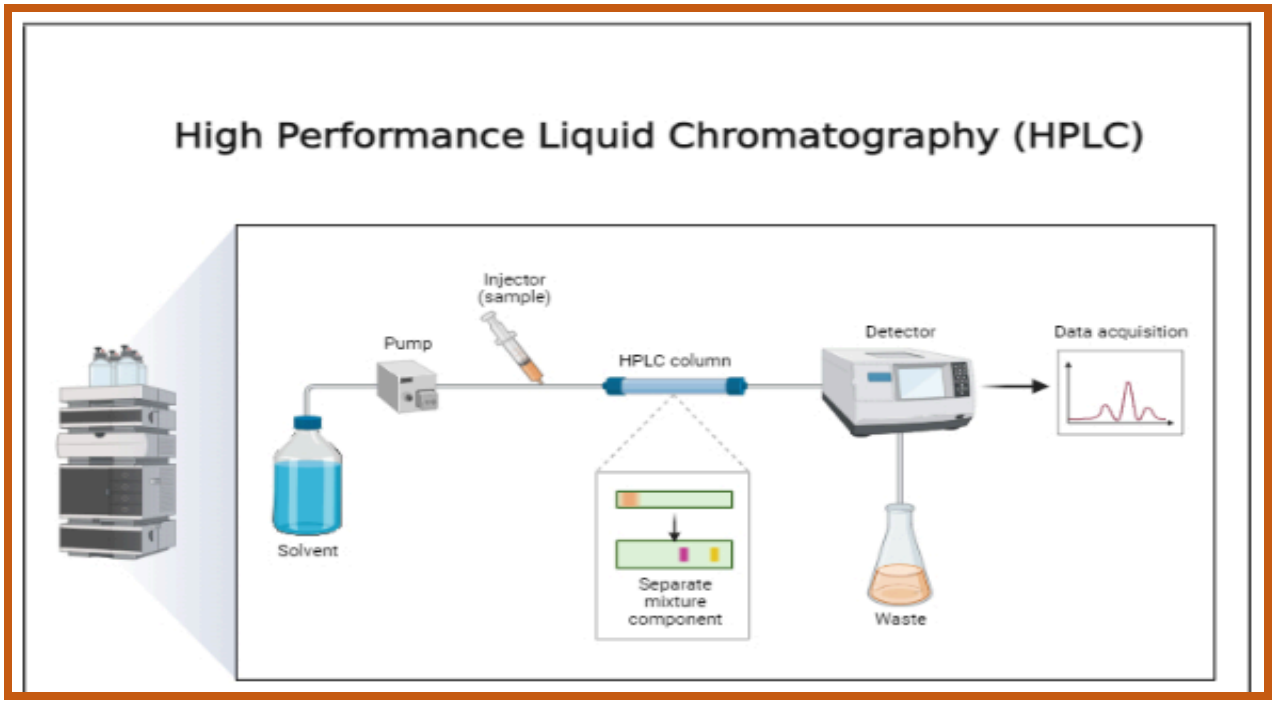

Figure 6: High Performance Liquid Chromatography; Instrumentations and process (Aseem, 2023)

1.8 Aim of Study:

To assess the safety and pharmacokinetic profile of 2-amino-3-hydroxy_Anthraquinone about novel anticancer molecules, this study will employ the paraclinical mouse as a model. This study aims to ascertain the compound's maximum tolerated dose (MTD) and evaluate its toxicological impact on essential organs, offering crucial information about its safety profile. The study examines bioavailability, half-life, and dosing intervals to determine the pharmacokinetics and distribution of molecules as well as their absorption and excretion parameters. Understanding these aspects, it is important to guarantee the stability of drugs for the use of therapeutics. This study aims to analyze the cancer-specific particle and tumour regression in treated subjects compared to control groups in evaluating compound efficiency.

This research aims to determine whether 2-amino acid, 3-amino, and 3-hydroxyanthraquinone offer advantages and provide a distinguishable cancer treatment option

by addressing safety and pharmacokinetics for reducing toxicity and improving therapeutic outcomes. By elucidating the potential for the compounds, this study seeks to provide a foundation for further clinical treatments and conditions to address the significant limitation of current anti-cancer treatment options.

Targeted Mechanisms of Action:

The pathway by which 2-Amino, 3-Hydroxy-Anthraquinone causes anti-cancer properties. New evidence indicates that Anthraquinone derivatives such as 2-Amino, and 3-Hydroxy-Anthraquinone selectively kill cancer cells through direct damage to topoisomerase, blocking DNA replication and generating oxidative stress. These processes were pointed out in pilot experiments as the components that contribute to its anti-cancer effect. In addition, the targeting of UHRF1 (Ubiquitin-like, containing PHD and RINGER finger domains 1), a proliferation-related effector of epigenetic change, may be of benefit. In a related study, it was reported that small molecular tools for base flipping activity of UHRF1 may affect DNA binding and its downstream effects on DNA repair pathways and cancer cell growth (Zaayter et al., 2019). Based on these results, the present research indicates that 2-Amino and 3-Hydroxy-Anthraquinone may have an opportunity to operate in combination with such compounds, opening new horizons for those approaches. It is therefore the intention of this research to describe these pathways and understand their effectiveness for improving therapeutic outcomes thus offering potential for cancer therapy.

Addressing Current Limitation in Cancer Treatments:

Addressing the shortcomings of existing cancer treatment is one of the overarching goals of this study. For example, killing rapidly dividing cells is highly effective in chemotherapy but lacks specificity which often harms the healthy tissues and leads to extreme side effects. For

correct radiation therapy limitations were given to localized tumours which may not be affected by metastatic cancers. It remains expensive and poses the risk of autoimmune reaction, while immunotherapy holds significant potential (Nora, Pittini, and Osinaga, 2022). The 2-amino-3-hydroxide and anthraquinone provide a promising alternative to overcome these challenges by:

Lower Toxicity:

Minimizing damages to healthy tissues, its structure allows for selective targeting of cancer cells.

Improved Tolerability:

During treatment side effects reductions could improve the compliance and quality of the patient's life.

Versatility:

Through broad-spectrum its activity makes it effective against multiple types of cancer.

Laying the Groundwork for Clinical Trials:

With the help of this research author finds that for future clinical trials, it will serve as a foundation. For identification of potential risks and establishing a drug's pharmacological profile before in human, it is tested, all these are critical in preclinical study. This research aims to justify further investigations into clinical developments when both 2 Amino and 3-Hydroxy-Anthraquinone are safe and effective in animal models.

Contributions to Cancer Research and Therapeutics:

This study contributes to the broader field of cancer research, beyond the direct implication for drug development. The insights gained from the pharmacokinetics and mechanisms of action of 2-Amino, and 3-Hydroxy-Anthraquinone can inform the design for the same compounds and inspire new strategies for targeting cancer cells. Aiding in the development

of personalized medicine approaches, this study's outcomes may also highlight the biomarkers that predict response to the treatment.

Focusing on the comprehensive evolution of the safety efficacy of 2-Amino-3-Hydroxy-Anthaquinone as a novel anti-cancer agent is the aim of this study, which is very complex. This research seeks to establish the potential of this compound as a promising candidate for cancer therapy by addressing these critical aspects. The maximum tolerated dose and assess organ-specific toxicities guaranteed that the compound has a favourable toxicity profile when safety evolution is determined. The pharmacokinetic studies will provide valuable insights into absorption, distribution, metabolism, and excretion, offering a clearer understanding of the compound’s bioavailability and dosing requirements. Elucidating its underlying mechanism of action, the efficacy assessment aim is to explore its ability to inhibit tumour growth and induce cancer cell apoptosis.

In current cancer treatment, this research aims to address the major shortcomings in which toxicity, resistance, and limited specificity are included. The 2-amino-3-hydroxyanthraquinone would improve treatment outcomes and quality of life for patients when potentially safer and more targeted therapeutic options were introduced. Ultimately, Paving the way for advancements in cancer therapeutics and personalized medicine approaches through this preclinical study the findings will not only facilitate the further development of this molecule but also contribute to the broader field of one hydroxy-anthraquinone contributing to the improvement of cancer therapy (Cheng *et al.*, 2025).

Chapter 2: Material and Methods

2.1 Experimental Female Mice:

The experimental procedure was carried out using 24 healthy female laboratory mice that are more appropriate for use in studies relating to pharmacokinetic and toxicological research. For the reliability of results, species, strain, weight, as well as age of animals were chosen.

❖ **Species and Strain:**

BALB/c mice were used in the study and they are a standard inbred strain that is viewed to respond well to pharmacological drugs. They are used in toxicology and cancer research because they have a low genetic variation and immunogenicity, good genetic background, and adaption to drug metabolism.

❖ **Weight Range:**

The mice selected were middle-aged weighing between 25~35 grams, which is more suitable for pharmacokinetic studies of adult female mice. This weight range indicates a grown, physiologically normal adult population thereby minimizing the variation within ADME parameters. Mice below the weight of 25 grams or above the weight of 35 grams were also discarded to reduce variance and incorporate only standardized data.

❖ **Age Range:**

The mice were young adults, weighed between 25 and 35 grams and aged 8 weeks because the organism exhibits maximum metabolic activity at this stage. No juvenile or older mice were used in this research because juvenile mice's metabolic system may still be immature and older mice,

due to their age, will possess an impaired drug metabolism, changed renal clearance or immune-compromised status. Only the mice within this age range were selected to have strong, reproducible data regarding both pharmacokinetics and toxicity.

Inclusion Criteria:

To maintain experimental uniformity, only mice that met the following criteria were included:

- ✔ **Health Status**

Screened free of detecting any pathogens and other diseases or conditions before the study.

- ✔ **Weight and Age Compliance**

The weight is 25–35g limit and the age of the patients to be treated at 8 weeks.

- ✔ **Behavioural Normalcy**

Only those mice showing normal activity and feeding behaviours were used as normal controls to obtain healthy baseline values.

Housing Conditions:

The selected mice were maintained in a germ-free facility of the university animal facility using individually ventilated cages, specifically pathogen-free. This setup limited anew the chances of contracting diseases and kept off any form of interference from outside factors. The following conditions were maintained (NIH Cancer, 2024).

- **Temperature**

22 ± 2°C which is suitable to support rodent metabolism and health status while handling experiments.

- **Humidity**

50-60%, and are checked and regulated daily in order to help avoid problems with the respiratory system.

- **Light/Dark Cycle**

The light/dark cycle was maintained at 12/12 h, with lights on at 7:00 a.m. to mimic the circadian clock because this factor affects drug metabolism in mice.

- **Group Size**

Each cage contained three mice so the animals could exhibit more natural behaviours without stressing or fighting with other animals.

Bedding and Enrichment:

The cages were filled with aspen wood shavings for flooring material since it is non-toxic and has the quality of being very absorbent. Environmental enhancement was done using cardboard tubes and nest materials in this context; the animals were encouraged to exhibit natural behaviours including nest building. These actions improved the quality of animal life and minimized stress hence maintaining the homogeneity of physiological conditions required for the study (Mylène, et al., 2021).

Ethical Approval and Handling:

Any manipulations of animals and all experimental manipulations were performed in strict accordance with protocols approved by the Institutional Animal Ethics Committee and were conducted under the National Institutes of Health and other international guidelines for the care and use of laboratory animals (Guide for the Care and Use of Laboratory Animals, ARRIVE, and OECD). Special care was taken during dosing and sample collection to minimize distress (Karati & Kumar, 2022).

A. **Acclimatization Period:**

It took one week before mice were allowed to adapt themselves to their caging providing them with the required comfort before imposing an experiment.

B. **Handling Protocols:**

The manipulations to reduce stress and avoid potential suffering were conducted only by experienced handlers.

C. **Monitoring:**

The mice were observed daily for discomfort; changes in such behaviours as eating patterns; and loss of body weight.

Experimental Groups:

Mice were divided into groups based on dosing protocols:

Single-Day IV Dosing Group: Given a single intravenous (IV) dose of 200 mg/kg and collected samples at five different intervals: 30 minutes, 2 hours, 6 hours, 18 hours and 24 hours after dosing.

Three-Day IV Dosing Group: Similarly, a 3-day (IV) dose of 200 mg/kg was given, and samples were collected after 3 days.

Seven-Day IP Dosing Group: 200 mg/kg/day dose is given IP for seven consecutive days.

2.2 Chemicals and Drugs:

Table 2: Different Chemical drugs and formula

Chemical/Drug	Formula	Molecular Weight	Boiling Point	Volume	UN Number	Additional Information

Acetonitrile for Gradient HPLC	CH_3CN	41.05	82°C	4L	UN1648	High-purity chemical.
Methyl Alcohol for Gradient HPLC	CH_3OH	32.04	65°C	4L	UN1230	High-purity chemical.
Dimethyl Sulfoxide (DMSO)	$(CH_3)_2SO$	78.13	189°C	-	-	Used for drug preparation.
2-Amino, 3-Hydroxyanthraquinone	$C_{14}H_9NO_3$	239.23	-	-	-	Test compound for analysis.
Methanol	CH_3OH	32.04	65°C	-	-	Used for mobile phase preparation.
Normal Saline	NaCl in H_2O	-	-	-	-	Used for dilution and dosing.
HPLC Vials	-	-	-	2 mL	-	Screw-type, Lot No: 18108891, USA.
Syringe Filter	-	-	-	Φ 25 mm	-	Pore size 0.45 µm, Non-Sterile.

Need to achieve correct parameters:

This was due to the selection of high-purity chemicals, confirmation of the mobile phase composition and optimization of the HPLC conditions. This approach reduced variability and increased the sensitivity of the system which was useful when determining the low concentration of the drug in biological fluids (Nilmani, D'costa, Bothe, & Das, 2022).

Quality Assurance Measures:

All the measurements and other sequential processes were done in a controlled laboratory environment, and in addition, all the equipment used was calibrated regularly to ensure accuracy. Both the method of drug preparation and the method of HPLC analysis reported in this work were accurate, comprehensive and well-repeated throughout the study.

2.3 Apparatus Used

Table 3: Chemical Apparatus used in Drugs

Apparatus	Model/Type	Manufacturer	Origin	Purpose
Centrifuge	Eppendorf 5415	Eppendorf	Germany	Plasma and serum separation.
Open Field Test (OFT)	Behavioural Apparatus	-	Pakistan	Behavioural analysis.
Mouse Cages	Fengshi	Fengshi	China	Housing of laboratory mice.
Spray Bottle	-	-	Pakistan	For laboratory cleaning purposes.
USB Camera	Logitech C310	Logitech	Switzerland	Behavioural monitoring.
Petri Dishes	-	-	Pakistan	For sample handling.
Weighing Machine	Precision Scale	-	-	For accurate weight measurements.

The apparatus and equipment in this study were chosen judiciously to obtain the maximum possible accuracy and reliability in all experimentation. All instruments in use were calibrated and

maintained properly to ensure the correctness of the findings in the study (Zhao, Wang, Zhang, Liu, & Chen, 2019).

Laboratory Equipment

- Centrifuge 5415 R

The above showed a centrifuge used to enhance the separation of plasma and serum from blood samples.

Specifications:

Rotation speed: 6,000 rpm.

Time: 5 minutes.

Temperature: 4°C to make sure that the biological components within the extraction remain reliable.

The Centrifuge 5415 R is relatively small but very reliable for operating small samples that require high-density force. Its refrigerated feature allows for maintaining temperature-sensitive plasma and serum components at their capacity while undergoing centrifugation.

Disposable Membrane Filter Unit Syringe Filter (0.45 mm, Nylon/Polyamide)

Purpose: Applied earlier to separate plasma and serum samples before their introduction to HPLC vials.

- The filter was 0.45 micrometre; such a filter was useful to filter particulates that could complicate chromatographic analysis or reduce the life of the HPLC column.

- The filters were made out of polyamide or nylon material that has little protein, so that crucial analytes would remain unconsumed in the filtered sample.
- Proper filtration was adhered to so that there could be a high reproduction ability of the samples in a repeatable analysis.

Vial Screw 2 mL

Use: These vials had been employed for holding and transferring prepared samples as well as for HPLC evaluation.

- A standard borosilicate glass vial for storing sharp samples due to their chemical non-reactivity with mobile phase was used.
- Every vial was accompanied by a safety screw cap to avoid interaction of the samples with external substances or water loss in the process (Saré, Lemons, & Smith, 2021).

HPLC System

Model: Agilent 1260 Infinity HPLC System The efficacy of this product is evident in the HPLC analysis of four different components.

- This system was also fitted with a UV-Vis detector where 2-amino, 3-hydroxy anthraquinone was detectable at its λ max of 480 nm.
- Agilent 1260 Infinity is considered a benchmark instrument mainly for its high performance and deliver accurate and repeatable chromatographic separation.

Column: C18 Reversed-Phase Column

Specifications:

Dimensions: 4.6 x 250mm

Particle size: 5 microns

- The C18 column was employed in the reduction of the drug from the biological contents of plasma and serum samples.
- Reversed-phase capability allowed good retention and separation of 2-amino 3-hydroxy anthraquinone, causing the formation of very peaked and separated chromatographic humps.

Temperature-Controlled Column Compartment

- The column compartment was held at a constant temperature of 25 o C for obvious reasons to do with stability of retention times and peak shapes.
- The temperature should also be controlled because changes result in shifts in elution patterns and broad peaks, which influences the obtained results.

Additional Accessories and Consumables

Falcons Tubes Covered with Aluminium Foil

These tubes were used to contain prepared stock solutions of the drug to avoid photodegradation of the substance.

Mobile Phase Containers

In the prepared mobile phase, seventy per cent methanol and thirty per cent acetonitrile were transferred to high-purity containers (Schwartz, 2024).

Centrifuge Tubes

The blood samples during the plasma and serum preparation were collected and processed in centrifuge tubes.

The Role of Apparatus in the Study

The combination of high-quality instruments and accessories ensured:

Sample Integrity: Filtration and temperature conditions ensured plasma and serum samples stability to prevent changes during their processing.

Accuracy: Good and reliable separation of the drug was repaired through the validated C18 column and the HPLC settings (Rao, et al., 2022).

Reliability: The decision to use generic dry chemicals like borosilicate glass vials and nylon filters did not allow contamination or loss of analytes making the results credible.

Standard Drug Preparation for Optimization Protocol:

The drug 2-amino, 3-hydroxy anthraquinone was prepared with strict adherence to a validated protocol:

1. **Stock Solution Preparation**

A 10 mg quantity of the drug was dissolved in a mixture of 70% Methanol and 30% Acetonitrile (ACN). Methanol and ACN were chosen because they do not interfere with the stability of the compound throughout preparation and storage.

2. **Concentrations Prepared:**

The stock solution was diluted to achieve range concentrations of 20µg/mL, 40µg/mL, 60µg/mL, 80µg/mL, and 100µg/mL for a working solution. This range was determined based on the drug detection limit and suitability of the HPLC system (Mattiuzzi & Lippi, Current Cancer Epidemiology, 2019).

3. **Storage Conditions:**

The prepared stock solution and working concentrations were put in amber vials with a view of preventing the photodegradation of the drug. These vials remained stored in the refrigerator at 20- 40°C to achieve a steady state up to the study period. Amber vials can cut off the light factor more effectively, and light has an adverse impact on the chemical formation of the drug.

Other Reagents and Chemicals

All the chemicals, used in the present work were of analytical grade and may be utilised for HPLC analysis. These included:

Methanol for Gradient (HPLC-Grade):

Methanol was also employed as the mobile phase in the HPLC analysis, and for dissolving the drug substance. It also had high purity to cause or interfere with the HPLC runs.

Acetonitrile for Gradient (HPLC-Grade):

Therefore, Acetonitrile was chosen since it is a solvent with low viscosity for the flows in the HPLC system. Due to its compatibility with the drug and mobile phase, it was a necessary component of the procedure. The drug concentrations were determined using high-performance liquid chromatography HPLC. The mobile phase and chromatographic conditions were optimized and validated to achieve accurate and reproducible results:

Mobile Phase Composition:

In the mobile phase, MeOH formed 70% and ACN 30%. This combination was chosen since it provides the best baseline resolution and suitable peak shape of 2-amino, and 3-hydroxy anthraquinone.

Flow Rate:

The flow rate was held constant at 0.6 mL/min so that the drug would be well eluted from the column while other factors did not allow more pressure to build on the column.

Column Specifications:

A C18 reversed-phase column with 5-micron particulate matter was employed, measuring 4.6 x 250mm. This type of column is suitable for separating compounds with similar characteristics and providing reproducibility of the drug's retention time.

Sample Preparation for HPLC:

Firstly, a stock solution was prepared by dissolving 10 mg of the drug in 10 mL of a solvent mixture (70% methanol, 30% acetonitrile). From this stock solution, five different concentrations were prepared: 20 µg/mL, 40 µg/mL, 60 µg/mL, 80 µg/mL, and 100 µg/mL. Each prepared concentration was transferred into 2.0 mL screw-capping HPLC vials. These concentrations were then injected into the HPLC, with each concentration being run three times for analysis.

Every solution was prepared to the standard meant to eliminate any variations. The solutions were first passed through filter paper to eliminate any debris that may affect the HPLC results. The solutions were filtered and after filtration, the solutions were to different clean and appropriately labelled HPLC vials to avoid confusion. As soon as the vials were ready, they were placed into the HPLC. To obtain such reliable values, each vial was analysed three times under the same conditions. The peak heights, retention time, and peak areas from the runs were obtained and archived for further use in future analysis. This approach provided data for all the prepared concentrations with a high degree of correctness depending upon the specific

concentration of the solution.

Figure 7 Laboratory equipment and materials used for High-Performance Liquid Chromatography (HPLC) analysis, including Agilent-certified vials, syringe filters, centrifuges with samples, and an HPLC system setup.

2.4 Treatment Protocol and Division of Animals

This treatment schedule for the study consisted of the pharmacokinetic, tolerance and risks associated with toxicity of 2-amino, 3 hydroxy anthraquinone. Three different dosing regimens were used and within each protocol, all the dosing times were selected with utmost care so that valid data could be obtained without compromising animal safety.

2.5 Preparation of Drug and Stock Solution (in Vivo Studies)

The staircase method was followed to prepare doses of 50 mg/kg, 100 mg/kg, 200 mg/kg and 500 mg/kg. While dosing, no mice were killed. The dose of 200 mg/kg was selected based on some limitations of safety considerations. This dose was dissolved in 4% DMSO and the final volume was brought forward by normal saline for injection in the animals.

For this study, eight groups of mice were created. The first schedules of groups were five groups received the 200 mg/kg dose at different time points, 30minutes, 2 hours, 6 hours, 18 hours and 24 hours. In all the experiments, all the groups were dosed at the same time. The behavioural analysis for each group was then made to assess the effects of dosing, and post-dosing. Blood samples were collected after each time point: for 30 minutes, 2 hours, 6 hours, 18 hours 24 hours respectively.

Another group of IV 3-day dosing received 200 mg/kg while blood samples were collected on the 3rd day. Further, a group was administered IP dosing for 7 days and blood samples were collected on the 7th day. When the blood samples are taken in plasma vials from all 3 protocols (IV one day, IV 3 days and IP seven days) plasma vials are then centrifuged, plasma extracted and then added deproteinized, get the supernatant layer and dilute this layer with Methanol, ACN and then filter. A CBC test was conducted during the dosing period of the week, and blood samples were taken before and after dosing for seven days.

Single-Day IV Dosing Protocol:

In the single-day IV dosing protocol, the drug was given as a bolus injection in the tail vein, at a concentration of 200 mg/ kg. Dosing was conducted at 8: Sample preparation was done at 4:00 a.m. to help control for variability caused by circadian rhythms, which are likely to affect the rate of metabolism and pharmacokinetics of most compounds. Following administration, blood samples were collected at five specific intervals: at 30 minutes, 2 hours, 6 hours, 18 hours and 24 hours post dosing.

Discovery of dose was accomplished through testing on mice at 50, 100, 200, 300 and 500 mg/kg of the drug. Specifically, no animals died at any of these doses hence suggesting a relatively high safety margin. Incorporating these findings, 200 mg/kg was selected for

subsequent pharmacokinetic dose and toxicological assessment because this dose was proven to yield optimal

effects with a low toxicity level. These considerations made the approach to both wavelength and dose selection testable, reproducible, and appropriate approaches to HPLC analysis and subsequent dosing protocols that would generate accurate information for assessing the drug's pharmacokinetic and safety profiles.

For the single-day IV dosing the drug was made by dissolving 200 mg of the compound in 4% DMSO diluted with normal saline in an equal ratio. This guaranteed that the drug was well in soluble form and safe for infusion into the patient's body. The dose was administered as a bolus injection via the tail vein of the mice at 8: 00 Thus, observations before are made to minimize variations that are prone to occur due to daily body cycles called circadian rhythms.

Following administration, mice were divided into groups corresponding to specific time intervals for blood collection: Half an hour, two, six, eighteen and twenty-four hours of continuous painting. The three mice were grouped together and all the groups were given the dose at the same time. At these time points, mice from different groups were sacrificed and their blood was taken using vials.

For the 30-minute group, blood was collected by the retro-orbital sinus technique at the time of euthanasia. The collected blood was aliquot into the clean vial and spun on a centrifuge at 6,000 rpm for 10 minutes to pellet down the plasma. The upper clear layer was pipetted out by transferring it into Eppendorf tubes known as the supernatant. The Plasma was then recently centrifuged for another two minutes to make certain that the sample was thoroughly separated and clarified. The plasma was then deproteinized by the addition of an equal volume of ACN.

The resulting mixture was then centrifuged at 6000 rpm for 5 minutes, the supernatant was then further diluted, filtered and 1 ml was pipetted into a separate HPLC vial.

The same process was followed in the 2-hour, 6-hour, 18-hour and 24-hour groups; blood samples were collected and prepared in the same manner. The HPLC system was employed in the analysis of the samples with the drug concentration in plasma highlighted for each corresponding time point depicted by a peak.

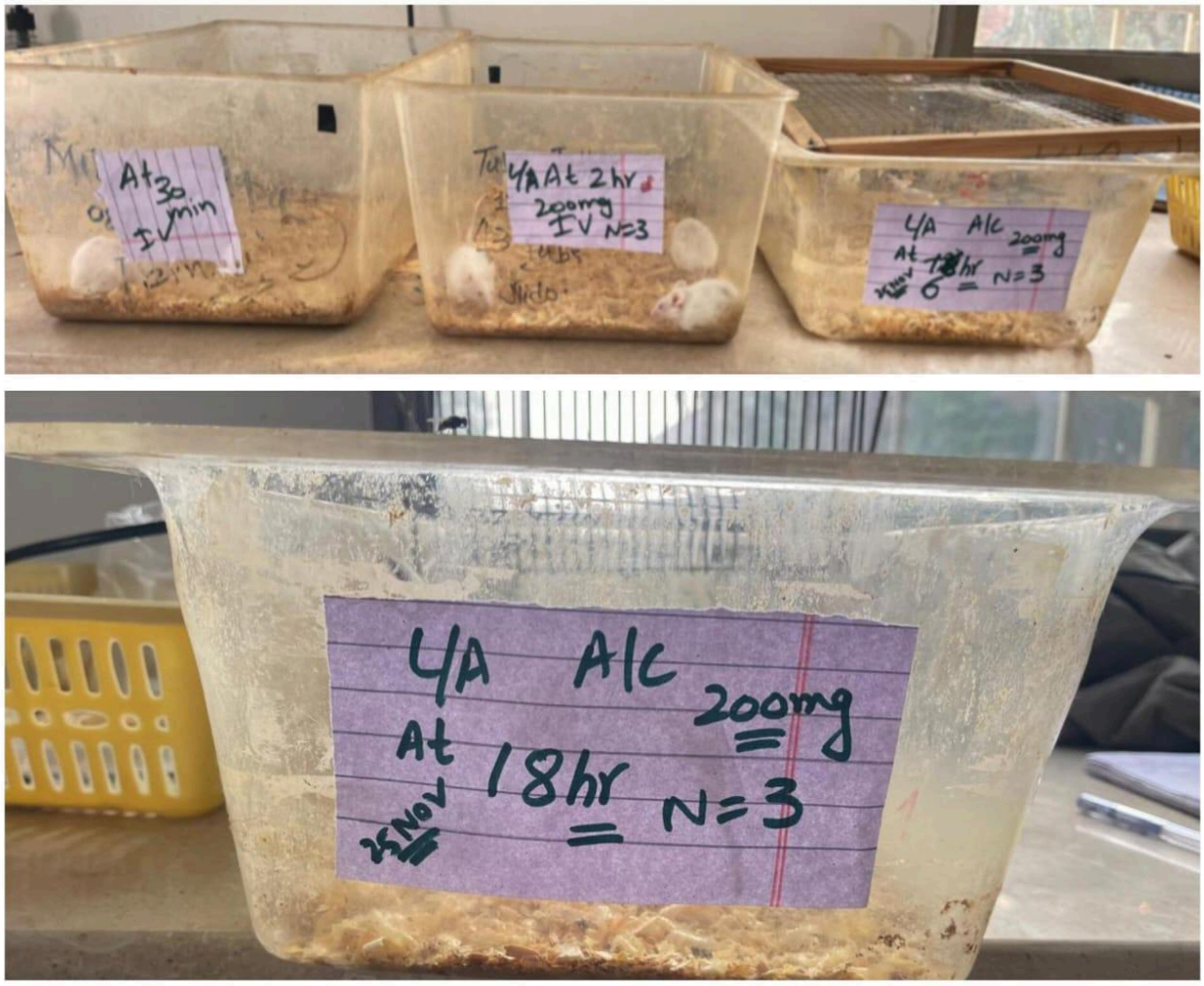

Figure 8 Single Day IV dosing for different time intervals of: 30 min, 2hr, 6hr, 18hr

Three-Day IV Dosing Protocol:

In the three-day IV dosing protocol, there was also used the same technique of the drug preparation: 200 nm of the compound was dissolved in 4% of DMSO and normal saline. The dose

was administered intravenously via the tail vein at 8:00 a.m. The principle variation in this protocol was the evaluation of the top line of cumulative effects as well as any variations in pharmacokinetics as a result of dosing reiteration. The samples were collected on the 3rd day.

Seven-Day IP Dosing Protocol:

In the seven-day dosing regimen the drug was given by intraperitoneal injection to prevent problems with injecting the material intravenously such as a puncture or scaring of used veins. A dose of 200 mg/kg was also dissolved in the same fashion as IV protocols and was injected for 7 consecutive days. Pre- and post-treatment blood samples were taken on Day 1 and Day 7 for estimation of drug accrued exposure and toxicities.

The first set of assays was performed on day 1 to determine the baseline values of the blood taken from mice before dosing. The pharmacokinetic profile and other effects attributable to the drug itself were determined on Day 7 after the last dose, at which time blood samples were collected. Plasma samples were processed following the same protocol: Included processes are filtration, deproteinization, dilution and also accompanied by centrifugation. These samples were then subjected to HPLC to document the drug peaks as well as quantify the concentration of the drug.

2.6 HPLC Analysis

Employing the composition of 70% Methanol and 30% Acetonitrile (ACN), we got a good flow of the samples during the HPLC analysis and got reasonable and significant peak resolutions. The flow rate for the column was kept at 0.6 mL/min which was optimized during

elution and has provided optimum peak shape. The optimal wavelength for detection was chosen using the staircase method where many different wavelengths were examined. The first samples were analysed using 420, 450, 480, 500 and 520 nm wavelengths. The higher intensity, area and height of the peaks were recorded in 480 nm, which has been selected for all further analysis. This

approach was ideal in providing the highest sensitivity and selectivity for the determination of the drug in plasma and serum matrices.

Blood Collection and Volumes

Blood samples were collected by retro-orbital sinus method, this method helped me collect small volumes at a very fast rate without the DNA getting lethal. The amounts of harvested blood ranged between 20-100 microliters since the amount of blood required for confirming call analysis varied. Whilst spiking, special precautions were taken not to excessively bleed the mice, based on their weight which could cause physiological stress.

Behavioural Studies

Observational behavioural tests were done before dosing and post-dosing to check for the existence of toxicity or side effects of the drug. Incorporation of these tests proved quite useful in understanding changes that occurred in motor activity, anxiety, and behaviour. Two validated tests were employed:

Open Field Test (OFT):

The OFT was employed in order to assess the locomotor activity and anxiety-like behaviour in mice. The test of animal behaviour consisted of putting an animal into a square enclosure and defining the time to move in it.

Figure 9 a. Motor activity monitor used to assess locomotion, detecting SM/FM and SR/FR readings; b. An open-field test conducted for anxiety

Inverted Screen Test:

This test was used to determine the relative torque for muscle strength and muscle coordination. Mice were put on DMAs the ability to grasp and locomote was tested on an inverted wire mesh grid. The amount of time they were able to stay on the grid without tripping was noted down. Abnormal movement or reduced grip can therefore show neuromuscular side

effects or sedation due to the drug. These behavioural tests were done together with the pharmacokinetic and toxicological results to give the overall efficacy of the drug to the animals.

Ethical Problems and Control:

All the procedures were done according to the institutional animal ethical permits. During the study, all the animals were observed to note discomfort, adverse effects or behavioural changes among the animals. This complimented health assessment checks on specific parameters such as body weight, activity and feed intake patterns daily. Any signs of untoward effects were observed when the animals were euthanized accordingly to minimize suffering (Mylène, et al., 2021).

The treatment protocols and sampling schedules were developed to yield good quality data, yet meet the principle of the '3Rs' of using laboratory animals; Replacement, Reduction, Refinement. This way, the cacuminal pharmacokinetics, safety, and tolerability assessment of the drug was done through the use of both short-term and extended dosing regimens.

2.7 Complete Blood Count (CBC) Analysis

Pre- and Post-Dosing CBC

The study revolves around the complete blood count (CBC) analysis for evaluating the prospective haemato-augmenting effect of the drug administered intraperitoneally (IP). Blood samples were then collected from the experimental group mice at 2 different time intervals: Day 1 pre-dosing and Day 7 post-dosing (of continuous seven days IP dosing). This afforded a comparison between the blood parameters of the mice before and after administration of the drug enabling valuable insights into the drug's impacts on health concerning haematology.

On Day 1, blood samples were taken from the mice for the baseline values of the major blood parameters. Blood samples were again taken on Day 7, after seven consecutive days'

administration of 200 mg IP dose, to check for variations in blood parameters. The study aimed to

identify any signs of haematological toxicity or bone marrow suppression caused by the drug and other changes associated with the drug administration in the blood composition (Schiliro & Firestein, 2021).

Parameters Analysed

The following blood parameters were analysed in terms of CBC analysis concerning the physiological response of the selected drugs.

Red Blood Cell (RBC) Count

The RBC count was important in determining the effectiveness of the mice's blood in transporting oxygen and maintaining normal circulation. The effect of the drug on RBC count could be noticed in cases where the mice were exposed to high doses of the drug through IP injection, between 200 mg for 7 days. RBC counts were very closely monitored over time to capture any changes which may suggest anaemia or any other form of dysfunctional RBCs. There was no significant decrease in RBC mean counts between pre-dose and post-dose suggesting that the administered drug does not inhibit the mice in terms of erythropoiesis or haemolytic reactions. The RBC counts were within the normal ranges for female mice and therefore were not considerable effects of the drug on oxygen transport capacity.

White Blood Cell (WBC) Count:

The levels of WBC were evaluated to establish the response of the immune system to the drug. Elevated levels of WBC indicate that there is an inflammatory process while low levels indicate immune suppression. In this study, it was found that WBC increased moderately after seven days of IP dose exposure, which is an indication of slight inflammation or perhaps the

effects of an immune response toward the drug. The increase, however, was not adequate to indicate marked toxicity or even infection. As evidenced by the study, the increase in WBC counts falls within a permissible range in female mice, with no apparent signs of high immune suppression or infection (Baade, Youlden, Kimlin, Aitken, & Biggar, 2024).

Level of Haemoglobin:

To evaluate the influence the drug experts on the oxygen-carrying potential of the blood, haemoglobin levels are monitored. The haemoglobin concentrations remained constant over the entire study period, without any significant drop noted in the post-dosing samples. This reflected no haemolysis or marked alterations in the function of red blood cells induced by the drug. Furthermore, the fact that haemoglobin experienced no significant drops bolstered the suggestion that the drug did not produce toxic effects on bone marrow or red blood cell production in the study period (NIH Cancer, 2024).

Platelet Count:

Platelets are mainly responsible for blood clotting and, thus any significant change in the count may indicate some bleeding or clotting disorder. Counting of platelets was done to check any possible incident that causes thrombocytopenia or thrombocytosis due to the study drug. Platelet counts were consistent for the entire duration of the study, without any significant difference pre- and post-dosing. This implies that the study drug did not interfere with platelets' production or their function, while no bad effect on blood clotting was noted (Michaeli, Michaeli, & Michaeli, 2023).

Equipment's Used:

The specialized analyser specific for CBC work has been calibrated by the analyser for rodent blood samples. According to the specialized analyser, the CBC will give precise readings

on the RBC, WBC, haemoglobin, and platelet counts. For all of the 1-day and 7-day-old mice, blood samples were all collected according to the protocol for minimum invasiveness-20 microliters to 100 microliters-from the eye of each mouse. These were then analysed in a machine using settings suitable for small rodent blood volumes so that results were both accurate and reproducible. The analytical machine is set to provide high results in terms of accuracy and reproducibility with small blood volumes collected from female mice. The samples were then run through the machine shortly after collection to avoid degradation of any blood components. The CBC analyser also suited the haematological variation due to treatment in female mice and gave data that would allow full assessment of the effects of the drug under study on these blood parameters during treatment.

Histopathology of Different Organs of Mice:

The subsequent section was devoted to the histopathological assessment of important target organs in mice the heart, liver, and kidneys. Histopathological examination is among the imperative criteria used for assessing both the therapeutic and toxic effects of drug candidates during preclinical studies. Histological analysis is one of the procedures that include the exposure of a tissue sample to microscopy use for the determination of structural and functional alteration induced by the test drug. This paper aims to evaluate the impact of intravenous injection of a test drug for seven consecutive days in female mice. Subsequently, biopsies of the liver, heart and renal tissues were taken for microscopical studies. These tissues were viewed under 10X and 40X to determine the differences between the normal tissue architecture with the ones that the drug could compromise. Other general areas looked at were: the shape and size of the cells observed; inflammations present; necrosis; fibrosis or any other abnormalities.

The objective of the study's outcomes was to identify if the drug caused toxicity or any other unwanted effects in those organs which are crucial to evaluate the safety of the compound. It also assisted in assessing the therapeutic effectiveness of the medicine so that without risk it can further be brought in clinical trials. Thus, the results of the study contribute the foundation for describing the damages and any adverse effects if they occurred during the experiment and distinguishing optimized dosages during human testing. Such a detailed assessment of the tissue integrity so contributed to laying down the relied drug for future therapeutic used.

Chapter 3: Results

3.1 Standard Tests

Interpretation of Figure 7: Peak Area vs. Concentration

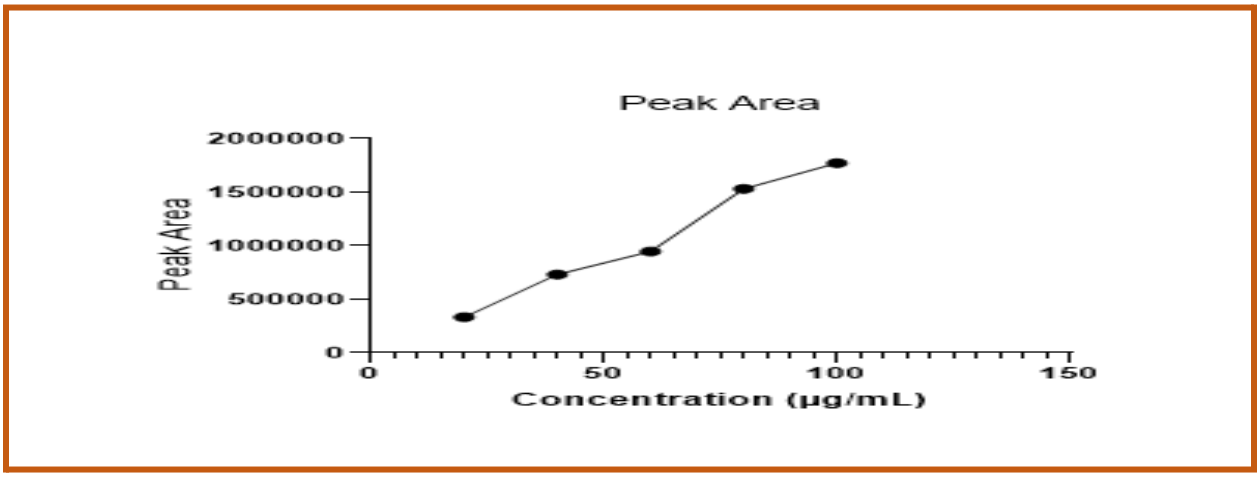

Figure 10: A positive linear relation is depicted in the graph between concentration (µg/mL) and area of peak, where progressive changes can be observed in higher peak areas at higher concentrations. This trend indicates a direct relationship between the two variables

Figure 7 depicts the area of the peak corresponds with the concentration of the sample that was analysed. When the concentration is increased from 20 µg/mL to 100µg/mL, the peak area increases in the same order hence it can be deduced that the two characteristics have a well-established physical relationship which is linear. The peak area values of 20µg/mL are approximately 398535-402143 and these values are higher with every doubling of concentration as the concentration increases to 40 ml, the peak area ranging from 732840-793234. Likewise, the average peak area increases to 951633 at 60 µg/mL for all three runs. The largest peak areas are recorded at the highest intensities of 80µg/mL is 1589166 and for 100 µg/mL on an average is 1688761. The steady increase in target concentrations and signal intensities for chromatographic analysis supports the hypothesis that increased concentrations correlate with signal intensities, indicating accurate analytical methods.

Interpretation of Figure 8: Peak Height vs. Concentration

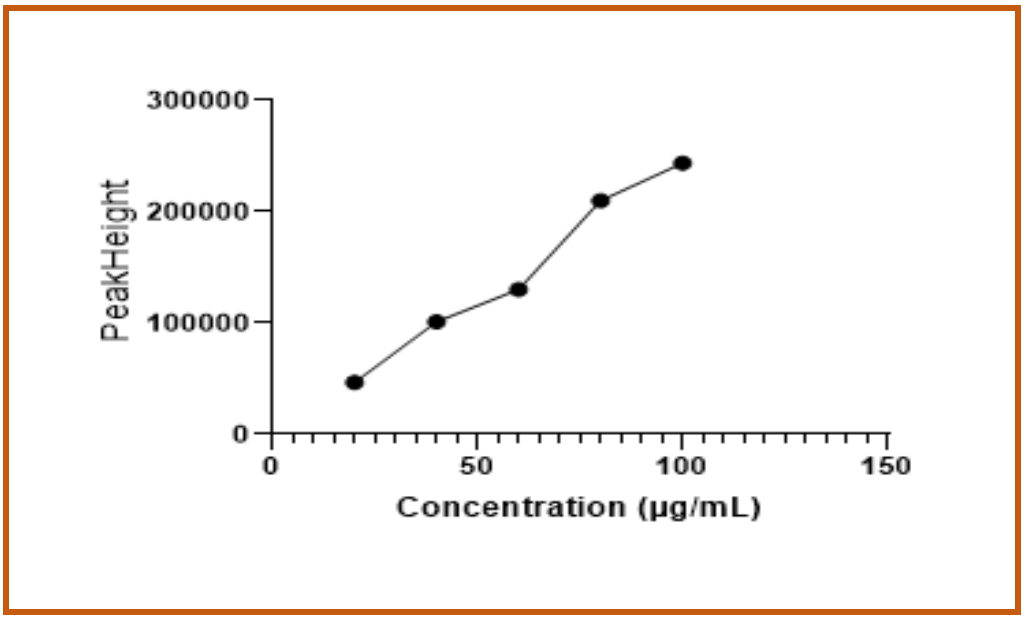

Figure 11: The graph shows a positive linear correlation between concentration (µg/mL) and height, in which the height increases with increasing concentrations. Such a trend suggests that it is proportional as expected

Figure 8 illustrates the variation of the peak height with respect to the actual concentration of the samples in the solution. When the concentration increases from 20 µg/mL to 100 µg/mL, the height of a peak substantially increases. The peak height decreases to a low signal strength of between 46897 and 54911 at 20 µg/ml. showing a relatively low signal strength at this concentration. When the concentration has reached 40 µg/mL the peak height approaches 101470 to 108941. As for 60 µg/mL the values are even higher, the average peak height is approximately 130653. These peak heights are assessed at 100 µg/mL and the peak heights ranges from 227081– 243806.

The current graph also corroborates with the previous results and stresses the fact that increased concentrations result in improved signal intensity, which is beneficial in quantitative evaluations. This relationship is especially valuable when investigating concentration-dependent

drug responses as seen in cancer treatments; peak height measurements can give direction to drug effectiveness and dosage adjustments.

3.2 Optimization Protocol

Standard Graph at 20mcg

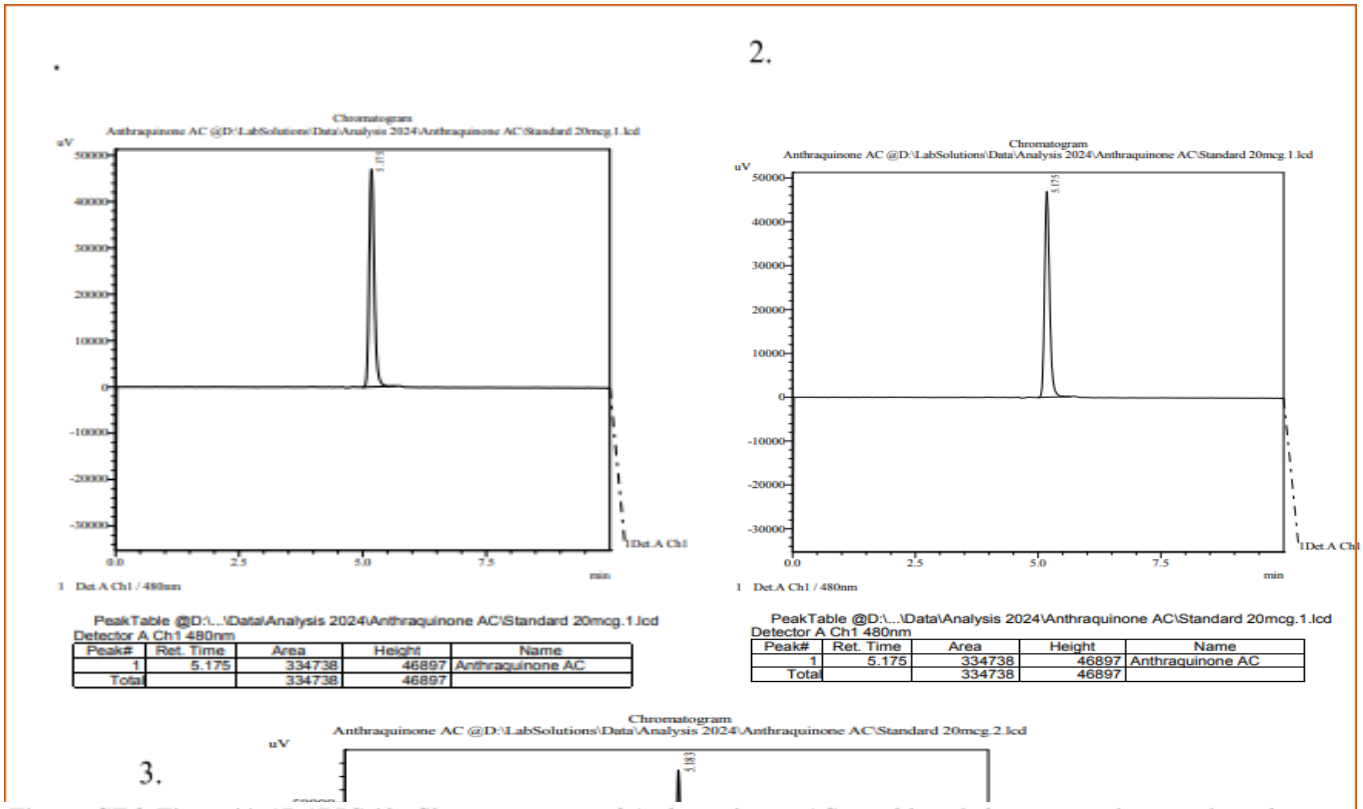

Figure SEQ Figure * ARABIC 12: Chromatograms of Anthraquinone AC at a 20-µg/ml concentration consistently showed a single peak with a retention time of 5.175 minutes. Peak areas varied, with the first at 334738 and the third at 398535. The method demonstrated specificity to Anthraquinone AC, with no interference from other compounds, confirming the stability and reliability of the analytical procedure

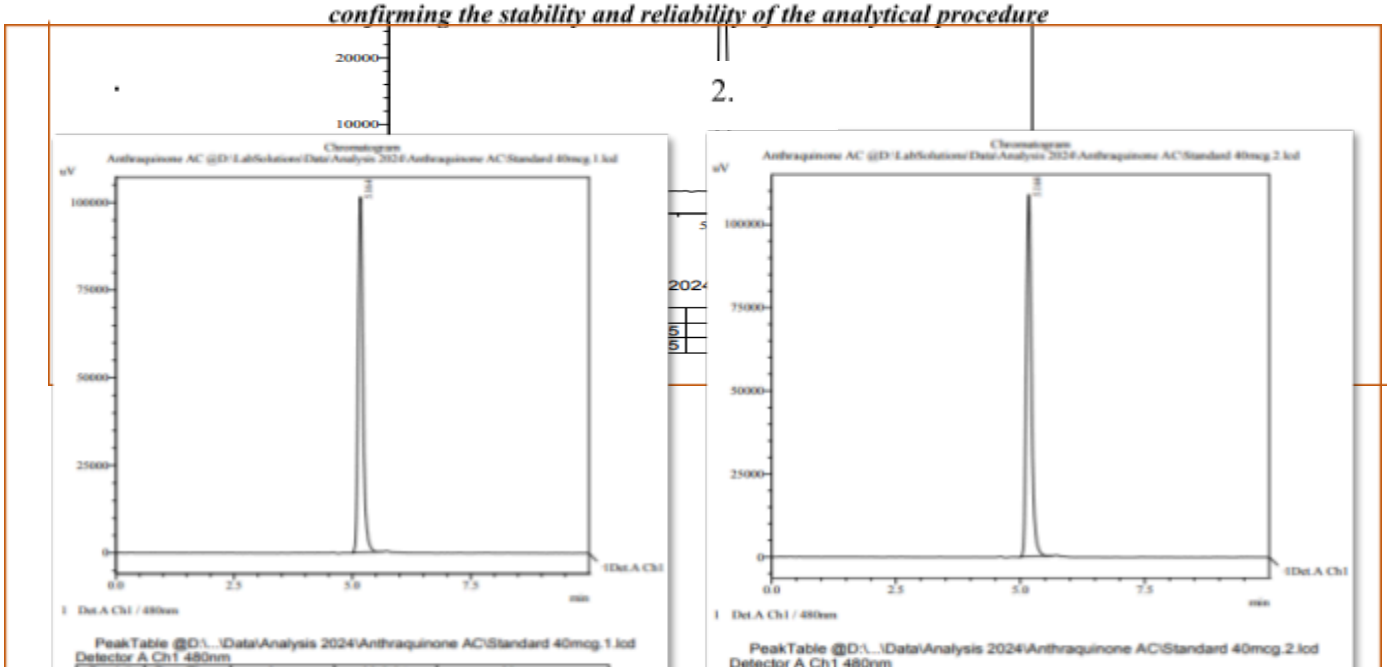

3.

Figure SEQ Figure * ARABIC 13: Chromatograms of Anthraquinone AQ at 40µg/ml concentration showed a single, consistent peak AQ across all graphs. The retention times were 5.164 minutes in all three peaks with an area of 793235. The method was specific to Anthraquinone AQ and did not detect interference from other compounds. The results confirm the stability and reliability of the analytical procedure

Standard 60mcg:

.

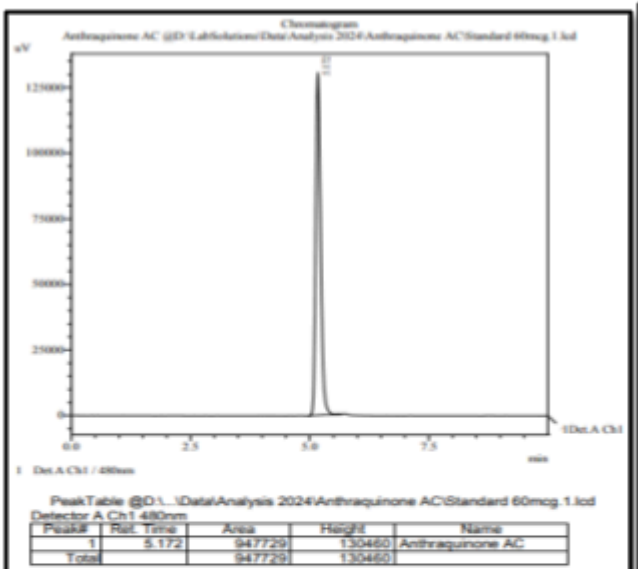

2.

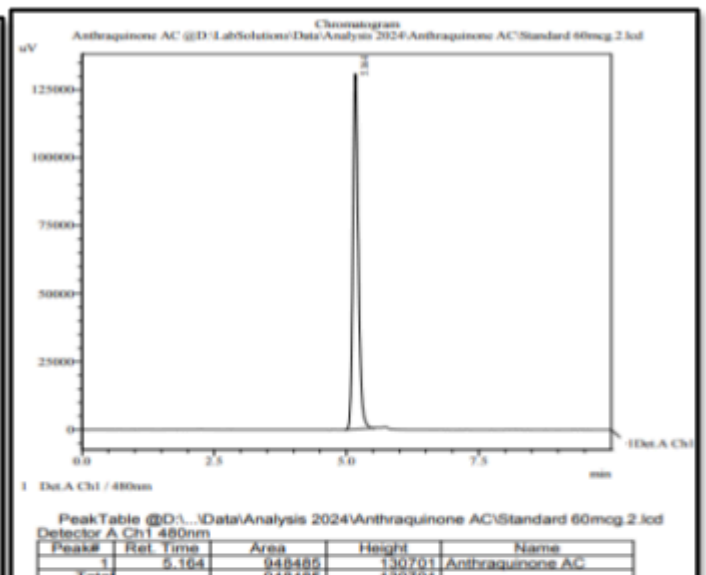

3.

Standard 80mcg:

.

2.

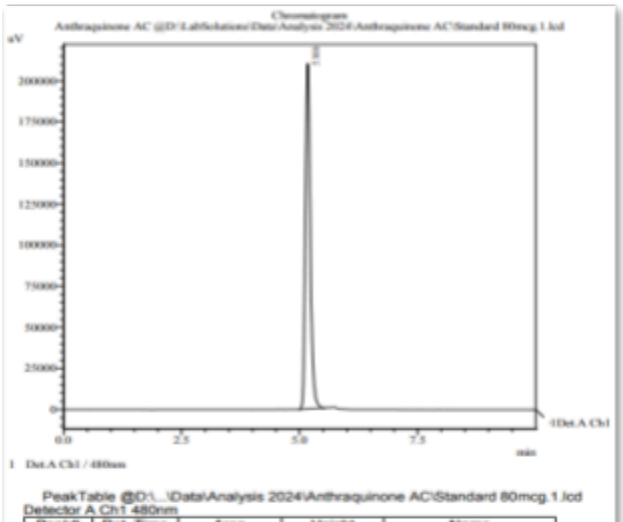

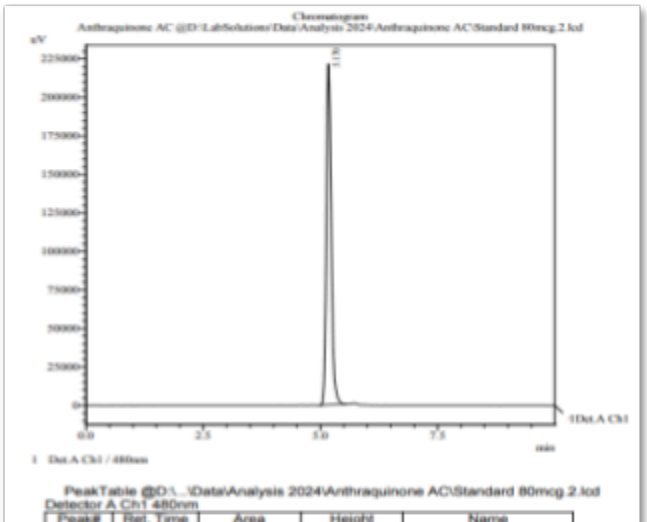

3.

Standard 100mcg:

.

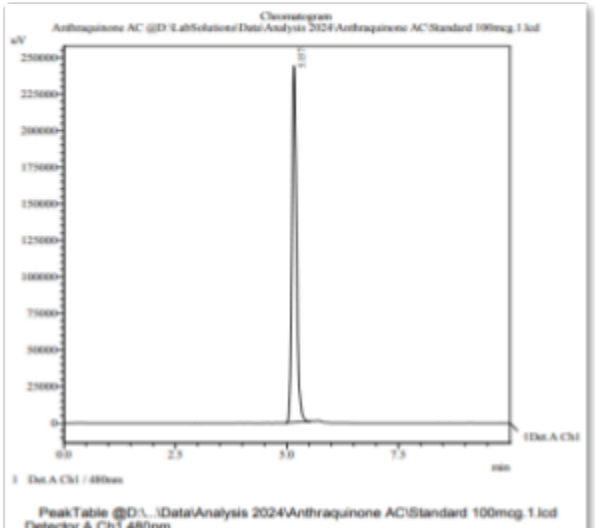

2.

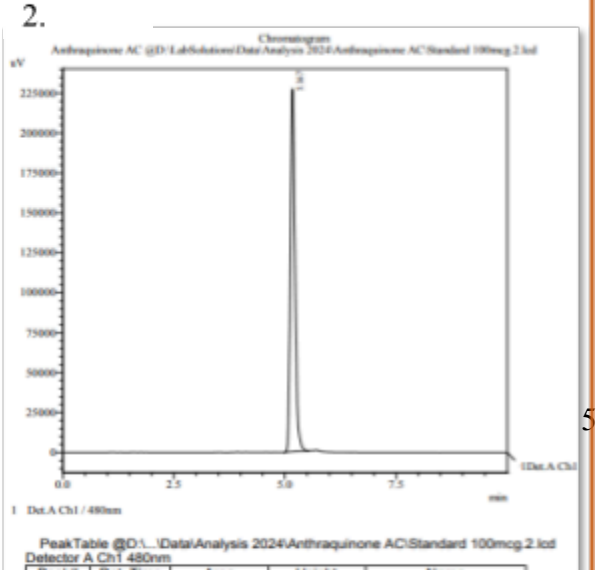

3.

*Figure SEQ Figure * ARABIC 16: This signifies a 100 µg/ml concentration. The presence of the drug is shown by a clear peak, and reliable and repeatable results are indicated by retention durations of 5.157 and 5.167. Peak 1 area was 1771757, peak 2 area was 1645802, and the third peak area was 1650724. The existence of the drug is confirmed by the presence of a distinct peak and stable chromatographic conditions, including temperature, flow rate, and column type*

3.3 Blank Plasma Analysis

Interpretation of Plasma:

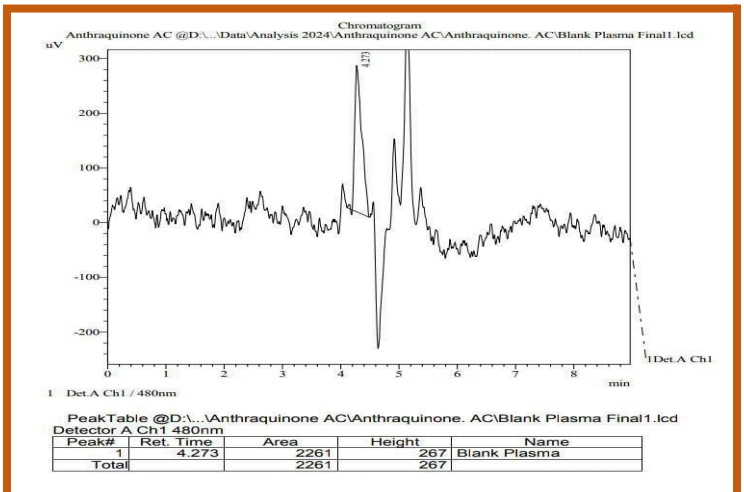

*Figure SEQ Figure * ARABIC 17: The chromatogram shows a sample analysis of plasma from blood derived from healthy mice, with no drug present and puff peaks representing plasma components only. The 4.273 min peak has an area of 2261mVs*

The blank chromatogram of plasma has only one peak with the retention time of 4.273 min, peak area is 2261 and peak height is 267. This is suggestive of only minimal internal contamination, thus ruling out substantial background activity and relative selectivity of the technique. This characteristic of the blank matrix being devoid of multiple peaks leads to its clearance for further analysis of either spiked or real samples.

Interpretation of Peak Area and Height for 30min-7 days:

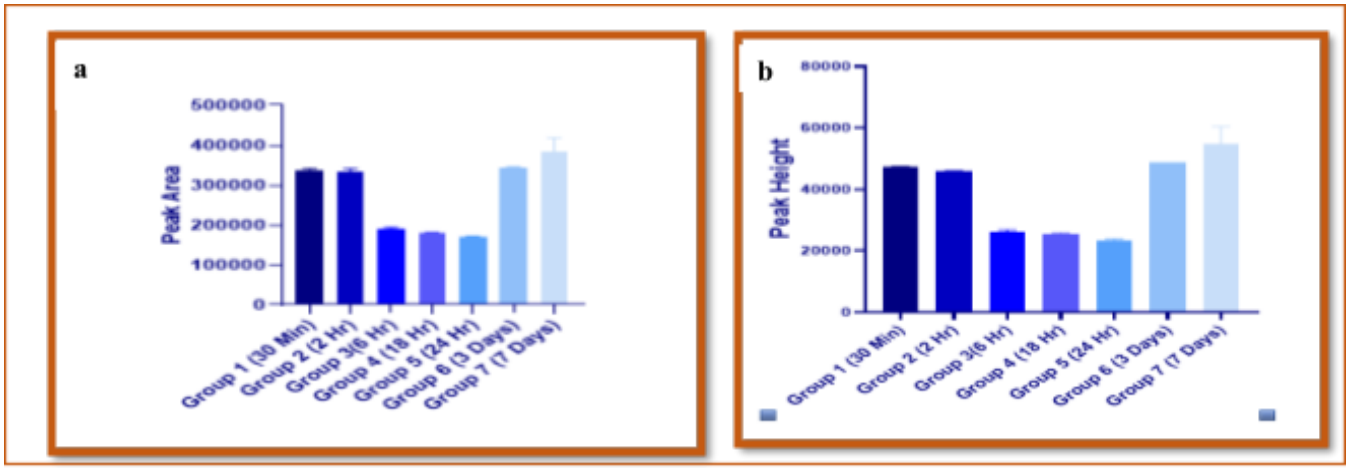

HPLC analysis of samples of plasma derived from six groups of animals treated with the drug at different time intervals is shown in Figure 15.

(a) Area Under the Curve (AUC): The bar graph analysis shows that moderate to high concentrations of the drug were detected in the plasma samples collected at 30 minutes and 2 hours after the administration with relatively low concentrations detected at 6, 18 and 24 hours. At 7 days, the concentration of the drug was visible as can be seen in the graph.

(b) Peak Height: Likewise, values of the maximum heights of the plasma drug concentration also corresponded to the AUC findings. The maximum peak heights were

measured at 30 minutes and 3 hours and indicated that most of the drug was present at those times.

3.4 Drug Analysis at Different Time Intervals

30 min:

.

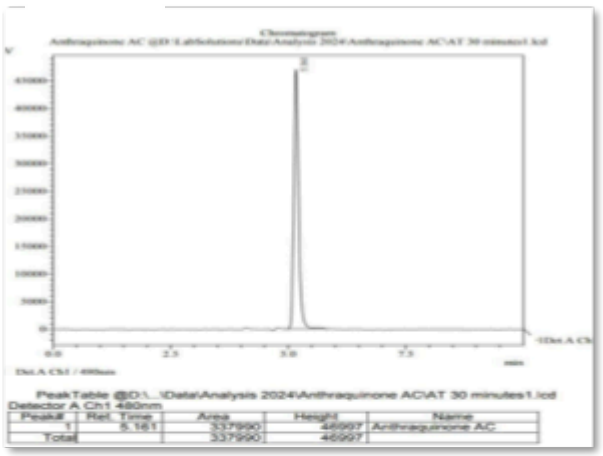

2.

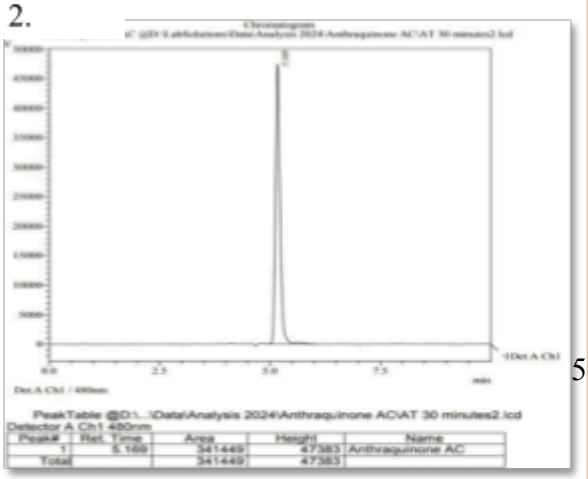

3.

Figure SEQ Figure * ARABIC 19: The chromatogram shows a single peak corresponding to Anthraquinone AQ at 30 minutes, with a retention time of 5.161 minutes. The difference occur in peak times is dependent on area. In the first peak the area was 46997 whereas in second and third peak, the area was 341449mVs

2 Hr:

.

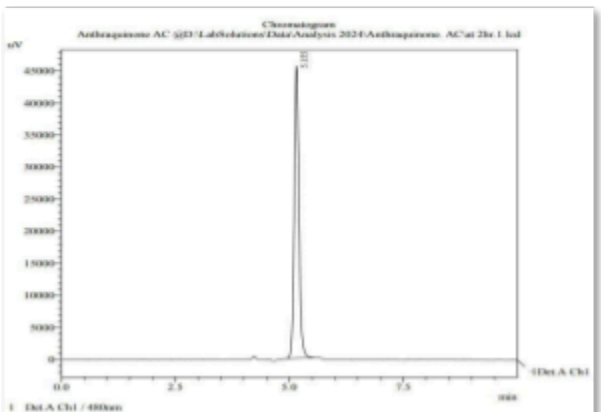

PeakTable @D:\LabSolutions\Data\Analysis 2024\Anthraquinone. AC\at 2hr.1.lcd
Detector A Ch1 480nm

Peak#	Ret. Time	Area	Height	Name
1	5.155	326707	46581	Anthraquinone AC
Total		326707	46581	

2.

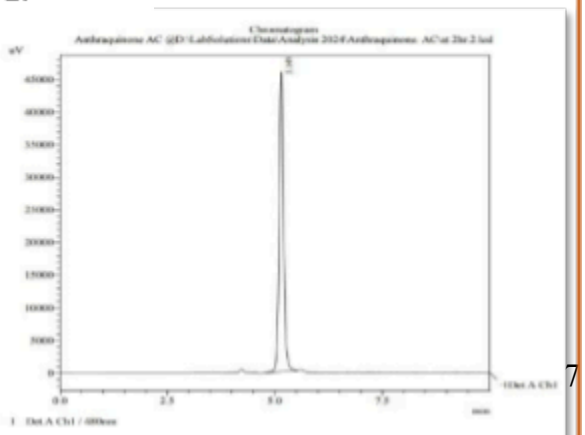

PeakTable @D:\LabSolutions\Data\Analysis 2024\Anthraquinone. AC\at 2hr.2.lcd
Detector A Ch1 480nm

Peak#	Ret. Time	Area	Height	Name
1	5.149	332910	46896	Anthraquinone AC
Total		332910	46896	

3.

*Figure SEQ Figure * ARABIC 20: The chromatogram at 2 Hrs shows a single peak corresponding to Anthraquinone AQ with a retention time of 5.155 minutes. At peak one, the area was 326707mVs, in the second peak the area was 33291, and in the third peak area was 342089mVs.*

6Hr:

.

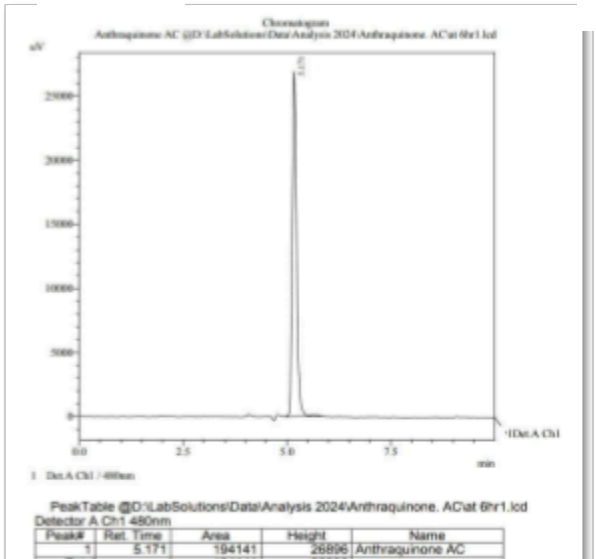

PeakTable @D:\LabSolutions\Data\Analysis 2024\Anthraquinone. AC\at 6hr1.lcd
Detector A Ch1 480nm

Peak#	Ret. Time	Area	Height	Name
1	5.171	194141	26896	Anthraquinone AC

2.

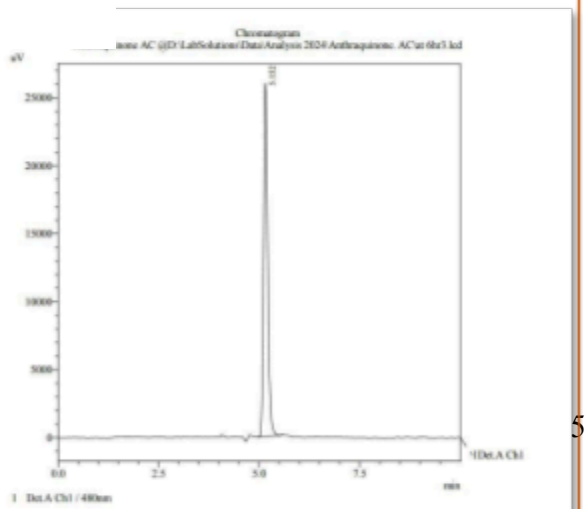

PeakTable @D:\LabSolutions\Data\Analysis 2024\Anthraquinone. AC\at 6hr3.lcd
Detector A Ch1 480nm

Peak#	Ret. Time	Area	Height	Name
1	5.152	183758	25978	Anthraquinone AC

3.

18Hr:

•

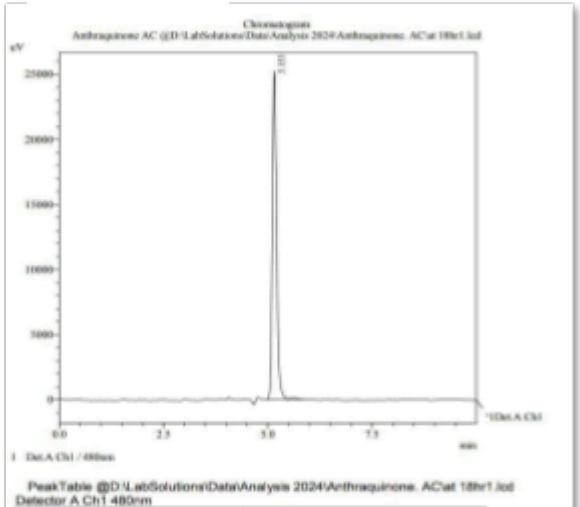
Chromatogram
Anthraquinone AC @D:\LabSolutions\Data\Analysis 2024\Anthraquinone. AC\at 18hr1.lcd
uV
25000
20000
15000
10000
5000
0
5.05
0.0
2.5
5.0
7.5
min
*1Det.A Ch1
1 Det.A Ch1 / 480nm
PeakTable @D:\LabSolutions\Data\Analysis 2024\Anthraquinone. AC\at 18hr1.lcd
Detector A Ch1 480nm

2.

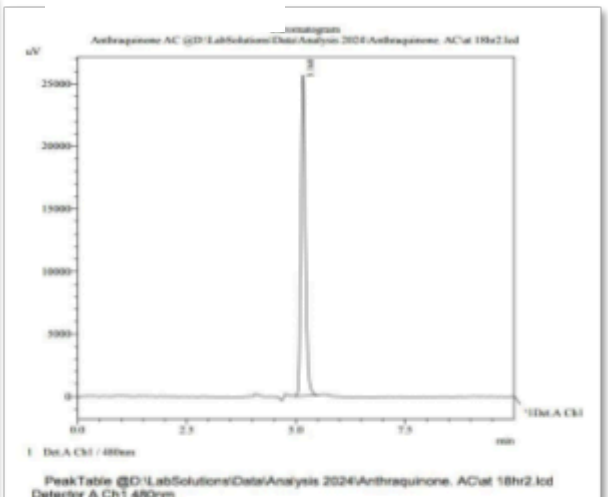
Anthraquinone AC @D:\LabSolutions\Data\Analysis 2024\Anthraquinone. AC\at 18hr2.lcd
uV
25000
20000
15000
10000
5000
0
5.05
0.0
2.5
5.0
7.5
min
*1Det.A Ch1
1 Det.A Ch1 / 480nm
PeakTable @D:\LabSolutions\Data\Analysis 2024\Anthraquinone. AC\at 18hr2.lcd

3.

24Hr:

.

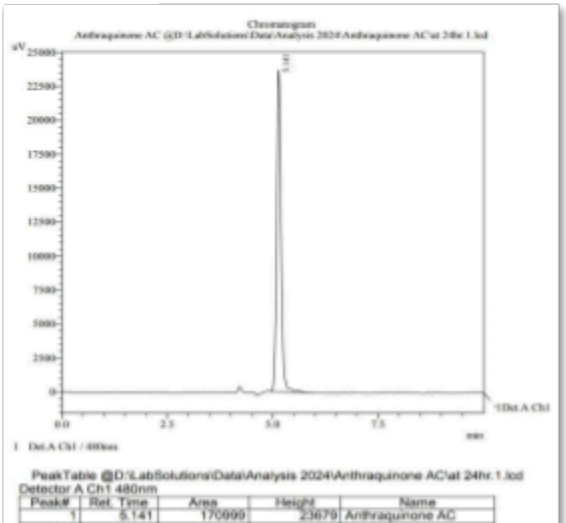
Chromatogram
Anthraquinone AC @D:\LabSolutions\Data\Analysis 2024\Anthraquinone AC\at 24hr.1.lcd
uV
5.141
1:Det.A Ch1
min
1 Det.A Ch1 / 480nm
PeakTable @D:\LabSolutions\Data\Analysis 2024\Anthraquinone AC\at 24hr.1.lcd
Detector A Ch1 480nm
Peak# Ret. Time Area Height Name
1 5.141 170999 23679 Anthraquinone AC

2.

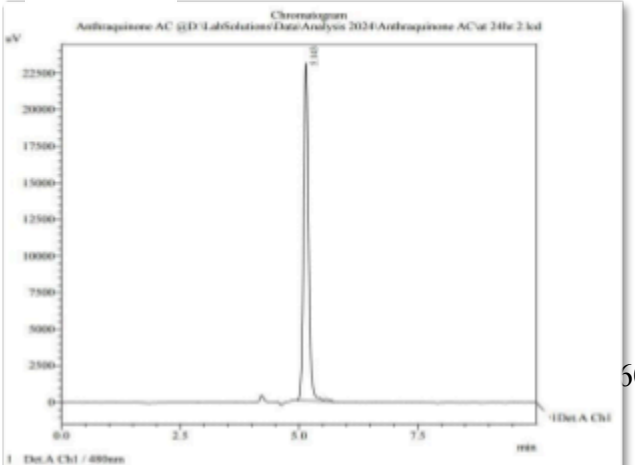
Chromatogram
Anthraquinone AC @D:\LabSolutions\Data\Analysis 2024\Anthraquinone AC\at 24hr.2.lcd
uV
5.140
1:Det.A Ch1
min
1 Det.A Ch1 / 480nm
PeakTable @D:\LabSolutions\Data\Analysis 2024\Anthraquinone AC\at 24hr.2.lcd
Detector A Ch1 480nm
Peak# Ret. Time Area Height Name

60

3.

3 Days:

.

2.

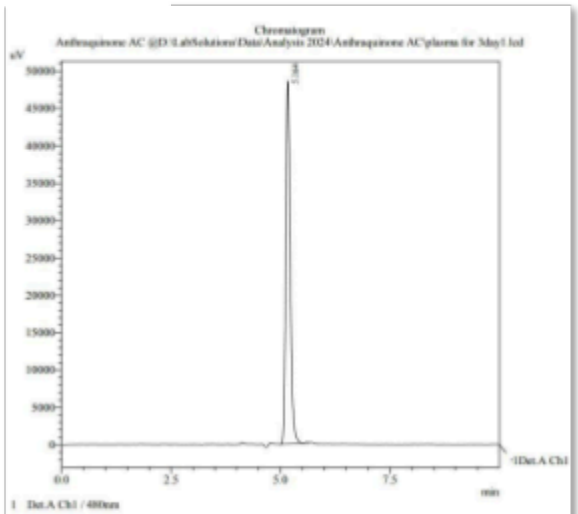
Chromatogram
Anthraquinone AC @D:\LabSolutions\Data\Analysis 2024\Anthraquinone AC\plasma for 3day1.lcd
mV
50000
45000
40000
35000
30000
25000
20000
15000
10000
5000
0
1
1Det.A Ch1
6.0
2.5
5.0
7.5
min
1 Det.A Ch1 / 480nm
PeakTable @D:\...\Data\Analysis 2024\Anthraquinone AC\plasma for 3day1.lcd
Detector A Ch1 480nm
Peak# | Ret. Time | Area | Height | Name

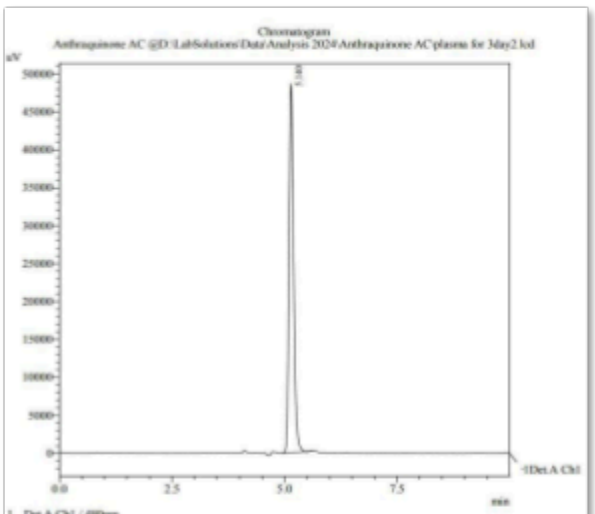
Chromatogram
Anthraquinone AC @D:\LabSolutions\Data\Analysis 2024\Anthraquinone AC\plasma for 3day2.lcd
mV
50000
45000
40000
35000
30000
25000
20000
15000
10000
5000
0
1
1Det.A Ch1
0.0
2.5
5.0
7.5
min
1 Det.A Ch1 / 480nm
PeakTable @D:\...\Data\Analysis 2024\Anthraquinone AC\plasma for 3day2.lcd
Detector A Ch1 480nm

3.

Figure SEQ Figure * ARABIC 24: The picture displays three Anthraquinone AQ chromatograms that were examined using a 480nm detector for 3 days. The molecule is consistently present in each chromatogram, which displays a single, identifiable peak. Peak 1 shows a retention time of 5.140mints. The area at peak 1 was recorded at 341354mVs, second peak area observed 341228mVs and the third peak area was recorded at 345801mVs

7 Days:

.

2.

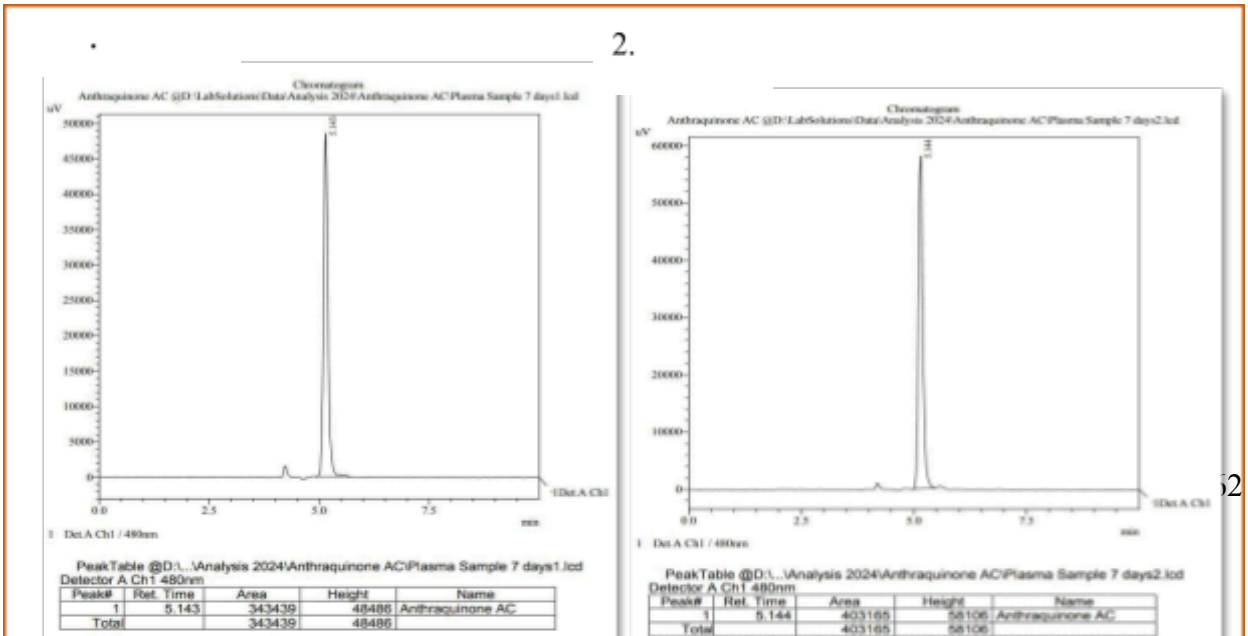

3.

.

Serum Sample for 7 Days

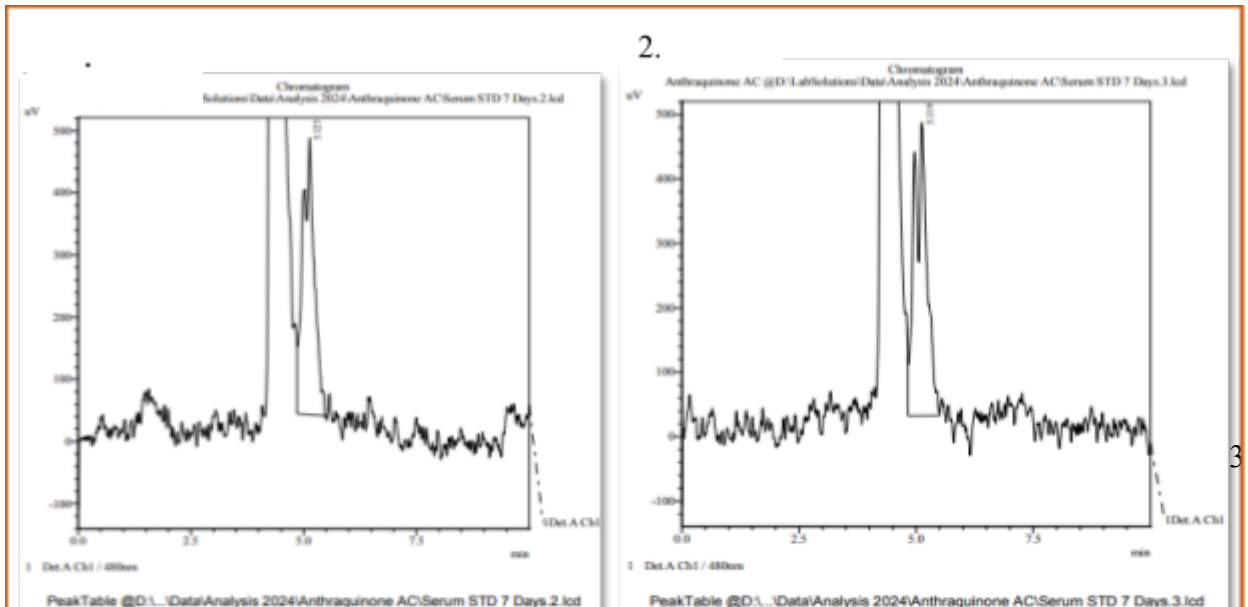

3.

Interpretation

Chromatograms provided here illustrate Anthraquinone AQ from the serum matrix after seven days of administration via the IP route. On the x-axis, the retention time in minutes is shown and the y-axis shows the detector response emphasizing the peak heights. The time taken detecting Anthraquinone AQ remains relatively close to 5.1 minutes across all the samples, the results are therefore stable and reproducible. Nevertheless, differences are registered in the peak area and other altimetrical parameters, regarding the assumed samples. The first graph indicates

an area of 8598 with a height of 453, the second graph gives an area of 8654 with a height of 455 and for the third graph, the area is 7940 and the peak height is 444 respectively. These variations raise the possibility of variable serum concentrations, which may be due to metabolic or pharmacokinetic differences existing between individuals. This analysis is necessary to understand the behaviour of the drug in terms of pharmacokinetics. Moreover, the serum analysis also highlighted that the AQ drug is protein-bound.

3.5 Behavioural Testing of the Drug

1. Open Field Test (OFT)

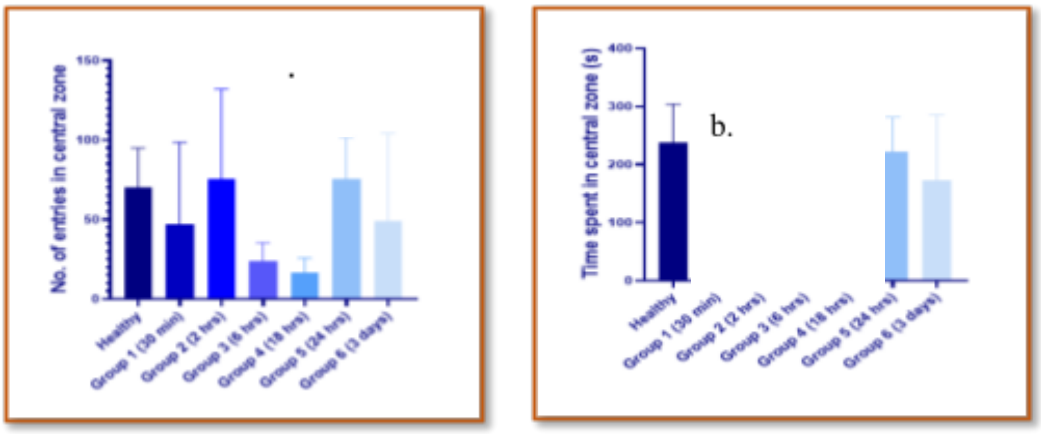

Figure SEQ Figure * ARABIC 27: fig a. The graph shows time-dependent variations in central zone entries compared to healthy controls, with error bars indicating data variability and fig b. time-dependent changes in the duration of time spent in the central zone compared to healthy controls, with error bars indicating data variability.

Interpretation of the Number of Entries and Time Spent in the Central Zone

The data reveals significant variability in both the number of entries to the central zone and the duration spent there, highlighting dynamic behavioural changes across different time points and conditions. The Healthy group shows relatively consistent entries (86, 83, and 42) indicating stable behaviour. In contrast, the experimental groups exhibit considerable fluctuations. At 30 minutes, entries vary widely (25, 11, and 106) reflecting high variability. By 2 hours, this erratic pattern continues with entries of 31, 139, and 57. At 6 hours, a gradual

decrease is observed (13, 36, and 23), suggesting reduced activity. By 18 hours, the entries reach their lowest range (13, 9, and 27), indicating minimal activity. However, entries rise again at 24 hours (80, 99, and 47) and 3 days (111, 31, and 6) although the coefficients of variation remain high, emphasizing the variability in responses.

The duration spent in the central zone also varies significantly between conditions, reflecting changes in behaviour over time. The Healthy group shows steady activity (270, 282, and 162 seconds) with moderate fluctuations, suggesting stable interaction with the central region. For the experimental groups, time spent is generally lower and more variable. At 30 minutes, durations (234, 126, and 388 seconds) are slightly less than the Healthy group. By 2 hours, there are significant changes (191, 408, and 159 seconds) potentially due to behavioural adjustments or stress. At 6 hours, the durations decrease further (158, 179, and 90 seconds) indicating reduced interaction. By 18 hours, the time is minimal (120, 187, and 146 seconds) suggesting sustained inactivity. After 24 hours, durations increase slightly (195, 390, and 180 seconds) indicating a revival of interest. However, by 3 days durations show contrasting values (364, 207, and 45 seconds) reflecting variable behavioral reactions. The time observation is lethargic but after time intervals no specific changes was observed in a behavioral testing of the drug. This means the drug is not affecting mice behaviors.

Interpretation SM/FM

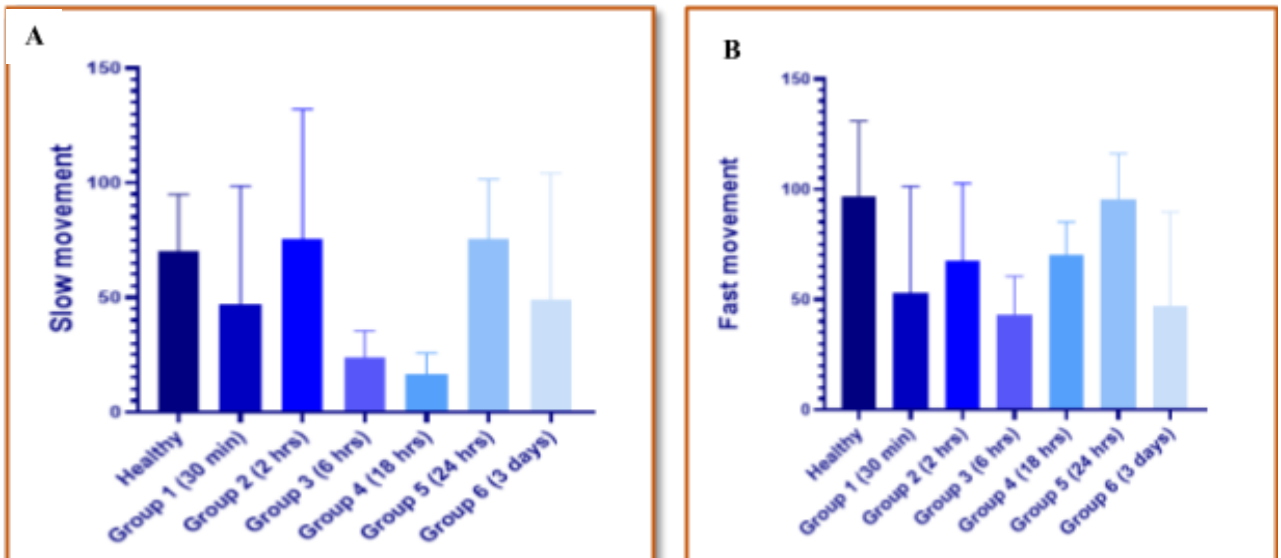

Interpretation for SM/FM

Figure 28 A illustrates the value of the cancer-related measurements in mice (SM/FM) at different time points after treatment. Firstly, normalisation values are 108, 124, and 59. Short-term fluctuations were observed at 30 minutes – two mice groups decreased their movement: from 108 to 25, and from 124 to 11, while the third group showed movement from 59 to 106. At 2 hours, dosed groups exhibit partial recovery and the one that presents a response exhibits a response time shift (11 → 57). At 6 hours, all groups show a reduction or plateau (13, 36, 23). At 18 hours, there is a significant decline (13, 9, 27) and at 24 hours movement increases (80, 99, 47). At the 3-day time point, time point-specific responses are regained.

Figure 25B SR/FR mice represent changes in the behaviour of subjects that underwent a cancer-related treatment process over some time. The normal initial values were 342, 376, and 179. At 30 minutes, there are marked reductions in rearing (342/184, 376/343) while one shows a dramatic rise in rearing (179/303). At 2 hours, decreases or plateau occurs (109, 225, 351). At 6 hours, variability remains marked (range 110 to 189) with one instance of a significant drop from baseline (351 to 109). There is a sharply defined increase at 18 hours in one mouse (902) and a slight decrease or stabilization in the others (312, 132). At 24h and 3 days, the responses vary, with near estimates of recovery (154, 462).

Interpretation of Inverted Screen Test

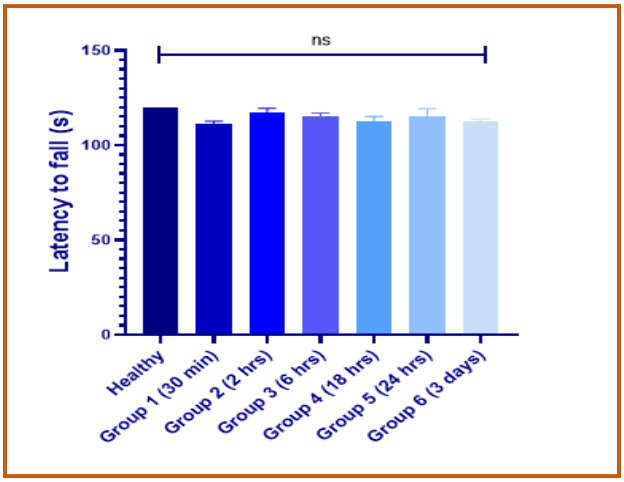

Figure SEQ Figure * ARABIC 29: Inverted screen test reported in the graph comparing the healthy control with different dosing groups at different time intervals

For the inverted screen test, there seemed to be

some difference between the samples. All of the mice were able to maintain 120 seconds during the test up to 6 hours post-treatment. At 18 hours, there were discovered moderate motor dysfunction in two mice, and at 24 hours the development of light dysfunction in one mouse (6 sec). Some subjects experienced a partial reduction of movement time (from 42 sec) or total recovery (to 120 sec) within the same time frame. There was a slight difference in motor coordination between the groups compared to the healthy controls, which consistently maintained 120 seconds.

Interpretation of the CBC

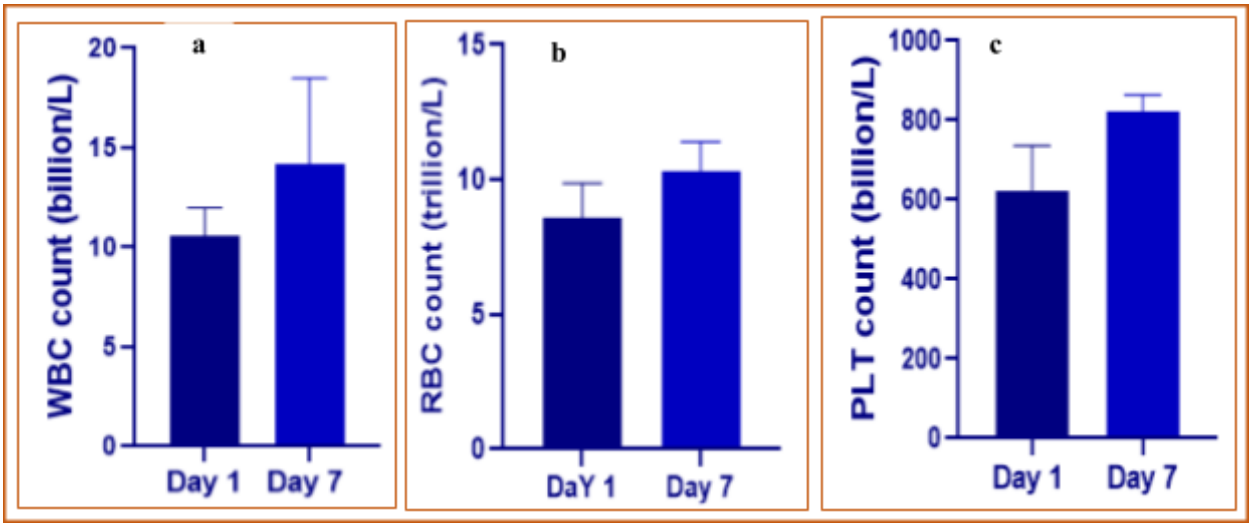

*Figure SEQ Figure * ARABIC 30: Comparison of WBC, RBC, and PLT levels on day 1 and after 7 days of dosing.*

Figure 30a illustrates the WBC count for 7 days dosing. When WBC count for mice1 was checked on 1st day it was 12.2 billion cells/L while when it was checked on day 7 the count was 17.3 billion cells/L. Similarly for mice 2 the WBC count was 9.8 billion cells/L on 1st day and on 7th day it increased to 16.0 billion cells/L. For mice 3 count for WBC WAS 9.7 billion cells/L while on 7th day it deceased to 9.3 billion cells/L. **Figure 30b** highlights RBC count for mice 1 on day 1 was 7.88 trillion cells/L where as it increased to 10.80 trillion cells/L on day 7.

For mice 2, 10.6 trillion cells/L were count on day 1 and increased to 11.10 trillion cells/L on day 7. For mice 3, the count of RBC on day 1 was 7.88 trillion cells/L which increased to 9.12 trillion cells/L. **Figure 30c** shows PLT on day 1 for mice 1 count was 674 billion cells/L and on day 7 it increased to 794 billion cells/L. For mice 2 the count on day 1 for PLT was 703 billion cells/L which increased to 870 billion cells/L. On day 1 for mice 1 count was 497 Billon cells/L which increased to 797 billion cells/L on day 7.

Overall, there was an increase in CBC at day 7 with comparison to Day 1.

3.6 Histopathology of Different Organs in Mice

Further, the next portion analyzed the histopathology of different organs in mice (heart, liver, and kidney). To assess the potential effects of a test drug that administered IV for 3 days in mice was the main focus of this study. To compare the healthy and diseased tissues of mice, the organs (liver, heart, and kidney) were examined at 10X and 40X magnification to identify the structural and functional changes. After analyzing this study evaluates to determine whether the drug induces toxicity or off-target effects in female mice to ensure the safety profile and efficacy the way for its clinical trials.

Heart Histopathology in Mice

Figure 31: Mice Heart Histology

Healthy Heart 10X	**Healthy Heart 40X**
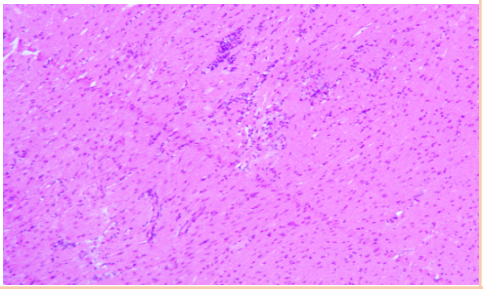	b. 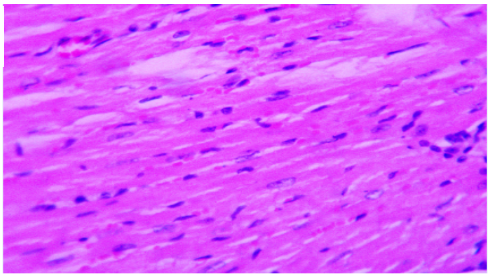
Diseased Heart 10X **Mice1 200mg/kg**	**Diseased Heart 40X**

b.

Mice 2 200mg/kg

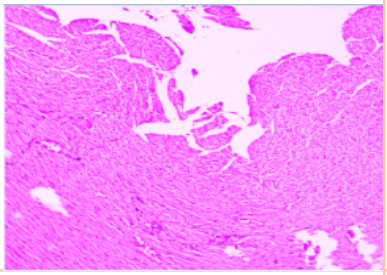

b.

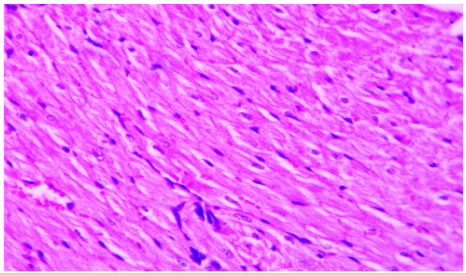

Mice 3 200mg/kg

a.

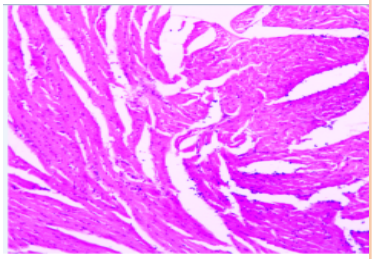

b.

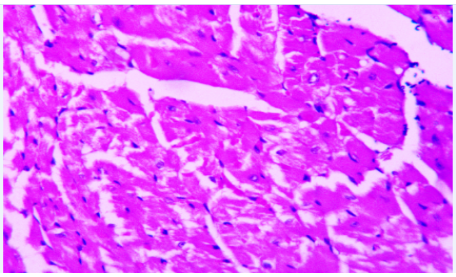

Mice with healthy and diseased hearts are shown side by side in the histopathology analysis. The Figure shows the comparison of healthy and diseased hearts of mice. There were two groups of mice one was healthy (control group) and the second was a diseased group. At 10X and 40X magnifications, the healthy heart tissue displays intact, well-organized cardiomyocytes with minimal extracellular matrix (ECM) deposition. The myocardial architecture remains undamaged, and no signs of fibrosis, inflammation, or cellular disorders exist. These findings demonstrate that the medication has no adverse effects on healthy heart tissue, supporting its safety profile (Davis, et al., 2023).

At 10X and 40X magnification, however, the diseased heart at a dosage of 200mg/kg did not exhibit any appreciable tissue damage. There were no dose-dependent changes in certain measures when compared to the control. During the experiment, there were no recorded deaths or clinical complaints associated with the treatment. In the heart, no tissue damage was observed; however, during slide preparation at 10x magnification, a slight change was noted. At 40x

magnification, no effects were detected in the cells or tissue. Overall, the findings showed that the drug does not worsen the condition. The fact that the outcomes for all three mice were the same emphasizes the drug's safety by showing that it has no side effects and may be utilized as a risk-free treatment. Thus, no diseased female mice nor the control female mice showed any appreciable histological changes in their internal organs.

Kidney Histopathology in Mice

Figure 32: Kidney Histology of Mice

<table>
<tr><th>Healthy Kidney 10X</th><th>Healthy Kidney 40X</th></tr>
<tr><td> 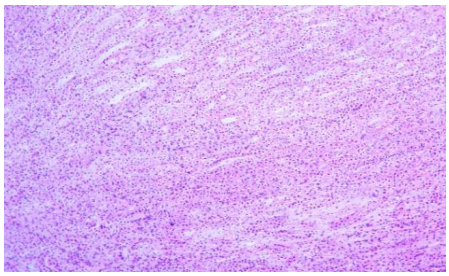 </td><td>b
 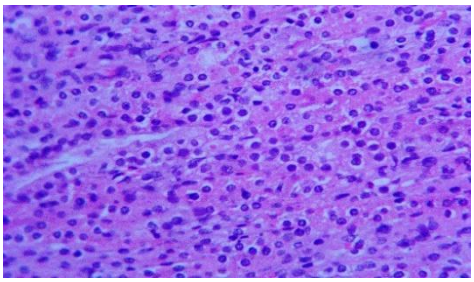 </td></tr>
<tr><td>Diseased Kidney 10X
Mice 1 200mg/kg
a.
 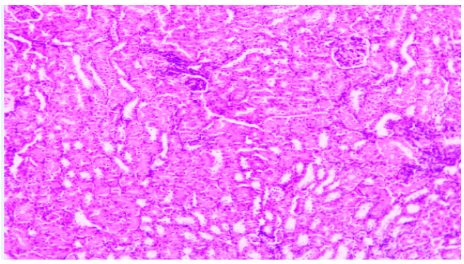 </td><td>Diseased Kidney 40X
b.
 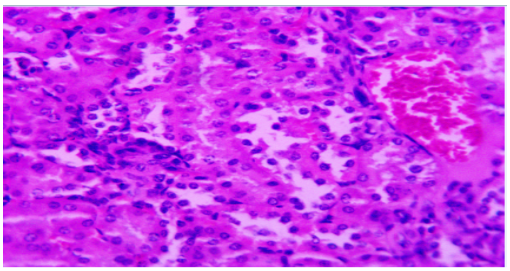 </td></tr>
<tr><td>Mice 2 200mg/kg
a.
 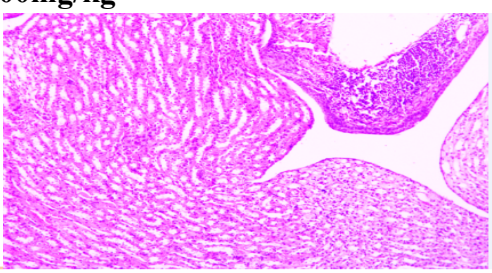 </td><td>b.
 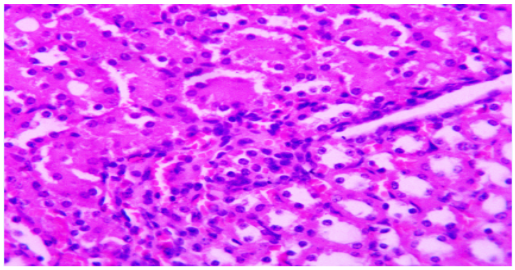 </td></tr>
</table>

Mice 3 200mg/kg

a.

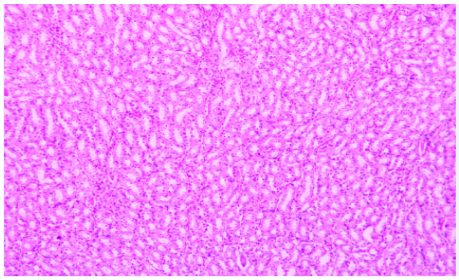

b.

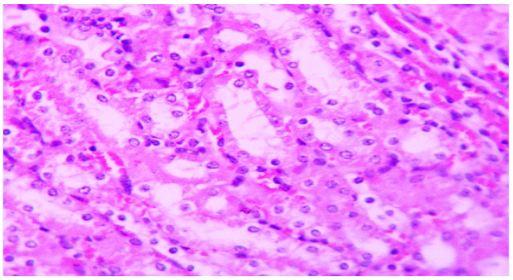

The provided histological images compare the kidney tissues of two mice groups from healthy (group 1) and diseased (group 2) mice under 10X and 40X magnifications with an average dose of 200mg/kg. The healthy kidney samples display normal renal architecture, including intact glomeruli, renal tubules, and interstitial spaces, without evidence of inflammation, fibrosis, or cellular damage. These findings serve as a baseline for evaluating the drug's safety (Rabah, 2010).

In the second group of mice, we did the IV dose of 200mg/kg for 3 days. After the third day of dosing the afflicted group of mice showed evidence of minor tubular injury and cellular infiltration, indicative of the underlying ailment. Nevertheless, no other physical changes were noticed that would indicate that the drugs rendered kidney damage worsened. The observed changes are compatible with the disease process rather than any drug-induced toxicity, and the kidney's structural integrity is maintained. Since there were no obvious indications or symptoms of toxicity at the initial dose of 200mg/kg the female mice extract was chosen for acute toxicity testing.

The findings demonstrated that diseased mice did not die or exhibit any other toxicity-related symptoms (Sireeratawong, et al., 2016). These findings strongly indicate that the drug under investigation has no harmful effects on the kidneys. Moreover, the lack of off-target effects further supports its therapeutic specificity. This is a critical consideration for

clinical applications, as the drug appears to act solely on its intended target without affecting other organs. These results provide a positive outlook for the drug's safety and potential for further development.

Liver Histopathology in Mice

Figure 33: Liver Histology of Mice

Healthy Liver 10X	**Healthy Liver 40X**
a. 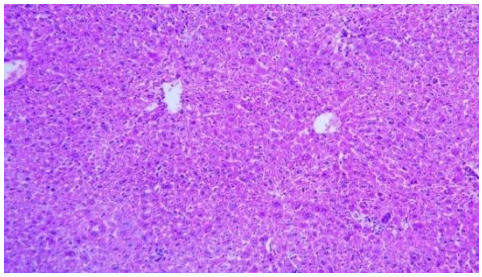	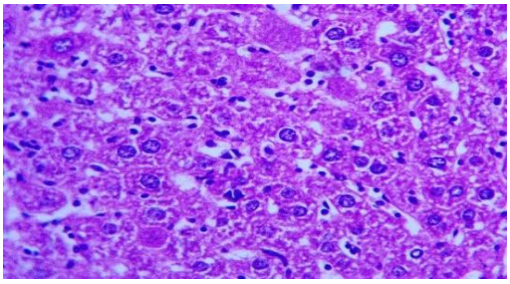 b.
Diseased Liver 10X **Mice 1 200mg/kg** a. 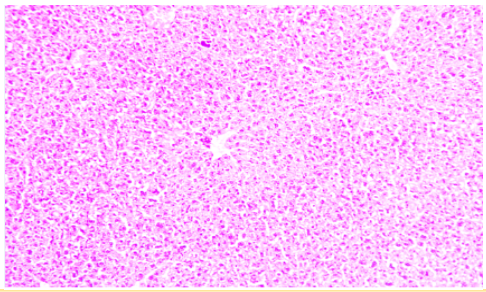	**Diseased Liver 40X** b. 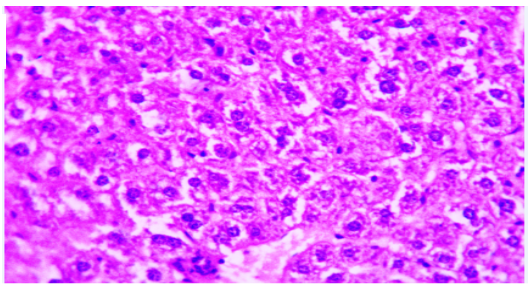
Mice 2 200mg/kg a. 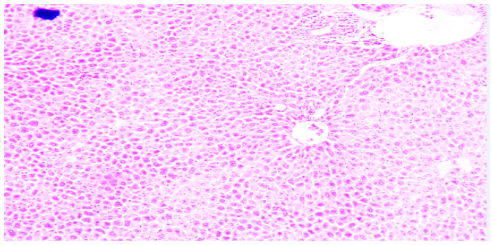	b. 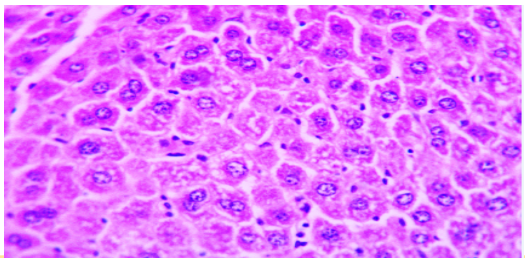

Mice 3 200mg/kg

a.

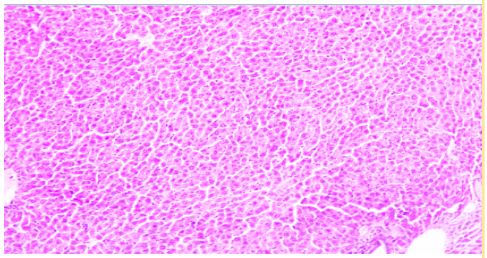

b.

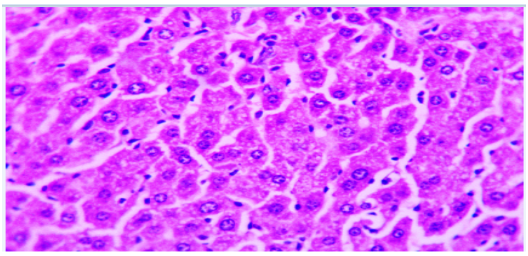

The liver slides in the control group appeared normal. The liver at this stage of development is made up of hepatocytes, blood sinusoids, and central and portal veins, as this image demonstrated. Hepatocytes come into greater contact with one another to create hepatic cords, as seen in the figure. These hepatocytes are big, flat, and normal in size, the control group's data at 10X and 40X revealed numerous hematopoietic cells (Hussien, et al., 2020).

In contrast, cellular infiltration and moderate hepatocyte degeneration are among the pathological alterations seen in the second group of female mice (diseased). The result was shown on the third day. Nevertheless, rather than being related to drug-induced liver damage, these results are consistent with the disease process. In every sample, the liver structure is largely unaltered and shows no further anomalies that could indicate negative medication effects (Ganguli, et al., 2012).

These findings show that the drug being studied does not aggravate liver disease or cause additional harm. Its organ safety profile is confirmed by the fact that there are no off-target effects in liver tissues. Without negatively impacting liver function or morphology, the drugs seem to perform precisely on their designated therapeutic target. This study offers compelling proof that the drug is safe and has no negative effects on the liver or various other organs. These results demonstrate the drug's potential for safe clinical use and

further advancement. The acceptable safety profile constitutes an important milestone for therapeutic application.

Chapter 4: Discussion and Conclusion

4.1 Discussion

This study aims to investigate the safety and cumulative effects of 2-amino,3-hydroxy anthraquinone through different dosing protocols that employ the technique of HPLC as the primary protocol. Different drug penetration techniques were utilized in this study as administration routes and time points (50mg/kg, 100mg/kg, 200mg/kg, 300mg/kg, 400mg/kg, and 500mg/kg) to collect the comprehensive data on the drug behaviour in mice. Initially, a stock solution was prepared with a ratio of 1:1 in a solvent mixture of Methanol and Acetonitrile. The stock solution was prepared in a Vortex machine with varying concentrations of mixture i.e. 20µg/mL, 40µg/mL, 60µg/mL, 80µg/mL, and 100µg/mL. Once the mixture was done the solution was transferred to the HPLC for analysis. However, based on previous safety testing 200mg/kg was chosen for accurate analysis of HPLC and found an authentic concentration of the drug in plasma (Mosaad, Samir, & Ibrahim, 2017). Thus, the three-day dosing protocol provides cumulative effects of intravenous dosing on drug safety and the seven-day dosing protocol assesses the impact of lengthy dosing on drug safety, accumulation, and toxicity. The use of the HPLC technique is reliable and demonstrates the effectiveness of different dosing protocols allowing efficacy and safety under long-term exposure. Further, the study also analyzed the optimization of drug (2-amino, 3-hydroxy anthraquinone) efficacy and safety.

When tested at a different concentration ranging (from 50 to 500 mg/kg), demonstrated favourable outcomes especially in terms of behavioural analysis, CBC (Complete Blood Count) analysis, and historical assessment. These finding of the study indicates better treatment efficiency. Suggesting a dose-dependent effect that was both effective and safe, the concentration with this range showed better results in terms of response and stability. Indicating that the drug is

well tolerated by the subject with no sign of significant adverse effect, especially in the behavioural assessment, the analysis of the plasma revealed a positive outcome (Siddamurthi, Gutti, & Jana, 2020). For determining the drug's potential for therapeutic use, especially in cancer research, where both safety and efficiency are paramount, this finding is critical.

On the subjective activity level, the data did not indicate any major negative impact of the drug. Throughout the study, the behavioural analysis revealed variety and variation in response of the experimental groups. The overall trends did not show any significant impairment in behaviour, which further supports the safety profile of the drug. However, the number of entries into the central zone, which serves as a behavioural measure, displayed some fluctuation. The analyte levels remained stable or showed signs of recovery at a certain time point when the data on peak area and height in plasma also suggest that the drug did not cause any notable degradation or toxicity.

Further, CBC analysis revealed minor fluctuations in mice, the count of WBC increased in some stages indicating immune activation while other counts indicated a slight decrease in the results. The changes occurred in these resulting drug-influencing immune responses but there is no major changes or alterations were observed in the blood counts. It means the drug is on the safer side within the tested dose range. Similarly, the count of platelets also showed a mild effect in coagulation of dynamics but no significant suggestion was seen in safety concerns of the drug. To offer a comprehensive reference resource for identifying normal (control) structures pertinent to the most significant diseased mouse heart, liver, and kidney, this histology atlas was developed. However, to meet the challenges of phenotyping the growing number of mice with developmental cardiac, kidney, and liver abnormalities whether spontaneous or brought on by chemicals or genetic modification it is designed to help pathologists and biomedical scientists.

For liver, heart, and kidney we took three mice and performed IV dosing to check the cancerous cells on different days. According to the results on day 3, the results were compiled and compared with the normal cells of the female mice. The above histology analysis of the mice showed that it provides compelling evidence on the safer side of the drug efficacy.

This drug also lacks off-target effects in the heart, liver, and kidney tissues. From the histoanalysis of the heart, when comparing normal cells with diseased no significant changes were seen to the drug. It means the healthy cells maintained their normal arrangement and morphology whereas the diseased group of mice showed mild existing pathological features. These features include the disorganization of fibrosis, which is consistent with the underlying process instead of drug-induced damage. Therefore, after analysis, we can say that no drug exacerbates the heart pathology of the female mice resulting safety profile for heart tissues. Both diseased and control group cells were analyzed at 10X and 40X magnification. The diseased cells utilize 200mg/kg of IV dosage.

Likewise, in liver histology, the cells like blood sinusoids, hepatocytes, and vascular structures in the control group of mice appeared normal while intacting hepatic cords and no signs of cellular stress. According to the results, small changes in hepatocytes and degeneration of cellular cells were seen in the diseased mice but no significant changes were observed.

In a similar study conducted by Vallerand et al, the loss of drugs damages the portion of the mouth. Their study demonstrated a correlation between excessive RA administration and hair loss when injecting IV dosage in female mice. All-trans-retinoic acid (atRA), a metabolite of RA, has been found in the retina of treated adult mice, and the dark eye was also observed during morphological examination. The sclera is the outer shell of connective

tissue in the eye. It is hypothesized that atRA regulates the expression of multiple genes that impact alterations in the scleral extracellular matrix, which in turn modify ocular size and refraction (Vallerand, et al., 2018).

In addition, previous studies were conducted to check the efficacy and safety of drugs (2-amino, 3-hydroxy anthraquinone) but no such work has been done on safety measures. According to the study of Andrey E. Shchekotikhin et al in 2020, he administered anthrafuran, a novel anticancer drug, which has demonstrated consistent effects in murine tumour models. P388 leukaemia, Ca755 mammary adenocarcinoma, LLC lung carcinoma, and T47D human breast cancer xenografts were among the transplanted tumour models used in this work to evaluate the anticancer efficacy and acute toxicity of anthrafuran given orally in Balb/c nude mice. For all examined tumour models, their study demonstrated strong antitumor activity; the best course of treatment was 70–100 mg/kg administered daily for five days. They found that when human breast cancer xenografts were put into naked mice, the anticancer effect was verified. Single doses of 70–100 mg/kg for five days constitute the ideal course of treatment for oral anthrafuran, which significantly inhibits tumour growth or prolongs the life of many tumour models (Shchekotikhin, et al., 2020).

In a study akin to drug-protein binding, Zaayter et al. found UHRF1 inhibitors that block the recognition and flipping of 5mC by targeting the 5'-methylcytosine (5mC) binding pocket of the SRA domain. Biophysical testing, molecular modeling, and virtual screening are all part of a multidisciplinary approach. The crucial function of base flipping for DNMT1 recruitment was highlighted by the discovery of an anthraquinone drug that blocked the base-flipping process and reduced total DNA methylation (Zaayter et al, 2019).

Likewise, Shaheer Malik et al.'s 2021 study found that anthraquinones and their derivatives have demonstrated promising anticancer activities against a variety of cancer cell lines and targets. After being converted to hydrophilic glucuronides, this antidrug anthraquinones are readily digested and eliminated by the kidneys. Additionally, synthetic anthraquinone derivatives have demonstrated promise as medicinal agents for several diseases. Inhibition of cancer cell proliferation, invasion, migration, metastasis, cellular apoptosis, tumour angiogenesis, host immune response modulation, antioxidant, anti-inflammatory, and reversing tumour cell multidrug resistance are some of their antitumor properties. According to their study, more investigation is required to determine hit/lead-like compounds for future development and to comprehend the toxicity and safety assessment of anthraquinone derivatives (Malik, et al., 2021).

The study of Tomoki Nakamura et al focused on determining the lethal dose of Acridine orange (AO), a compound which is used for cancer therapy. This drug was injected intravenously in mice to check the results. The lethal dose of LD50 is crucial in toxicology and represents a substance to causes 50% of deaths in mice. The study of Tomoki identified safe doses for AO before clinical trials in cancer treatment. Their study also suggested intravenous administration of AO at different time intervals in mice by careful monitoring of the mice for symptoms of mortality and toxicity. The authors also visualize the potential side effects of AO as well to check the behaviour of this drug. In our study, this drug efficacy is related and focused on the safety and effectiveness of the drug. The study of Nakamura analyzed the lethal dose of AO drug but in our study, we analyzed the safety and efficacy of AQ drug. We ensure that our drug is safe for potential and clinical trials (NAKAMURA, et al., 2014).

4.2 Limitations

However, some questions have to be discussed concerning the study on efficacy, safety and pharmacokinetics of 2-amino-3-hydroxy-anthraquinone. The research utilized 24 female BALB/c mice, which authors considered an acceptable number for preliminary studies while can be insufficient to provide coverage of more extensive biological variation. These lesions are done on male mice and other genetic strains making the results less generalizable and may exclude gender or genetic bias in drug response. The study specifically concerned dose regimens of single-day IV, three days IV, and seven days IP administration, which leave one guessing about the compound's influence during long-term or chronic treatment (Ioele *et al.*, 2022).

The used behavioural tests included the Open Field Test (OFT) and Inverted Screen Test to study motor activity and neuromuscular coordination in the animals, however, these tests might not have identified potential neurological and psychologically altered states of behaviours. One of these limitations is that there are no benchmarking studies that used conventional anti-cancer agents (Zhang *et al.*, 2023). Unfortunately, its formulation does not offer any clear advantages or disadvantages over existing treatments if it has not been benchmarked against them. Furthermore, getting high purity of active compounds on tumour cells while excluding other interacting cellular components is another potential limitation, as the settings of a highly controlled environment of a laboratory differ from those of the actual world, including other influencing variables such as varying lighting conditions, dietary habits, other diseases, etc. affecting the drug's efficiency and side effects (Crombag *et al.*, 2016).

4.3 Recommendations

Future research should target increasing the diversity among test subjects. The use of both males and females has increased, in addition to other strains to ensure variation in genetics

and physiology. A larger sample would also enhance the efficiency of the results because statistical power and reliability would also increase. Further research should also examine its chronic use and other forms of administration including administration via the oral route (Ostios-Garcia *et al.*, 2024).

Further, behavioural suggestions should extend to cognitive and emotional evaluations that may also allow an understanding of certain neurological side effects. Further, comparative research works with the primary anti-cancer medication are needed to compare the results, to reveal the advantages or shortcomings of the analyzed drug. More practical study is the simulation of people and classroom conditions where various levels of stress, or co-pathologies are present and it is proposed that the experimental designs afford greater generalizability of these results to the clinical domain.

Studying biomarkers could help gain a better understanding of the molecular basis of the drug's action as well as understand which biomarker could be used to select patients for future clinical trials. It is crucial to create an outline for building an approach, enabling the project to proceed directly to clinical trials. This involves calculating known hazards, planning assessments rating human equivalent dosages, and meeting regulatory objectives (Waseem *et al.*, 2024).

Other studies include any economic achievability that can be done to look at the cost of producing drugs. This is especially important to make the drug available to poor areas of the world where affordable cancer treatments are most required. Concerning these areas, further research can be conducted focusing on the development of the therapeutic effect and clinical use of 2-amino-3-hydroxy-anthraquinone contributing to the improvement of cancer therapy (Cheng *et al.*, 2025).

References

Animesh, S., & Revandkar, A. (2024). Cancer Pathogenesis: Molecular and Cellular Mechanisms of Tumor evolution, Therapy-Resistance and Immune Evasion. *Frontiers in Cell and Developmental Biology*, 3-10. Retrieved from https://www.frontiersin.org/research-topics/59699/cancer-pathogenesis-molecular-and-cellular-mechanisms-of-tumor-evolution-therapy-resistance-and-immune-evasion#:~:text=Cancer%20pathogenesis%20is%20a%20pathophysiological,solid%20tumors%20and%20blood%20cel

Aseem, A. (2023, September 2). *HPLC – High-Performance Liquid Chromatography*. Retrieved from BioTech Reality: https://www.biotechreality.com/2023/09/hplc-high-performance-liquid-chromatography.html

Azees, P. A., Natarajan, S., Amaechi, B. T., Thajuddin, N., & Phuong, T. N. (2022). An empirical review on the risk factors, therapeutic strategies and materials at nanoscale for the treatment of oral malignancies. *Process Biochemistry, 118*(6), 283-293. Retrieved from https://www.sciencedirect.com/science/article/abs/pii/S1359511322001295

Baade, P. D., Youlden, D. R., Kimlin, M. G., Aitken, J. F., & Biggar, R. J. (2024). Estimating the change in life expectancy after a diagnosis of cancer among the Australian population. *BMJ Open, 5*(4), 1-10. Retrieved from https://bmjopen.bmj.com/content/5/4/e006740

Chow, C. Y., Lie, E. F., & Wu, C.-H. (2022). Clinical implication of genetic composition and molecular mechanism on treatment strategies of HER2-positive breast cancers. *Frontier Oncology*, 12. doi:https://doi.org/10.3389/fonc.2022.964824

Cleveland. (2024, November 27). *Chemotherapy*. Retrieved from ClevelandClinic: https://my.clevelandclinic.org/health/treatments/16859-chemotherapy

Clark, J. D., Gebhart, G. F., Gonder, J. C., & Keeling, M. E. (1997). Special Report: The 1996 Guide for the Care and Use of Laboratory Animals. *ILAR journal / National Research Council, Institute of Laboratory Animal Resources*, 41-48.

Cnops, V., Iyer, V. R., Parathy, N., Wong, P., & Dawe, a. G. (2022). Test, rinse, repeat: A review of carryover effects in rodent behavioral assays. *Neuroscience & Biobehavioral Reviews*, 1-10.

Das, A., Roy, S., Mondal, P., Datta, A., Mahali, K., Loganathan, G., & Dharumadurai, D. (2016). Studies on the interaction of 2-amino-3-hydroxy-anthraquinone with surfactant micelles reveal its nucleation in human MDA-MB-231 breast adinocarcinoma cells. *RSC Advances, 6*(34), 1-41. doi:doi:10.1039/c6ra00062b

Davis, J. R., Banskota, a., Levy, J. M., & Newby, G. A. (2023). Efficient prime editing in mouse brain, liver and heart with dual AAVs. *Nature Biotechnology, 42*, 253-264.

Donnarumma, F., Schober, M., Greilberger, J., Matzi, V., Lindenmann, J., Maier, A., . . . Wintersteiger, R. (2011). Method development and validation for the analysis of a new anti-cancer infusion solution via HPLC. *Journal of Separation Science, 34*(2), 135-141. doi:doi.org/10.1002/jssc.201000574

Evans, M. A. (2024, November 27). *The Limitations and Challenges of Cancer Therapies*. Retrieved from IndeeLabs: https://www.indeelabs.com/articles/the-limitations-and-challenges-of-cancer-therapies

Feeney, T., & Villanueva, T. (2023). Communicating the benefits and harms of anticancer drugs. *BMJ Open*, 623. Retrieved from doi: https://doi.org/10.1136/bmj.p623

Ganguli, M. N., Singh, R. K., & Mitra, A. (2012). Toxicological evaluation of Kasisa Bhasma, an ayurvedic organo metallic preparation. *International Journal of Research in Ayurveda and Pharmacy, 3*(3), 381-386. Retrieved from

https://www.researchgate.net/publication/291193383_Toxicological_evaluation_of_Kasisa_Bhasma_an_ayurvedic_organo_metallic_preparation

Gencturk, S., & Unal, G. (2024). Rodent tests of depression and anxiety: Construct validity and translational relevance. *Cognitive, Affective, & Behavioral Neuroscience*, 191–224.

Globocan. (2024, February 1). *GLOBOCAN 2022: Latest global cancer data shows rising incidence and stark inequities*. Retrieved from UICC: https://www.uicc.org/news/globocan-2022-latest-global-cancer-data-shows-rising-incidence-and-stark-inequities

Herck, S. V., & Geest, B. G. (2020). Nanomedicine-mediated alteration of the pharmacokinetic profile of small molecule cancer immunotherapeutics. *Acta pharmacologica sinica, 41*, 881-894. Retrieved from https://www.nature.com/articles/s41401-020-0425-3

HPLC. (2022, November 3). *HPLC Testing & UPLC Testing*. Retrieved from Impact Analytical: https://www.impactanalytical.com/hplc-testing-uplc-testing/#:~:text=HPLC%20stands%20for%20High%20Performance,of%20a%20mixture%20or%20compound.

Hussien, B., Intissar, N., & Waheed, I. (2020). The Effects of Different Concentrations of Retinoic Acid on the Histological Structure of Liver of Adult Albino Female Mice and Their Prenatal Fetuses. *Journal of Biology, Agriculture and Healthcare , 10*(18), 24-41. Retrieved from https://www.researchgate.net/publication/344445766

Izzah, I. N., & Ibharm, S. F. (2020). Chemotherapy–Types, Side Effects and Resistance. *Journal of Tomography System and Sensor Application, 3*(2), 32-43. Retrieved from https://www.tssa.my/index.php/jtssa/article/view/111

Junwei, H., Zhao, R., Xia, W., Chang, C.-W., You, Y., Hsu, J.-M., & Nie, L. (2020). PD-L1-mediated gasdermin C expression switches apoptosis to pyroptosis in cancer cells and facilitates tumour necrosis. *Nature cell biology, 22*(10), 1264-1275.

Karati, D., & Kumar, D. (2022). Exploring the structural and functional requirements of Phyto-compounds and their synthetic scaffolds as anticancer agents: Medicinal chemistry perspective. *Pharmacological Research - Modern Chinese Medicine, 4*, 100123. doi:https://doi.org/10.1016/j.prmcm.2022.100123

Kim, H. J., Schweiker, S., Powell, K., & Levonis, S. (2022). An efficient and robust HPLC method to determine the sialylation levels of human epithelial cells. *Plos One*. doi:https://doi.org/10.1371/journal.pone.0257178

KSV, A. B., Dissanayake, D., Gunatilake, M., Velu, V. K., & Modagan, P. (2023). A short review on behavioural assessment methods in rodents. *Bioinformation*, 866–870.

Lawal, B., Kuo, Y.-C., Sumitra, M. R., & Wu, A. T. (2021). In vivo Pharmacokinetic and Anticancer Studies of HH-N25, a Selective Inhibitor of Topoisomerase I, and Hormonal Signaling for Treating Breast Cancer. *Journal of Infammation Research, 14*(22), 4901-4913. Retrieved from https://pmc.ncbi.nlm.nih.gov/articles/PMC8473721/

Livestrong. (2024, October 4). *Life Expectancy*. Retrieved from Livestrong: https://livestrong.org/resources/life-expectancy

Lei, Z.-N., Tian, Q., Teng, Q.-X., & Wurpel, J. (2023). Understanding and targeting resistance mechanisms in cancer. *MedComm, 4*(3), e265. doi:10.1002/mco2.265

Lezak, K. R., Missig, G., & Jr, a. W. (2017). Behavioral methods to study anxiety in rodents. *Dialogues Clin Neurosci*, 181–191.

Mattiuzzi, C., & Lippi, G. (2019). Current Cancer Epidemiology. *Journal of Epidemiology and Global Health, 9*(4), 217-222. doi:10.2991/jegh.k.191008.001

Mattiuzzi, C., & Lippi, G. (2019). Current Cancer Epidemiology. *Journal of Epidemiology and Global Health, 9*(4), 217-222. doi:DOI: https://doi.org/10.2991/jegh.k.191008.001

Michaeli, D. T., Michaeli, J. C., & Michaeli, T. (2023). Advances in cancer therapy: clinical benefit of new cancer drugs. *Aging, 15*(12), 5232-5234. Retrieved from https://pmc.ncbi.nlm.nih.gov/articles/PMC10333065/

Mosaad, R. M., Samir, A., & Ibrahim, H. M. (2017). Median lethal dose (LD50) and cytotoxicity of Adriamycin in female albino mice. *Journal of Applied Pharmaceutical Science, 7*(3), 77-80. doi:DOI: 10.7324/JAPS.2017.70312

Mylène, T., Hennequart, M., Cheung, E. C., Zani, F., Hock, A. K., Legrave, N., & Maddocks, O. D. (2021). Serine synthesis pathway inhibition cooperates with dietary serine and glycine limitation for cancer therapy. *Nature Communication, 12*(5), 366. Retrieved from Nature communications .

Neha, T., Gheldof, A., Tatari, M., & Christofori, G. (2012). EMT as the ultimate survival mechanism of cancer cells. *In Seminars in cancer biology*, 194-207. Retrieved from https://www.sciencedirect.com/science/article/abs/pii/S1044579X12000491

Nature. (2024, November 27). *Decoding the signs of response to cancer immunotherapy*. Retrieved from Nature Portfolio: https://www.nature.com/articles/d42473-019-00064-0#:~:text=Only%2020%2D40%25%20of%20patients,trigger%20severe%20auto%2Dimmune%20reactions.

NIH Cancer. (2022, May 31). *Targeted Therapy to Treat Cancer*. Retrieved from NIH Cancer Institute: https://www.cancer.gov/about-cancer/treatment/types/targeted-therapies

NIH Cancer. (2024, November 27). *Cancer Risk Factors*. Retrieved from National Cancer Institute: https://www.cancer.gov/about-cancer/causes-prevention/risk/hormones

NIH Cancer. (2024, November 27). *Immunotherapy to Treat Cancer*. Retrieved from NIH Cancer: https://www.cancer.gov/about-cancer/treatment/types/immunotherapy

Nilmani, D'costa, M., Bothe, A., & Das, S. (2022). Chapter Five - CDK regulators—Cell cycle progression or apoptosis—Scenarios in normal cells and cancerous cells. *Advances in Protein Chemistry and Structural Biology, 135*, 125-177. doi:https://doi.org/10.1016/bs.apcsb.2022.11.008

Noorani, I. (2020). Chapter 1: Introduction. *Thesis*, 1-30. Retrieved from https://ftp.sanger.ac.uk/pub/resources/theses/in1/chapter1.pdf

Nora, B., Pittini, A., & Osinaga, E. (2022). Targeting tumor glycans for cancer therapy: successes, limitations, and perspectives. *Cancers, 14*(3), 645. Retrieved from https://www.mdpi.com/2072-6694/14/3/645

NSW. (2024, November 27). *Cancer risk factors*. Retrieved from Cancer Institute: https://www.cancer.nsw.gov.au/about-cancer/cancer-basics/cancer-risk-factors

Puneet, S., & Lim, B. (2022). Targeting apoptosis in cancer. *Current oncology reports, 24*(3), 273-284.

Rabah, S. O. (2010). Acute Taxol nephrotoxicity: Histological and ultrastructural studies of mice kidney parenchyma. *Saudi Journal of Biological Sciences, 17*(2), 105-114. Retrieved from https://www.sciencedirect.com/science/article/pii/S1319562X10000161#aep-section-id40

Rao, Z., Zhu, Y., Yang, P., Chen, Z., Xia, Y., & Qiao, C. (2022). Pyroptosis in inflammatory diseases and cancer. *Theranostics, 12*(9), 4310-4329. doi:10.7150/thno.71086

Ruan, J., & Yao, Y. (2020). Behavioral tests in rodent models of stroke. *Brain Hemorrhages*, 171-184.

Sabourian, R., Mirjalili, S. Z., Namini, N., Chavoshy, F., & Hajimahmoodi, M. (2020). HPLC methods for quantifying anticancer drugs in human samples: A systematic review. *Analytical Biochemistry, 610*, 113891. doi:https://doi.org/10.1016/j.ab.2020.113891

Saré, R. M., Lemons, A., & Smith, a. C. (2021). Behavior Testing in Rodents: Highlighting Potential Confounds Affecting Variability and Reproducibility. *Neuro-Developmental Disorders: Bench-to-Bedside*, 1-10.

Schiliro, C., & Firestein, B. L. (2021). Mechanisms of Metabolic Reprogramming in Cancer Cells Supporting Enhanced Growth and Proliferation. *Cells, 10*(5), 1056. doi:https://doi.org/10.3390/cells10051056

Schwartz, S. M. (2024). Epidemiology of Cancer. *Clinical Chemistry, 70*(1), 140-149. doi:https://doi.org/10.1093/clinchem/hvad202

Siddamurthi, S., Gutti, G., & Jana, S. (2020). Anthraquinone: a Promising Scaffold for the Discovery and Development of Therapeutic Agents in Cancer Therapy. *Future Medicinal Chemistry, 12*(11), 1037-1069. doi:https://doi.org/10.4155/fmc-2019-0198

Sireeratawong, S., Jaijoy, K., & Khonsung, P. (2016). Acute and chronic toxicities of Bacopa monnieri extract in Sprague-Dawley rats. *BMC Complementary and Alternative Medicine, 16*(249). Retrieved from https://bmccomplementmedtherapies.biomedcentral.com/articles/10.1186/s12906-016-1236-4

Zaayter, L., Mori, M., Ahmad, T., Ashraf, W., Boudier, C., Kilin, V., . . . Mely, a. Y. (2019). *A Molecular Tool Targeting The Base-Flipping Activity of Human UHRF1*. Retrieved from 10.1002/chem.201902605

Zhao, X.-S., Wang, H.-Y., Zhang, L.-L., Liu, Y.-H., & Chen, H.-Y. (2019). Prevalence and risk factors associated with the comprehensive needs of cancer patients in China. *Health and Quality of Life Outcomes, 17*(102), 34-67. Retrieved from https://hqlo.biomedcentral.com/articles/10.1186/s12955-019-1171-4

Appendix A

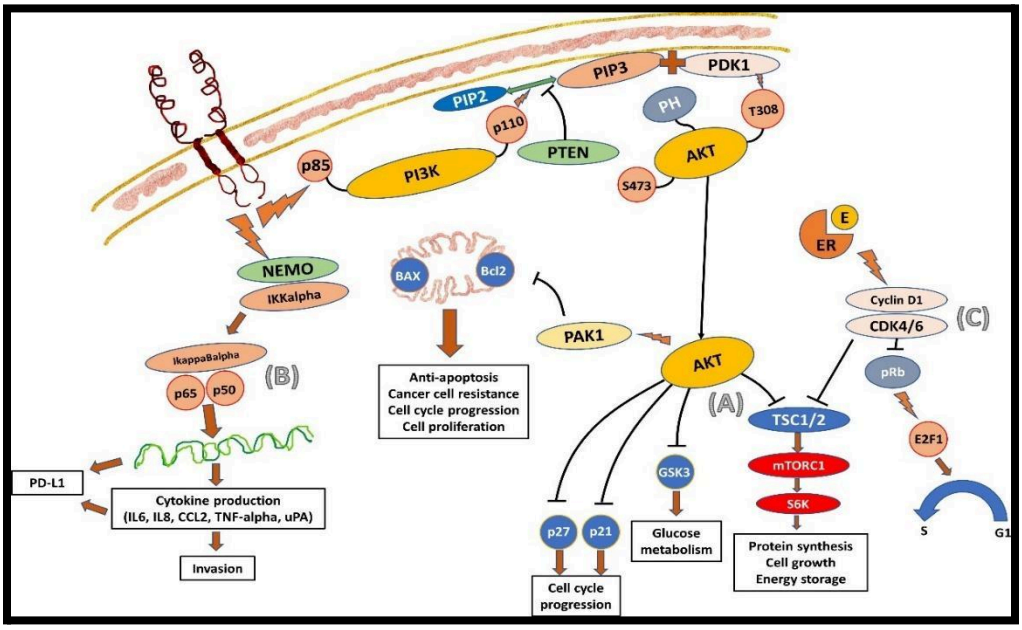

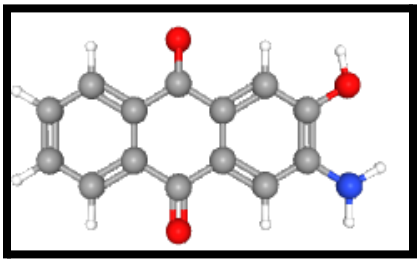

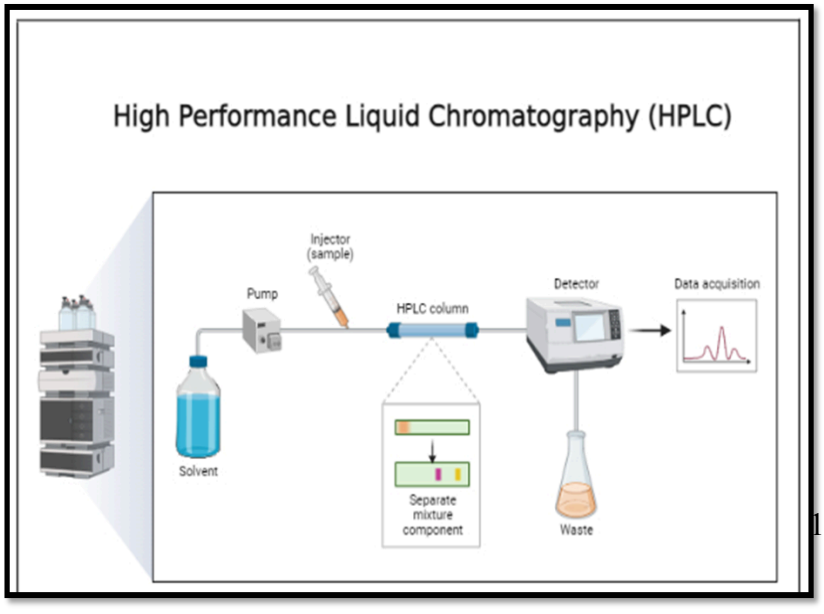

Appendix B

Chemical/Drug	Formula	Molecular Weight	Boiling Point	Volume	UN Number	Additional Information
Acetonitrile for Gradient HPLC	CH_3CN	41.05	82°C	4L	UN1648	High-purity chemical.
Methyl Alcohol for Gradient HPLC	CH_3OH	32.04	65°C	4L	UN1230	High-purity chemical.
Dimethyl Sulfoxide (DMSO)	$(CH_3)_2SO$	78.13	189°C	-	-	Used for drug preparation.
2-Amino, 3-Hydroxyanthraquinone	$C_{14}H_9NO_3$	239.23	-	-	-	Test compound for analysis.
Methanol	CH_3OH	32.04	65°C	-	-	Used for mobile phase preparation.
Normal Saline	NaCl in H_2O	-	-	-	-	Used for dilution and dosing.
HPLC Vials	-	-	-	2 mL	-	Screw-type, Lot No: 18108891, USA.
Syringe Filter	-	-	-	Φ 25 mm	-	Pore size 0.45 µm, Non-Sterile.

Appendix C

Appendix D

Apparatus	Model/Type	Manufacturer	Origin	Purpose
Centrifuge	Eppendorf 5415	Eppendorf	Germany	Plasma and serum separation.
Open Field Test (OFT)	Behavioural Apparatus	-	Pakistan	Behavioural analysis.
Mouse Cages	Fengshi	Fengshi	China	Housing of laboratory mice.

Spray Bottle	-	-	Germany	For laboratory cleaning purposes.
USB Camera	Logitech C310	Logitech	Switzerland	Behavioural monitoring.
Petri Dishes	-	-	Pakistan	For sample handling.
Weighing Machine	Precision Scale	-	-	For accurate weight measurements.

Appendix E

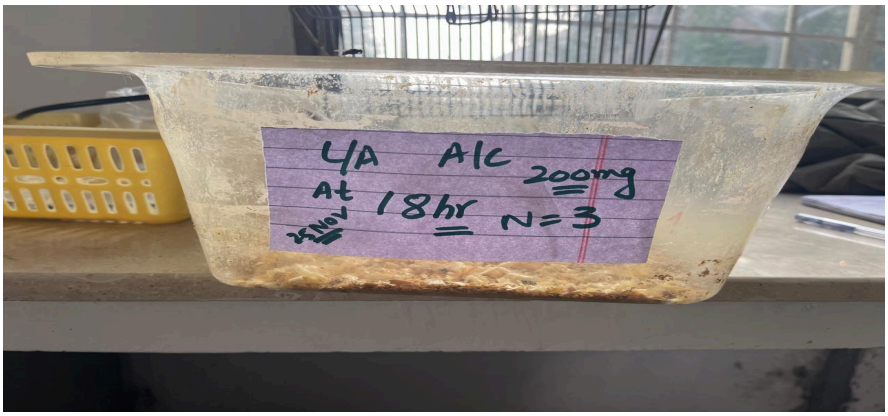

Appendix F

Height vs. Concentration

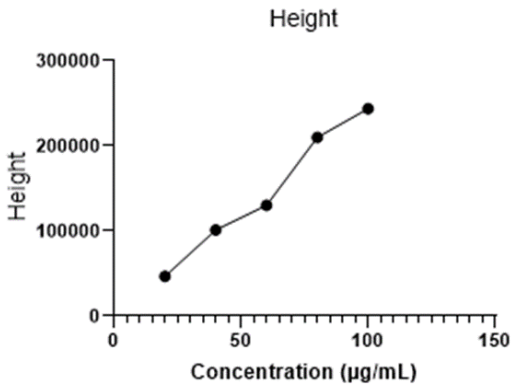

Peak Area vs. Concentration

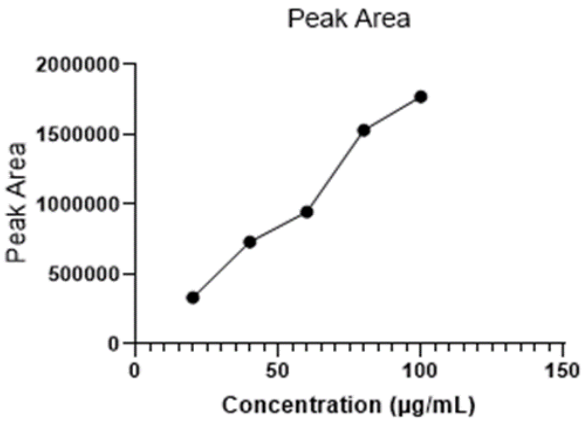

Standard Graph (Average Area and Height)

Standard Graph for 20 mg

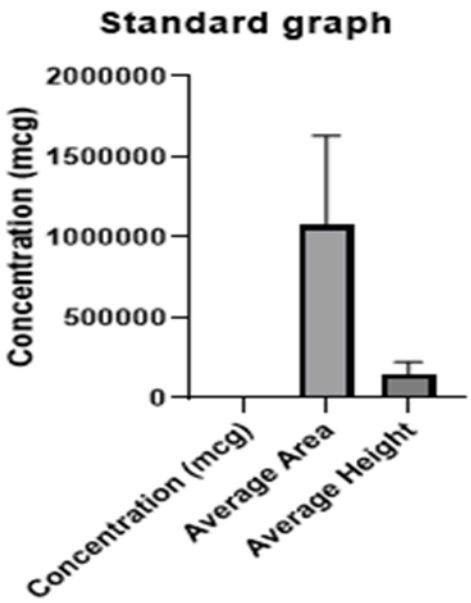

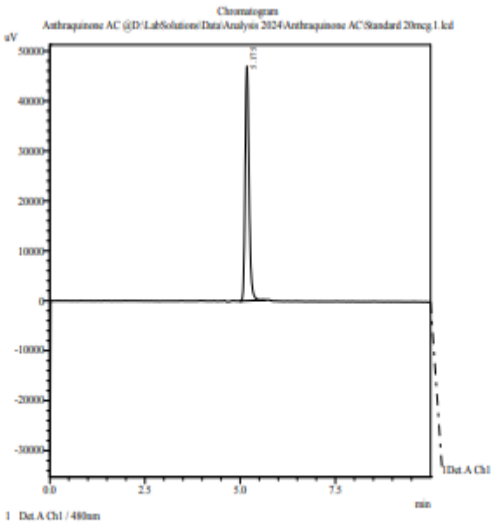

PeakTable @D:\...\Data\Analysis 2024\Anthraquinone AC\Standard 20mcg.1.lcd
Detector A Ch1 480nm

Peak#	Ret. Time	Area	Height	Name
1	5.175	334738	46897	Anthraquinone AC
Total		334738	46897	

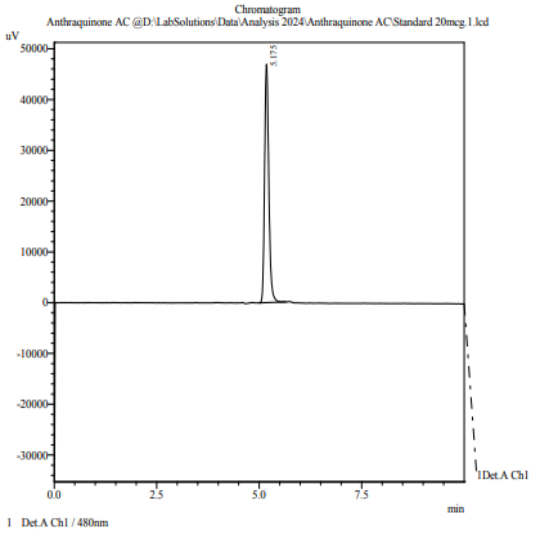

PeakTable @D:\...\Data\Analysis 2024\Anthraquinone AC\Standard 20mcg.1.lcd
Detector A Ch1 480nm

Peak#	Ret. Time	Area	Height	Name
1	5.175	334738	46897	Anthraquinone AC
Total		334738	46897	

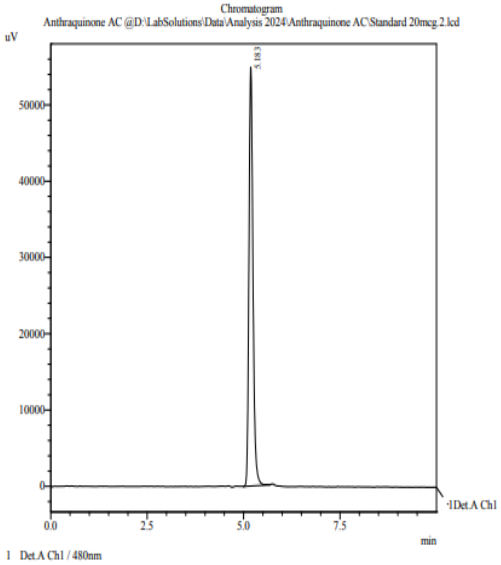

PeakTable @D:\...\Data\Analysis 2024\Anthraquinone AC\Standard 20mcg.2.lcd
Detector A Ch1 480nm

Peak#	Ret. Time	Area	Height	Name
1	5.183	398535	54860	Anthraquinone AC
Total		398535	54860	

Standard 40 mcg

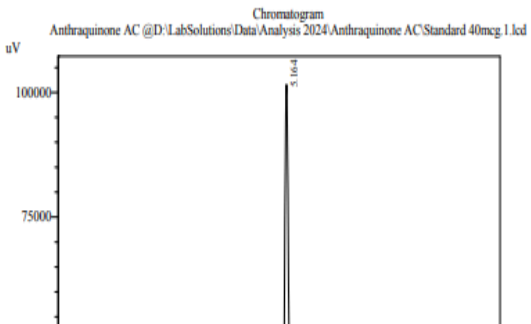

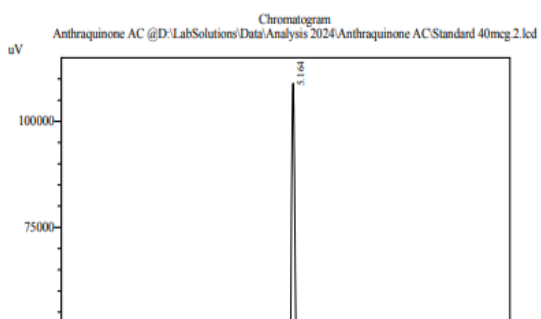

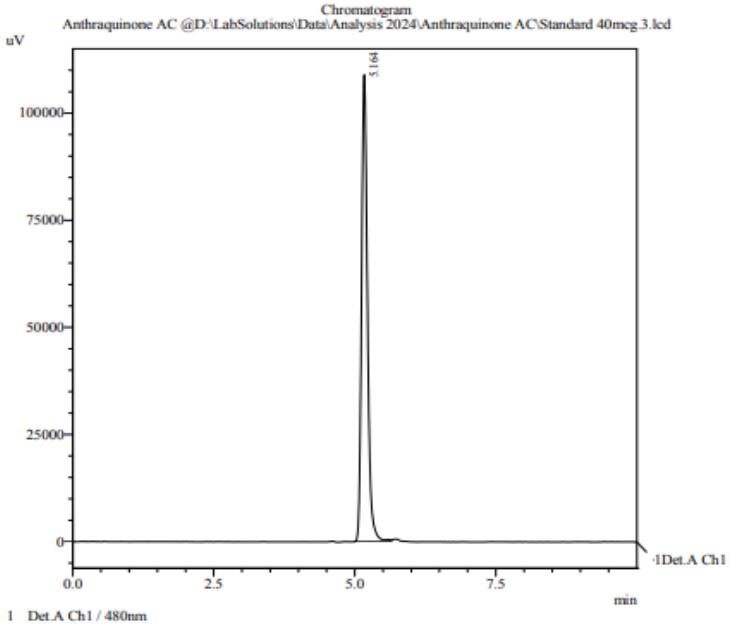

PeakTable @D:\...\Data\Analysis 2024\Anthraquinone AC\Standard 40mcg.3.lcd
Detector A Ch1 480nm

Peak#	Ret. Time	Area	Height	Name
1	5.164	793234	108941	Anthraquinone AC
Total		793234	108941	

Standard 60mcg

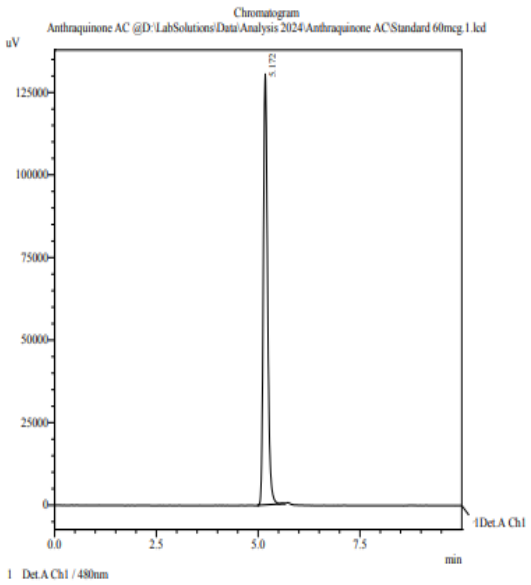

PeakTable @D:\...\Data\Analysis 2024\Anthraquinone AC\Standard 60mcg.1.lcd
Detector A Ch1 480nm

Peak#	Ret. Time	Area	Height	Name
1	5.172	947729	130460	Anthraquinone AC
Total		947729	130460	

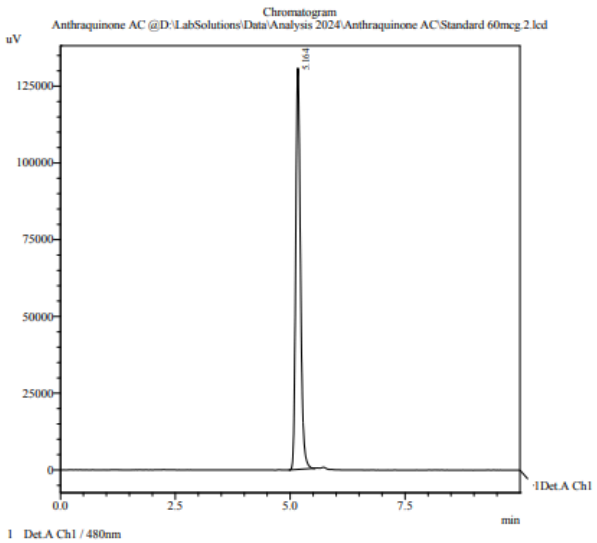

PeakTable @D:\...\Data\Analysis 2024\Anthraquinone AC\Standard 60mcg.2.lcd
Detector A Ch1 480nm

Peak#	Ret. Time	Area	Height	Name
1	5.164	948485	130701	Anthraquinone AC
Total		948485	130701	

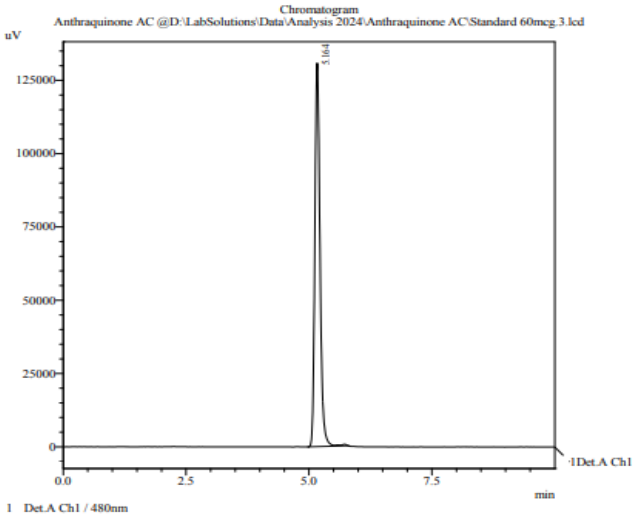

PeakTable @D:\...\Data\Analysis 2024\Anthraquinone AC\Standard 60mcg.3.lcd
Detector A Ch1 480nm

Peak#	Ret. Time	Area	Height	Name
1	5.164	958684	130798	Anthraquinone AC
Total		958684	130798	

Standard 80mcg

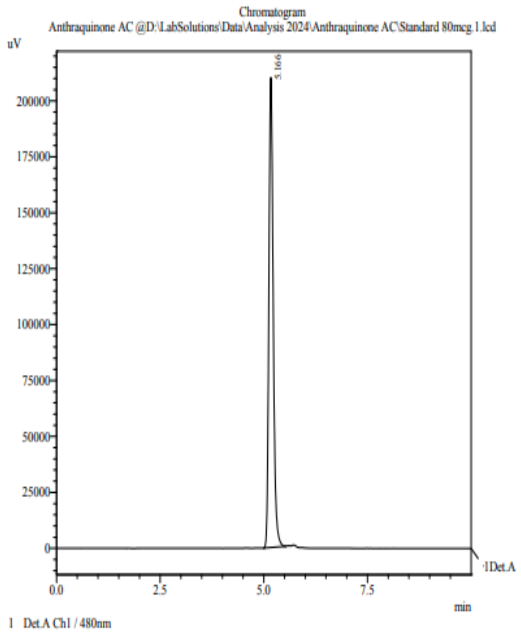

PeakTable @D:\...\Data\Analysis 2024\Anthraquinone AC\Standard 80mcg.1.lcd
Detector A Ch1 480nm

Peak#	Ret. Time	Area	Height	Name
1	5.166	1532381	210049	Anthraquinone AC
Total		1532381	210049	

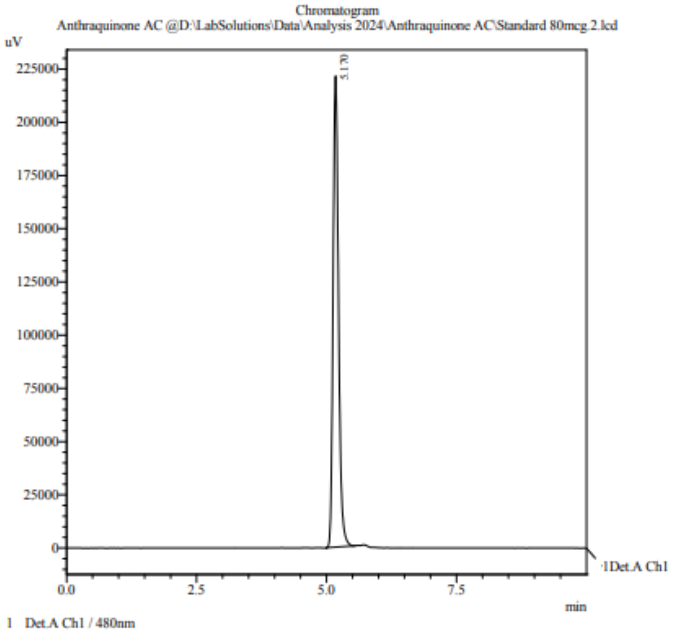

PeakTable @D:\...\Data\Analysis 2024\Anthraquinone AC\Standard 80mcg.2.lcd
Detector A Ch1 480nm

Peak#	Ret. Time	Area	Height	Name
1	5.170	1611164	221278	Anthraquinone AC
Total		1611164	221278	

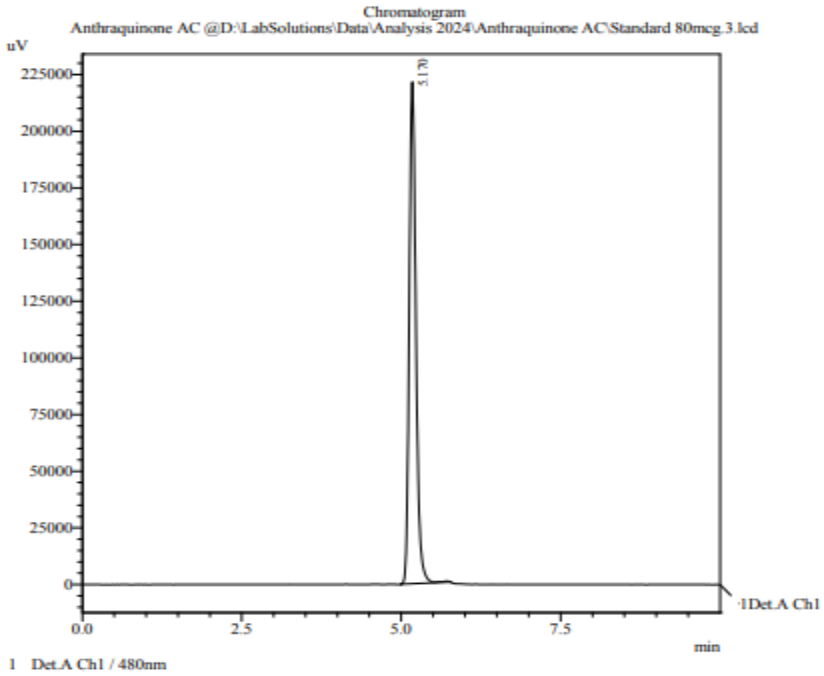

PeakTable @D:\...\Data\Analysis 2024\Anthraquinone AC\Standard 80mcg.3.lcd
Detector A Ch1 480nm

Peak#	Ret. Time	Area	Height	Name
1	5.170	1617953	221337	Anthraquinone AC
Total		1617953	221337	

Standard 100mcg

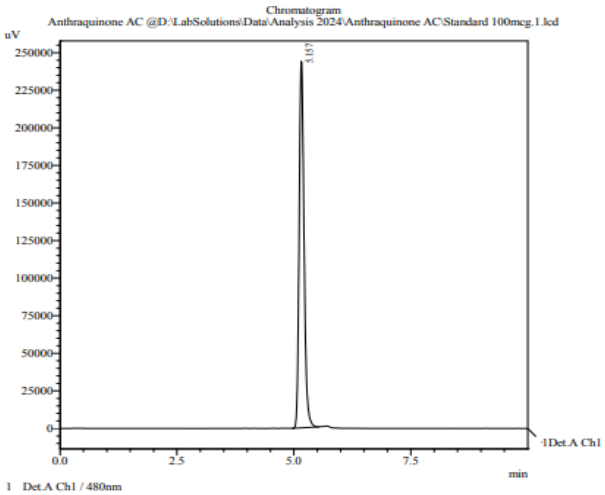

PeakTable @D:\...\Data\Analysis 2024\Anthraquinone AC\Standard 100mcg.1.lcd
Detector A Ch1 480nm

Peak#	Ret. Time	Area	Height	Name
1	5.157	1771757	243806	Anthraquinone AC
Total		1771757	243806	

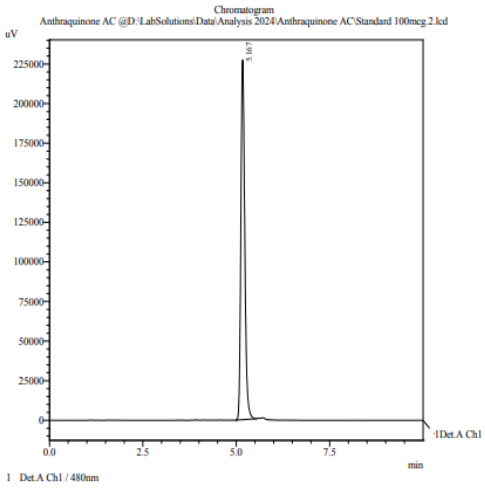

PeakTable @D:\...\Data\Analysis 2024\Anthraquinone AC\Standard 100mcg.2.lcd
Detector A Ch1 480nm

Peak#	Ret. Time	Area	Height	Name
1	5.167	1645802	227081	Anthraquinone AC
Total		1645802	227081	

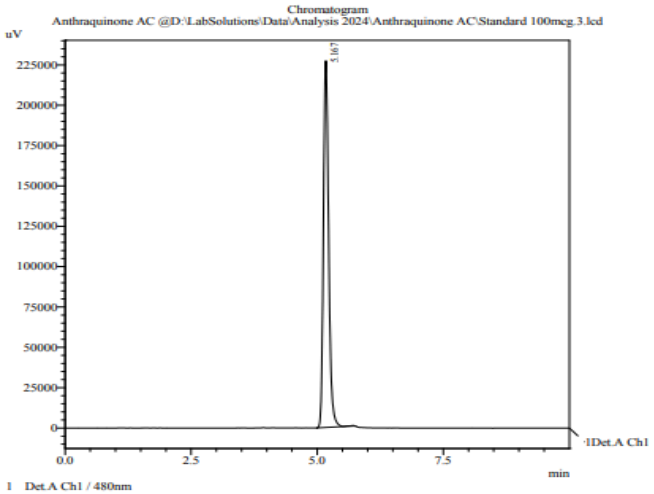

PeakTable @D:\...\Data\Analysis 2024\Anthraquinone AC\Standard 100mcg.3.lcd
Detector A Ch1 480nm

Peak#	Ret. Time	Area	Height	Name
1	5.167	1650724	227118	Anthraquinone AC
Total		1650724	227118	

Blank Plasma

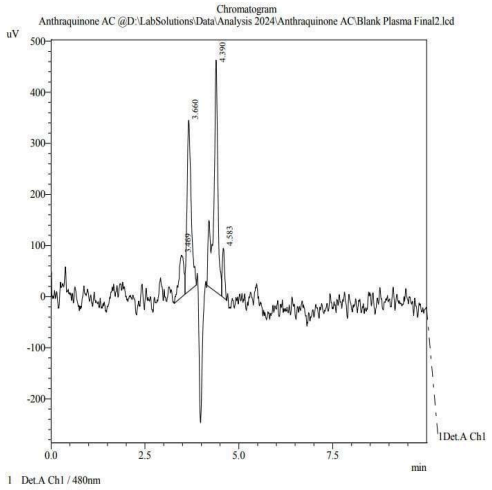

PeakTable @D:\...\Data\Analysis 2024\Anthraquinone AC\Blank Plasma Final2.lcd
Detector A Ch1 480nm

Peak#	Ret. Time	Area	Height	Name
1	3.469	795	83	RT3.469
2	3.660	2554	335	RT3.660
3	4.390	3609	454	RT4.390
4	4.583	410	96	RT4.583
Total		7368	968	

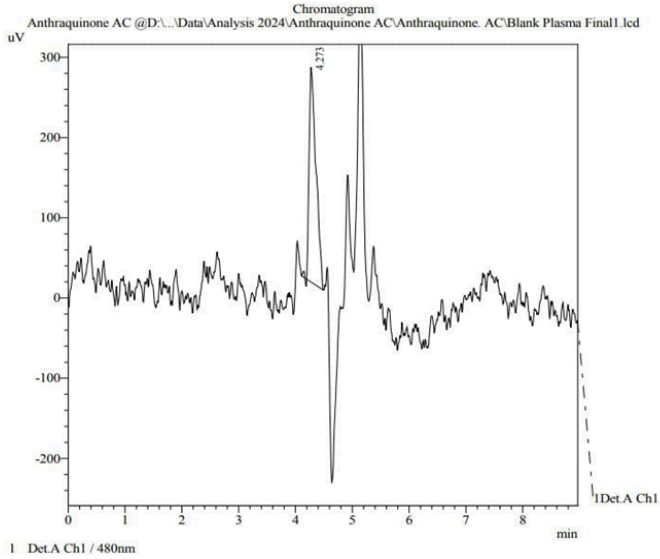

PeakTable @D:\...\Anthraquinone AC\Anthraquinone. AC\Blank Plasma Final1.lcd
Detector A Ch1 480nm

Peak#	Ret. Time	Area	Height	Name
1	4.273	2261	267	Blank Plasma
Total		2261	267	

IV Dosing

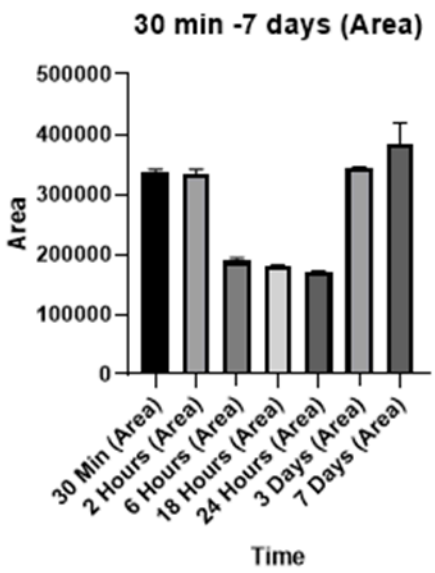

30min – 7 days (height)

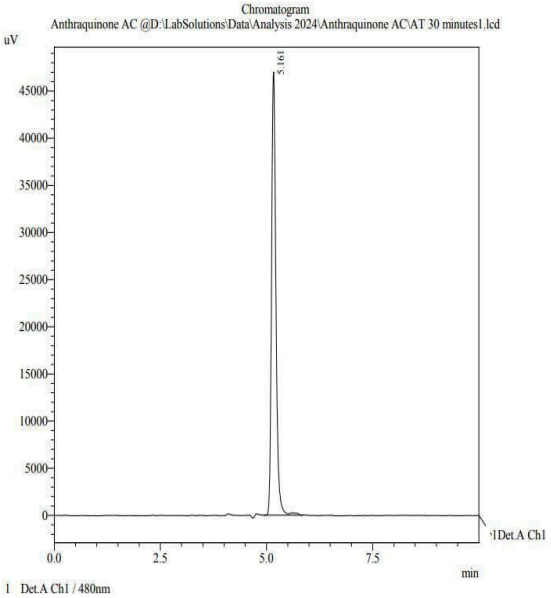

PeakTable @D:\...\Data\Analysis 2024\Anthraquinone AC\AT 30 minutes1.lcd
Detector A Ch1 480nm

Peak#	Ret. Time	Area	Height	Name
1	5.161	337990	46997	Anthraquinone AC
Total		337990	46997	

30 min

2

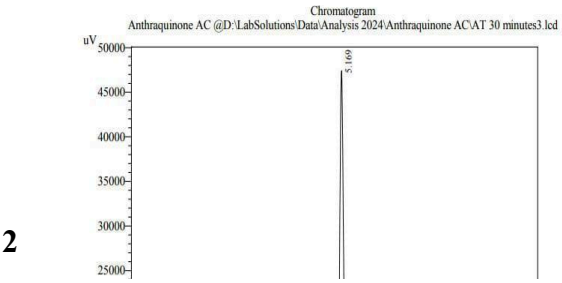

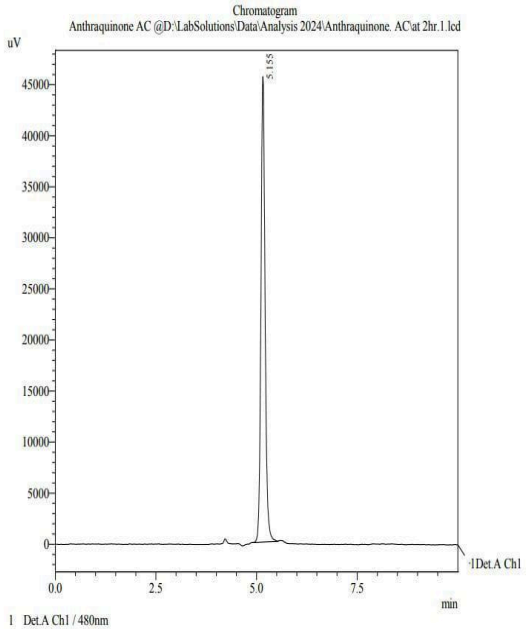

PeakTable @D:\LabSolutions\Data\Analysis 2024\Anthraquinone. AC\at 2hr.1.lcd
Detector A Ch1 480nm

Peak#	Ret. Time	Area	Height	Name
1	5.155	326707	45581	Anthraquinone AC
Total		326707	45581	

A Ch1

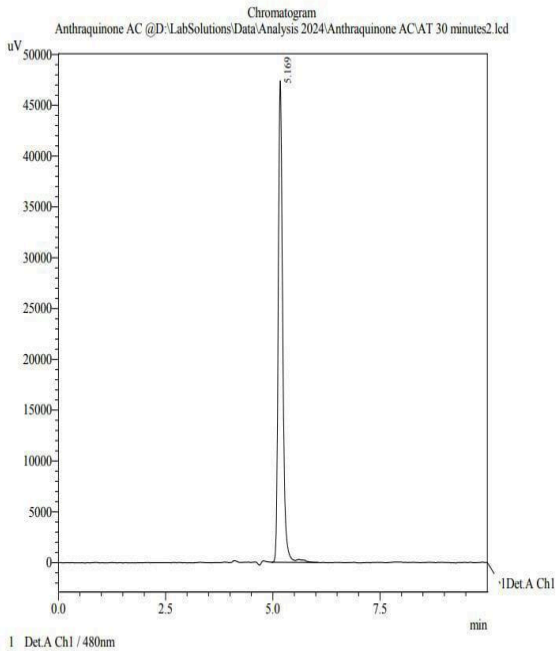

PeakTable @D:\...\Data\Analysis 2024\Anthraquinone AC\AT 30 minutes2.lcd
Detector A Ch1 480nm

Peak#	Ret. Time	Area	Height	Name
1	5.169	341449	47383	Anthraquinone AC
Total		341449	47383	

Hr

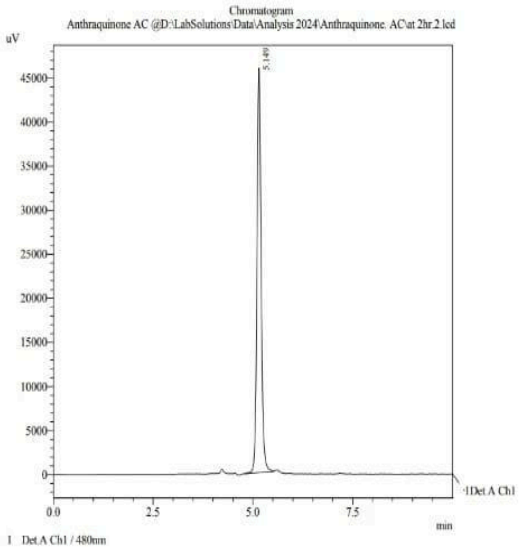

PeakTable @D:\LabSolutions\Data\Analysis 2024\Anthraquinone. AC\at 2hr.2.lcd
Detector A Ch1 480nm

Peak#	Ret. Time	Area	Height	Name
1	5.149	332910	45896	Anthraquinone AC
Total		332910	45896	

6Hr

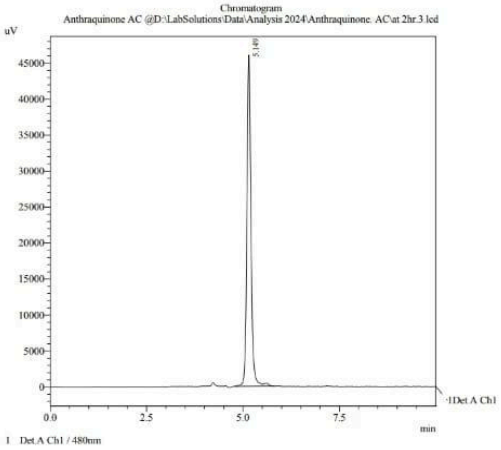

PeakTable @D:\LabSolutions\Data\Analysis 2024\Anthraquinone. AC\at 2hr.3.lcd
Detector A Ch1 480nm

Peak#	Ret. Time	Area	Height	Name
1	5.149	342089	46023	Anthraquinone AC
Total		342089	46023	

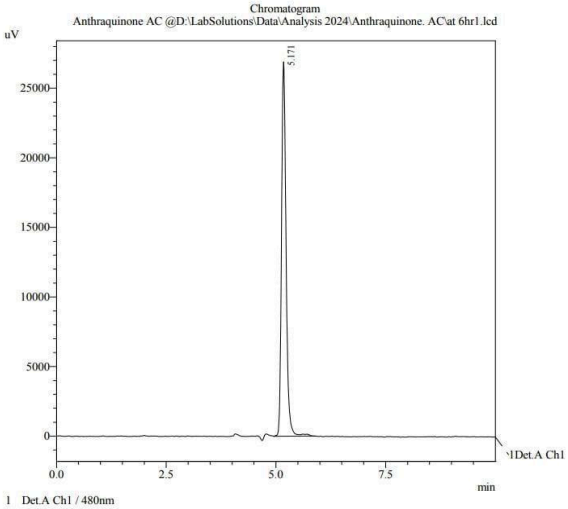

PeakTable @D:\LabSolutions\Data\Analysis 2024\Anthraquinone. AC\at 6hr1.lcd
Detector A Ch1 480nm

Peak#	Ret. Time	Area	Height	Name
1	5.171	194141	26896	Anthraquinone AC
Total		194141	26896	

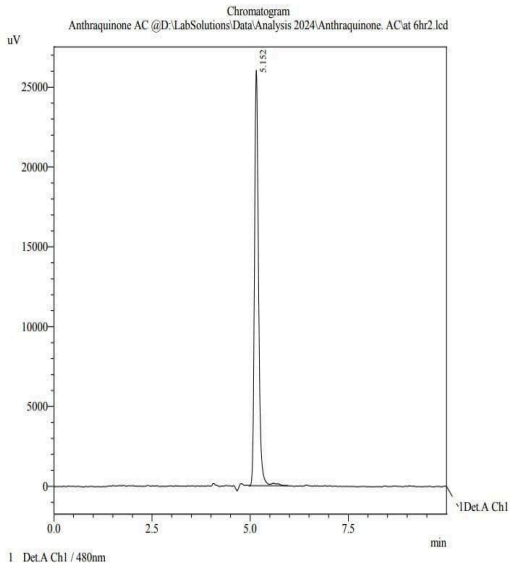

PeakTable @D:\LabSolutions\Data\Analysis 2024\Anthraquinone. AC\at 6hr2.lcd
Detector A Ch1 480nm

Peak#	Ret. Time	Area	Height	Name
1	5.152	188176	26023	Anthraquinone AC
Total		188176	26023	

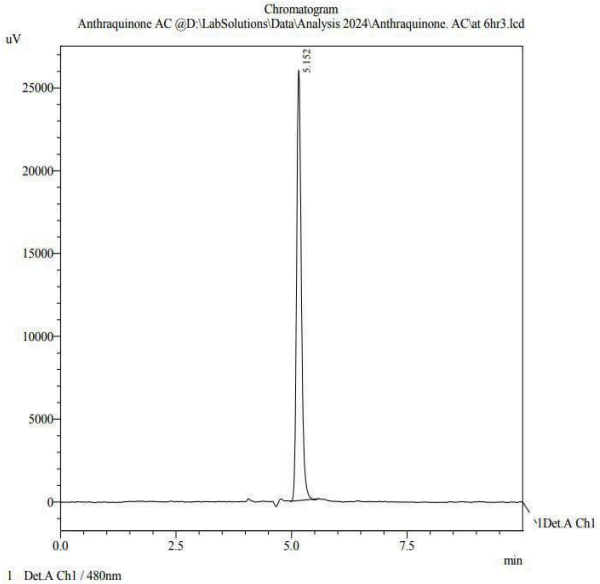

PeakTable @D:\LabSolutions\Data\Analysis 2024\Anthraquinone. AC\at 6hr3.lcd
Detector A Ch1 480nm

Peak#	Ret. Time	Area	Height	Name
1	5.152	183759	25978	Anthraquinone AC
Total		183759	25978	

18Hr

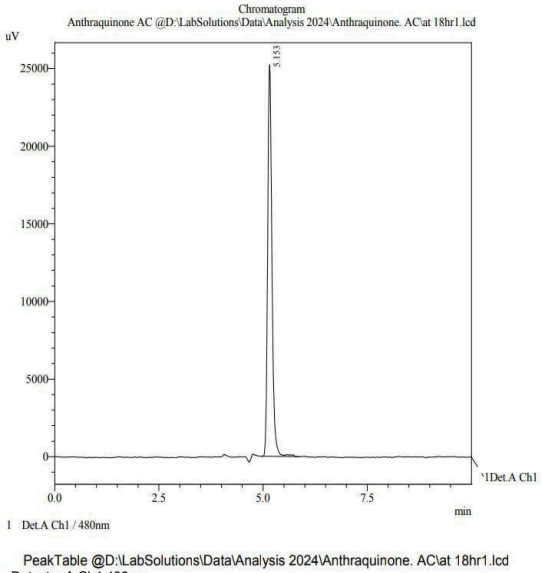

PeakTable @D:\LabSolutions\Data\Analysis 2024\Anthraquinone. AC\at 18hr1.lcd
Detector A Ch1 480nm

Peak#	Ret. Time	Area	Height	Name
1	5.153	180344	25215	Anthraquinone AC
Total		180344	25215	

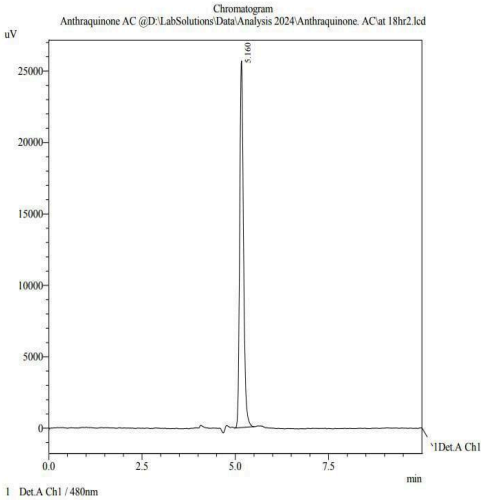

PeakTable @D:\LabSolutions\Data\Analysis 2024\Anthraquinone. AC\at 18hr2.lcd
Detector A Ch1 480nm

Peak#	Ret. Time	Area	Height	Name
1	5.160	181548	25655	Anthraquinone AC
Total		181548	25655	

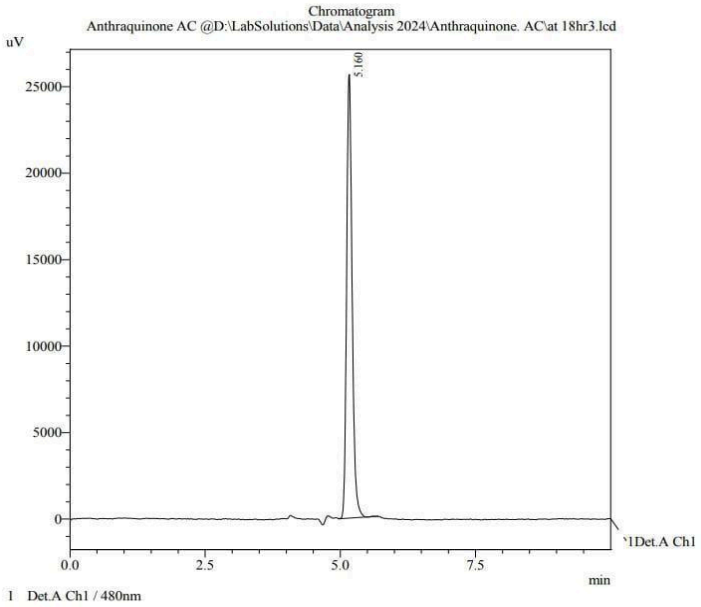

PeakTable @D:\LabSolutions\Data\Analysis 2024\Anthraquinone. AC\at 18hr3.lcd
Detector A Ch1 480nm

Peak#	Ret. Time	Area	Height	Name
1	5.160	181276	25649	Anthraquinone AC
Total		181276	25649	

24Hr

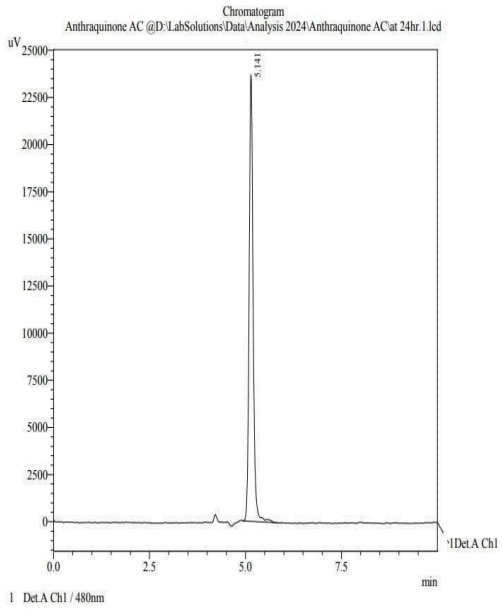

PeakTable @D:\LabSolutions\Data\Analysis 2024\Anthraquinone AC\at 24hr.1.lcd
Detector A Ch1 480nm

Peak#	Ret. Time	Area	Height	Name
1	5.141	170999	23679	Anthraquinone AC
Total		170999	23679	

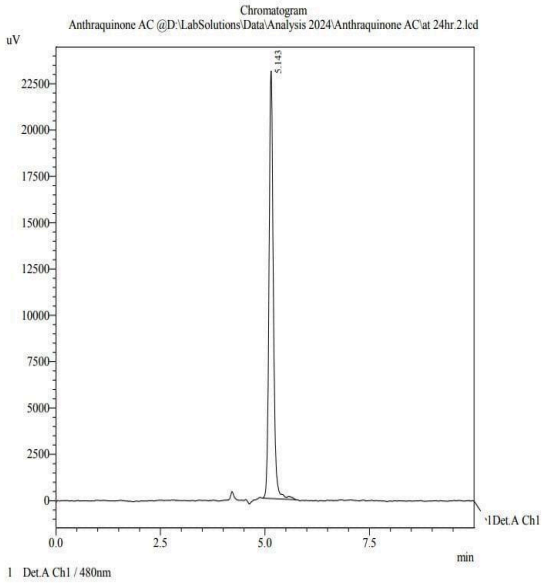

PeakTable @D:\LabSolutions\Data\Analysis 2024\Anthraquinone AC\at 24hr.2.lcd
Detector A Ch1 480nm

Peak#	Ret. Time	Area	Height	Name
1	5.143	166482	23062	Anthraquinone AC
Total		166482	23062	

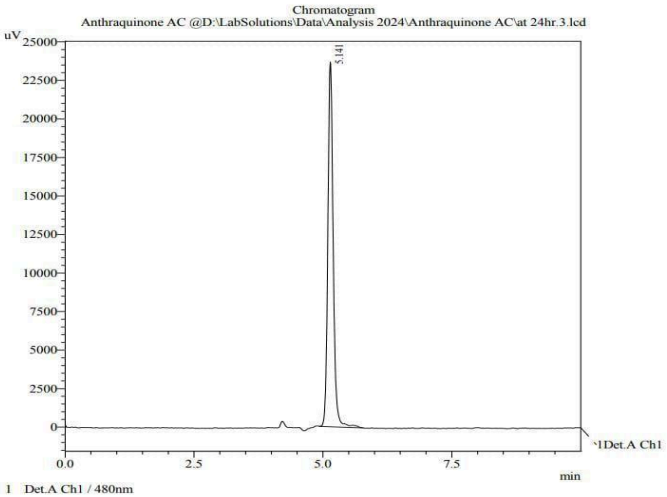

PeakTable @D:\LabSolutions\Data\Analysis 2024\Anthraquinone AC\at 24hr.3.lcd
Detector A Ch1 480nm

Peak#	Ret. Time	Area	Height	Name
1	5.141	171016	23679	Anthraquinone AC
Total		171016	23679	

3 Days

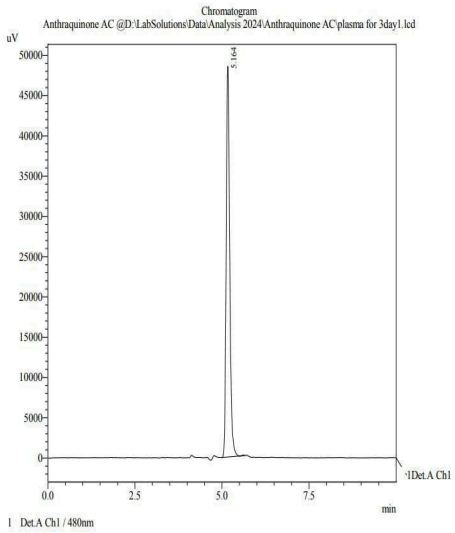

PeakTable @D:\...\Data\Analysis 2024\Anthraquinone AC\plasma for 3day1.lcd
Detector A Ch1 480nm

Peak#	Ret. Time	Area	Height	Name
1	5.164	341354	48502	Anthraquinone AC
Total		341354	48502	

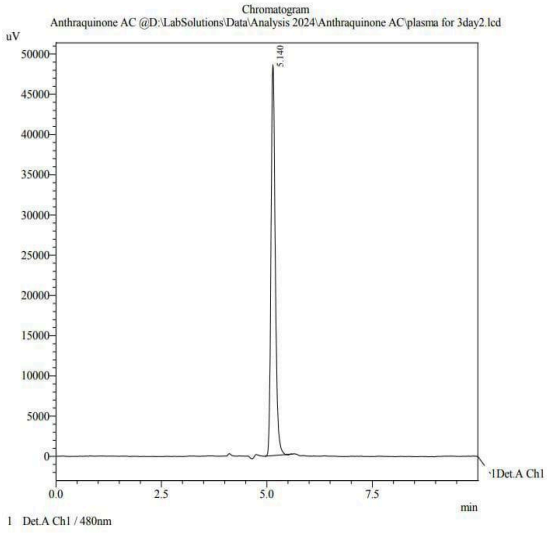

PeakTable @D:\...\Data\Analysis 2024\Anthraquinone AC\plasma for 3day2.lcd
Detector A Ch1 480nm

Peak#	Ret. Time	Area	Height	Name
1	5.140	341228	48575	Anthraquinone AC
Total		341228	48575	

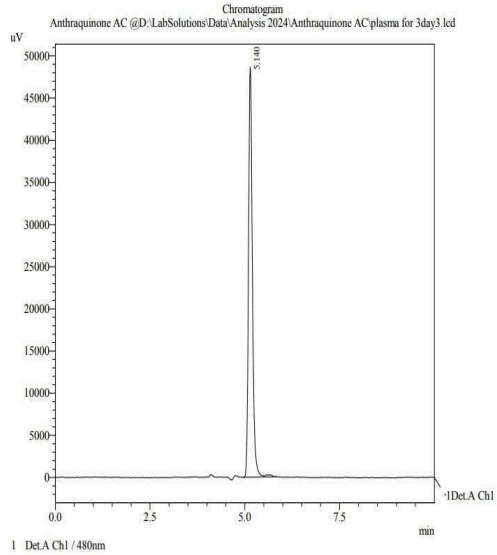

PeakTable @D:\...\Data\Analysis 2024\Anthraquinone AC\plasma for 3day3.lcd
Detector A Ch1 480nm

Peak#	Ret. Time	Area	Height	Name
1	5.140	345801	48636	Anthraquinone AC
Total		345801	48636	

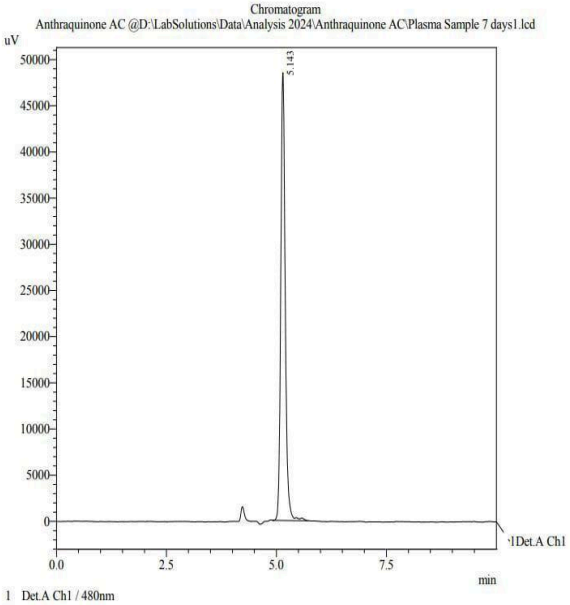

PeakTable @D:\...\Analysis 2024\Anthraquinone AC\Plasma Sample 7 days1.lcd
Detector A Ch1 480nm

Peak#	Ret. Time	Area	Height	Name
1	5.143	343439	48486	Anthraquinone AC
Total		343439	48486	

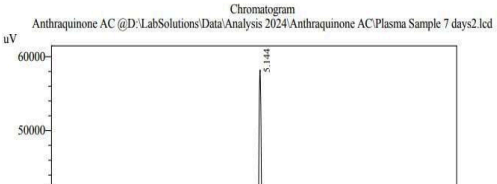

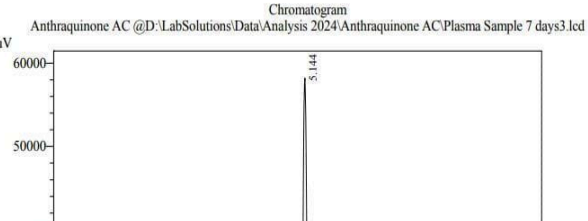

Open Field Test (OFT)

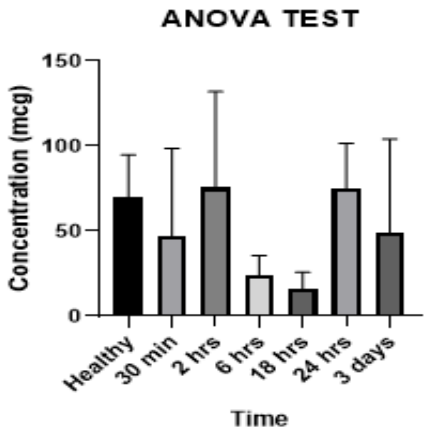

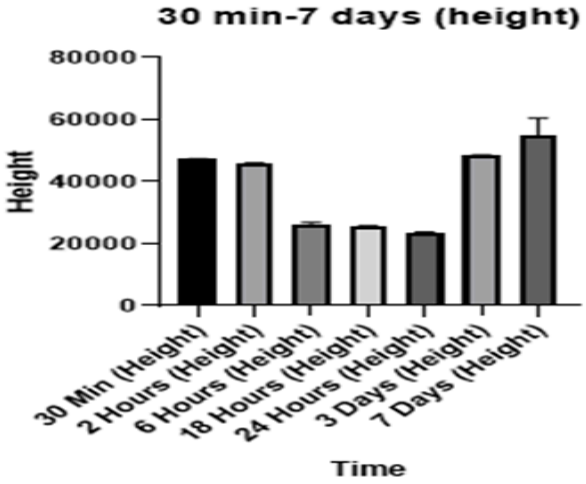

Number of Entries to the

Central Zone

Time Spent in the Central Zone (seconds)

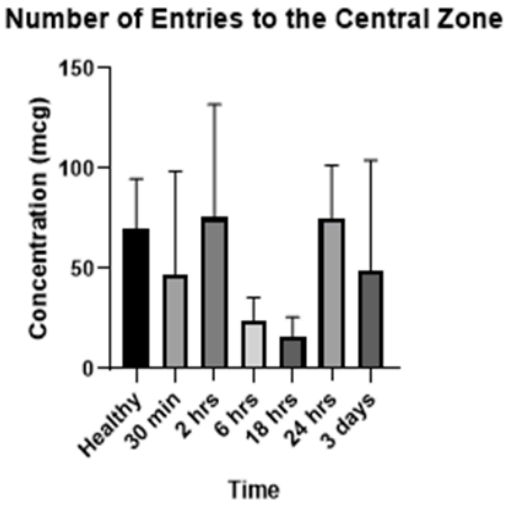

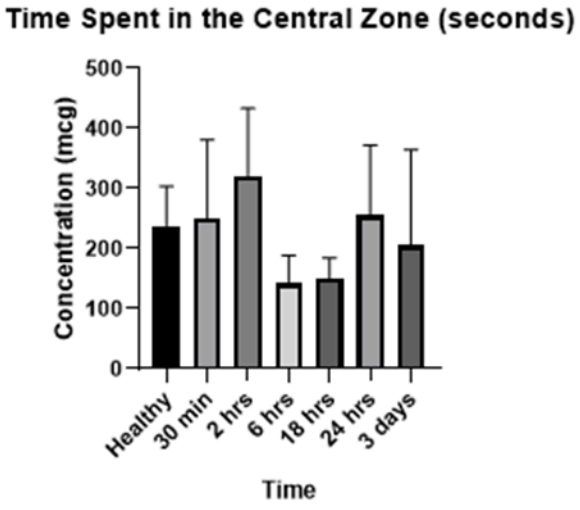

SM/FM

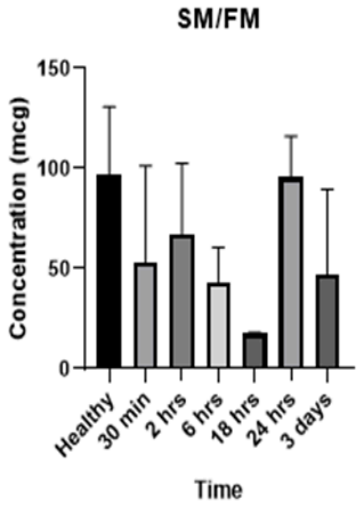

SR/FR

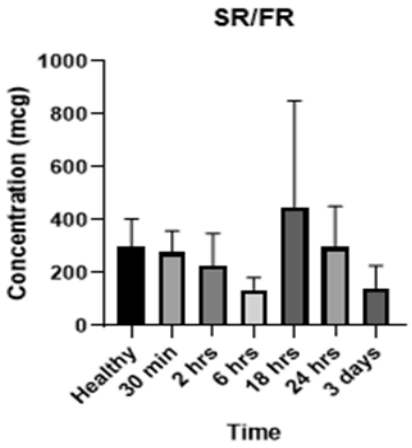

Inverted Screen Test

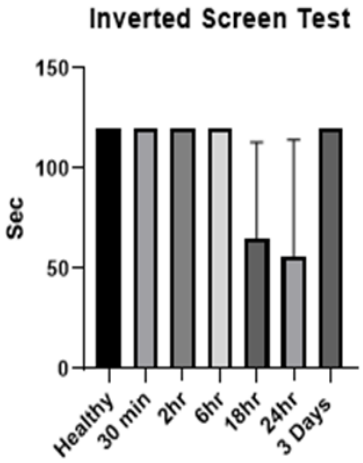

CBC

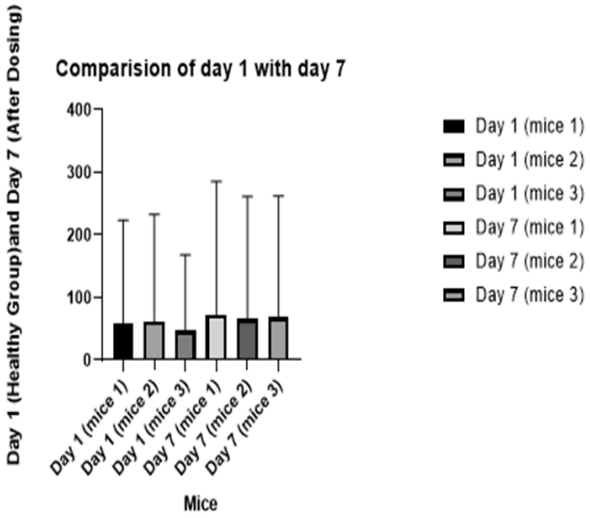

Appendix G

Heart Histopathology in Mice

Healthy Heart 10X	Healthy Heart 40X
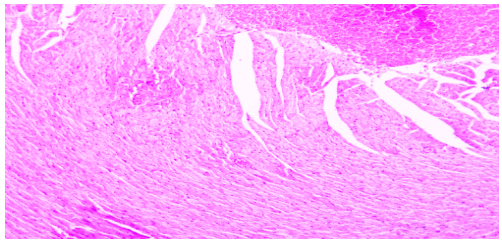	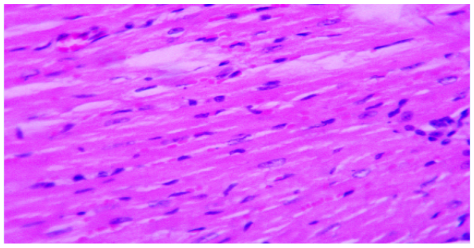
Diseased Heart 10X **Mice 1 200mg/kg** 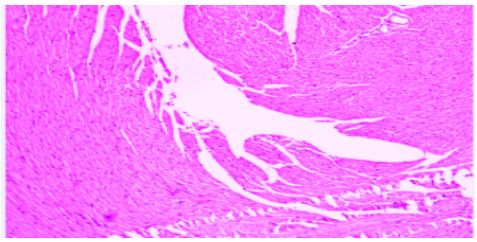	**Diseased Heart 40X** 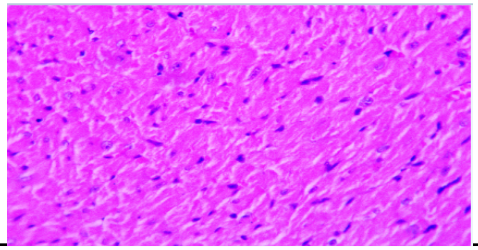
Mice 2 200mg/kg 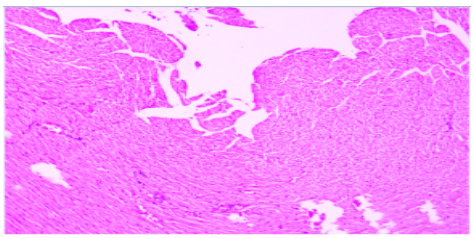	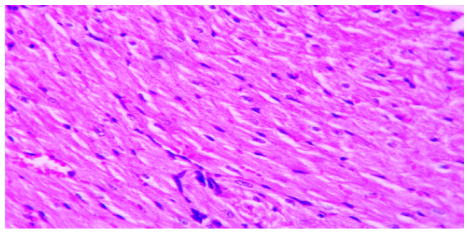
Mice 3 200mg/kg 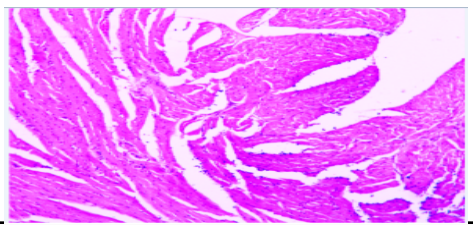	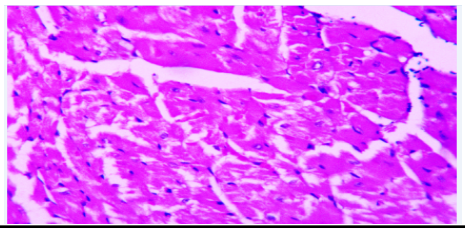

Kidney Histopathology in Mice

Healthy Kidney 10X	Healthy Kidney 40X
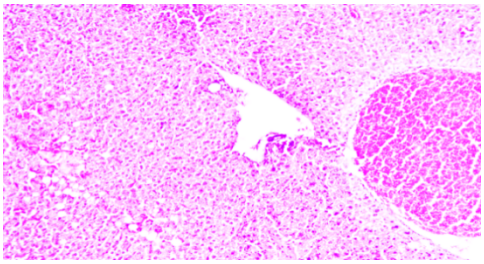	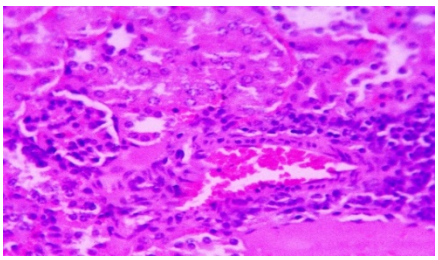
Diseased Kidney 10X **Mice 1 200mg/kg** 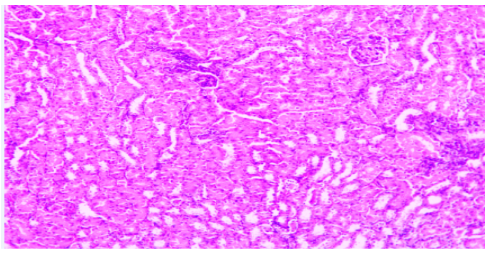	**Diseased Kidney 40X** 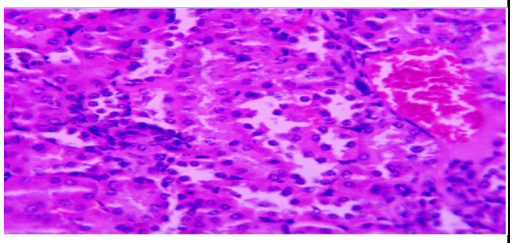
Mice 2 200mg/kg 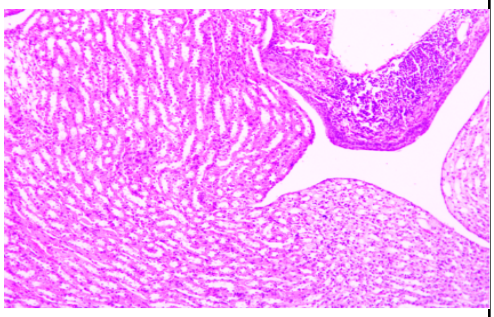	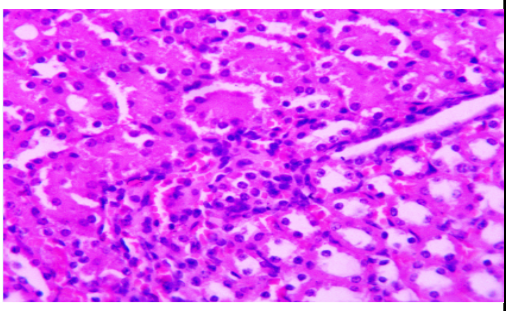
Mice 3 200mg/kg 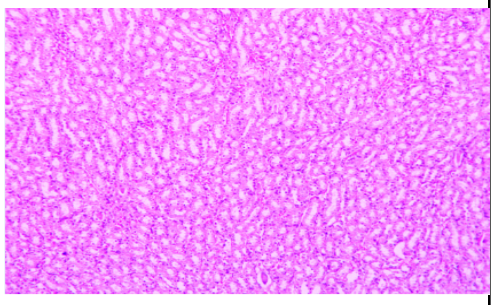	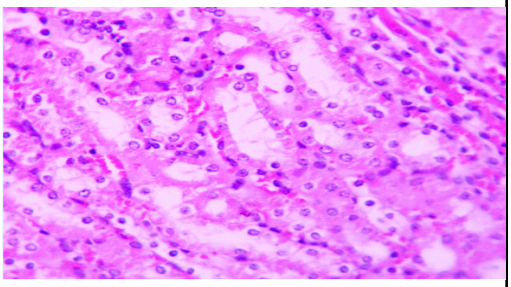

Liver Histopathology in Mice

Healthy Liver 10X	Healthy Liver 40X
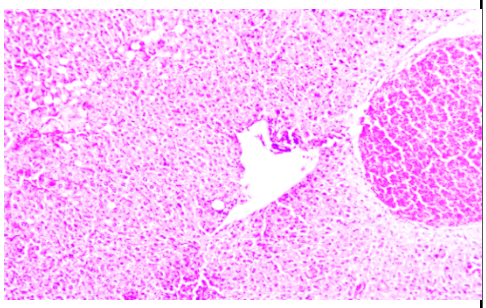	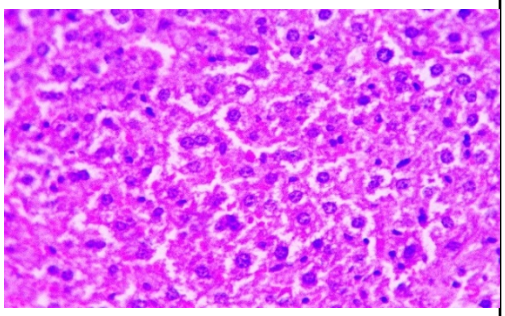
Diseased Liver 10X	**Diseased Liver 40X**
Mice 1 200mg/kg 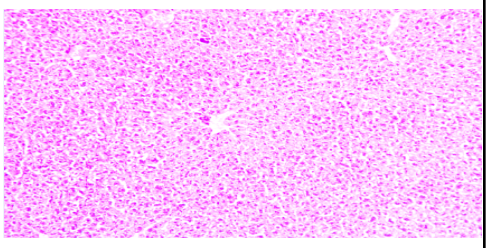	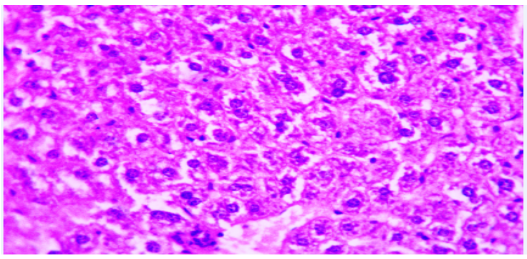
Mice 2 200mg/kg 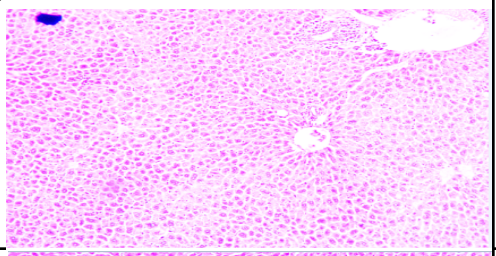	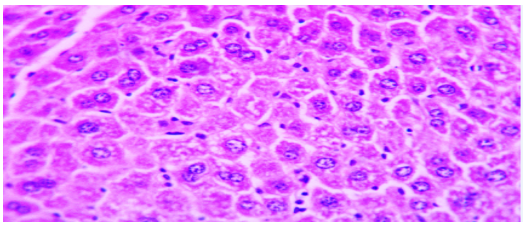
Mice 3 200mg/kg